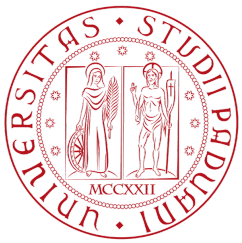

UNIVERSITA' DEGLI STUDI DI PADOVA

Dipartimento di Ingegneria Industriale

Corso di Laurea Magistrale in Ingegneria Energetica

TESI DI LAUREA MAGISTRALE

Evolution of Configurations of Evaporative Systems for Seawater Desalination

Relatore:
Prof. Andrea Lazzaretto

Laureanda:
Chiara Dall'Armi

Correlatore:
Dott. Sergio Rech

Anno Accademico 2017/2018

Abstract

A comprehensive analysis on the evolution of main evaporative desalination technologies is performed in this thesis, from the simplest configurations (single stage and single effect) to more complex and efficient solutions. In the first part, mathematical models are developed for MSF, MED, MED-TVC and MED-MVC systems, and simulations are run for different design conditions. The thermodynamic models, solved with EES software, utilize accurate properties for seawater, brine and pure water. Simulation results are discussed according to usual performance parameters (Performance Ratio PR and Recovery Ratio RR) along with a newly defined metric based on primary energy at input.

The second part of this work analyzes the performances of the above mentioned desalination systems through an exergy analysis based on SPECO method. In particular, a new approach is illustrated for the definition of fuel and product exergies accordingly to the real purpose of desalination plants. Decrease of chemical exergy related to freshwater mass flow rate is considered as system product, while all other exergy variations (decreases or undesired increases) are considered at the fuel side. Investigating performance of desalination systems through the newly defined approach for exergy analysis stressed out critical aspects of PR and RR. In addition, a comparison is done with other approaches for the calculation of exergy analysis, which points out the differences in exergy efficiencies due to different definitions of fuel and product of the desalination system.

Sommario

In questa tesi viene presentata un'analisi approfondita sull'evoluzione delle principali tecnologie evaporative di desalinizzazione, partendo dalle configurazioni più semplici (singolo stadio e singolo effetto) per giungere a quelle più complesse e performanti. Nella prima parte vengono sviluppati i modelli delle tecnologie MSF, MED, MED-TVC e MED-MVC, il cui funzionamento viene simulato in diverse condizioni di progetto. I modelli termodinamici, implementati nel software EES, fanno riferimento a proprietà accurate dell'acqua di mare, della salamoia e dell'acqua pura. I risultati delle simulazioni vengono discussi, in questa prima fase, facendo riferimento ai parametri di prestazione abitualmente utilizzati per l'analisi dei sistemi di desalinizzazione: Performance Ratio (PR) e Recovery Ratio (RR). Contestualmente, viene introdotta una nuova definizione di rendimento energetico basato sull'energia primaria in ingresso al sistema.

La seconda parte della tesi invece analizza i suddetti sistemi di desalinizzazione tramite un'analisi exergetica basata sul criterio SPECO. In particolare, viene seguito un nuovo approccio nella definizione di *fuel* e *prodotto* exergetici, coerente con lo scopo produttivo del sistema: la diminuzione di exergia chimica associata alla portata di massa desalinizzata costituisce l'unico prodotto desiderato del sistema, mentre le le altre variazioni di exergia, siano esse decrementi o incrementi non desiderati, vengono considerate parte del *fuel*. Dall'analisi dei sistemi secondo questo nuovo criterio, emergono alcune criticità dei parametri PR e RR utilizzati in precedenza. Vengono infine illustrati i valori del rendimento dell'impianto utilizzando diverse definizioni, mettendo in evidenza come diversi approcci, soprattutto nella definizione del *fuel* exergetico, possano condurre a valori anche molto discordanti.

Contents

List of Figures

List of Tables

Chapter 1

Introduction

Over the last decades, unsustainable development pathways have strongly compromised quality and availability of water resources. Rapid growth of urban areas and climate change are two of the main causes of the increasing number of regions that will suffer from water scarcity in the immediate future [22, 42]. In such a critical context, desalination systems started to be considered a viable option to produce freshwater, despite being energy-intensive technologies. Hence, it is essential to understand which working parameters affect the performance of desalination plants in order to move towards more sustainable processes. Among different desalination systems, evaporative technologies have the possibility to be powered, for instance, by solar thermal power plants or by low temperature waste heat resources. Therefore, despite being far from being considered efficient, they could represent the best option for applications in arid areas.

Many studies have been conducted on the performance analysis of evaporative desalination plants, even though most of them do not report an organic analysis of the evolution of configurations and design parameters of evaporative systems. More in detail, many of the analyses found in the literature on the performance of evaporative systems report evaluations based on different metrics, which makes it difficult to compare one technology to the others or to evaluate the best configuration among different ones.

Objective of this thesis is to present the evolution of evaporative systems for seawater desalination, starting from the simplest configurations (single effect and single stage configurations) and ending up with more complex and efficient solutions. For this purpose, analysis of configurations proposed in the literature is performed at first, in

order to understand working principles of the processes and to individuate the adequate parameters to describe the systems.

In the first part of Chapter 2, main desalination technologies available nowadays are described, so as to give a general framework of the object of the thesis. The second part of Chapter 2 illustrates metrics utilized so far for delineating the performance of desalination processes, focusing on critical aspects of these parameters.

Thereafter, in Chapters 3 to 6 mathematical models are built for the most significant evaporative configurations: Multi Stage Flash (MSF), Multi Effect Distillation (MED), Multi Effect Distillation with Thermal and Mechanical Vapor Compression (MED-TVC and MED-MVC). Models are validated with experimental data found in the literature and simulations are run under different design conditions. Models are solved with Engineering Equation Solver (EES) [49], which does not require a solution algorithm as those ones used in most previous studies.

Finally, Chapter 7 reports exergy analysis for different desalination configurations according to an exergy efficiency defined with a novel approach based on an accurate investigation of real processes and on the productive goal of the global system. A comparison is then presented among different definitions of efficiency.

Chapter 2

Desalination Technologies

Desalination technologies differ one from another according to the way dissolved salts are separated from seawater. Although this work analyzes the evolution of evaporative technologies, it is worth give a brief description of other types of desalination. The aim of the first part of this chapter is to describe the main features of both thermal and membrane technologies. In the second part, performance parameters utilized so far to analyze desalination systems are illustrated. An alternative definition of energetic efficiency is hence given at the end of this Chapter in order to overcome some critical features of other metrics.

2.1 Classification of Desalination Technologies

Desalination technologies can be classified according to different characteristics. The most diffused classification divides desalination technologies in *thermal* and *membrane* desalination systems. Among thermal desalination technologies it is worth mention: Multi Stage Flash (MSF), Multiple Effect Distillation (MED), Mechanical and Thermal Vapor Compression (MVC and TVC), Vacuum Freeze Desalination (VFD), Humidification-Dehumidification (HDH), Solar stills. Membrane technologies include: Reverse Osmosis (RO), Electrodialysis (ED), Forward Osmosis (FO), Membrane Distillation (MD).Desalination technologies can also be classified according to the type of energy used in the process.Table 2.3 and 2.2 show the two classifications of desalination technologies.

Beside evaporative technologies (MSF and MED), analyzed in this work, it is worth give a brief description of working principles of the other technologies.

Sea or Ocean	Temperature (°C)	TDS (ppm)
Baltic Sea	10	7000
Black Sea	20	20000
North Atlantic	17-25	29000
Pacific Ocean	25-30	33600
Atlantic South	25-30	36000
Adriatic Sea	26	31400
Indian Ocean	30-35	33800
Mediterranean	27	39000
Red Sea	30-35	43000
Arabian Gulf	30-35	50000
Australian Shark Bay	20-25	70000

Table 2.1: Temperature and Total Dissolved Salts in various Seas an Oceans. Temperatures refer to June 2018. [1, 60]

2.1.1 Membrane Technologies

Membrane are used in two commercially important desalting processes: Electrodialysis (ED) and Reverse Osmosis (RO). Each process uses the ability of membranes to differentiate and selectively separate salts and water. However, membranes are used differently in each of these processes, as described in the following sections.

Reverse Osmosis(RO)

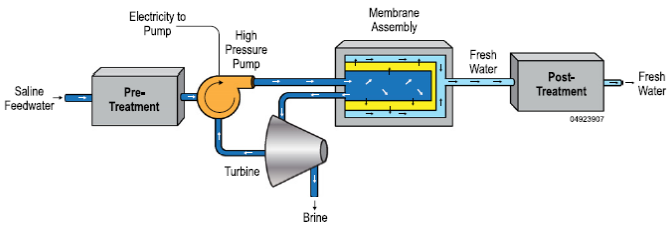

Figure 2.1: Reverse Osmosis Unit [58]

Reverse osmosis is a membrane separation process in which the water from a pressurized saline solution is separated from the solutes (the dissolved materials) by flowing

Type of process	Technology	Different configurations
Thermal	MSF	Once Through
		Brine Mixing
		Brine Circulation
		Vapor Compression
	MED	TVC
		MVC
	VFD	–
	HDH	–
Membrane	RO	Seawater
		Low salinity brackish water
	ED	–
	FO	–
	MD	–

Table 2.2: Thermal and membrane desalination technologies.

Type of Separation	Energy used	Process	Desalination method
Water from salts	Thermal	Evaporation	MSF MED TVC Solar distillation
Water from salts	Thermal	Filtration/Evaporation	MD
Water from salts	Mechanical	Evaporation Filtration	MVC RO
Salts from water	Electrical Chemical	Selective Filtration Ionic exchange	ED Ionic exchange

Table 2.3: Classification of Desalination Technologies according to the type of energy utilized.

through a semi-permeable membrane. No heating or phase change is necessary for this separation. The major energy required for desalting is to pressurize the feed water to a value higher than its osmotic pressure (about 28 bar) in order to be able to separate salts from water. Industrial plants normally pump the feed water to a pressure of 60-70 bar. In practice, as shown in Figure 2.1, saline feed water is pumped into a closed vessel where it is pressurized against the membrane. As a result, a portion of feed water passes through the membrane and, after a post treatment unit, is collected as fresh water. The remaining part of feed water(from 20 to 70 % of the feed water), with increased salt content, is discharged without passing through the membrane. This controlled discharge is fundamental to avoid problems such as precipitation of superheated salts and increased osmotic pressure across the membranes. Pretreatment unit is essential to guarantee that membrane surface remains clean; it usually consists of fine filtration and addition of chemical additives to inhibit precipitation and fouling on the membrane. Recent RO plants also provide for an energy recovery system (generally pressure exchangers) which increase pressure of feed seawater before entering the high pressure pump thanks to energy recovered from the rejected brine stream.[11, 14, 48, 58].

Electro-dialysis (ED)

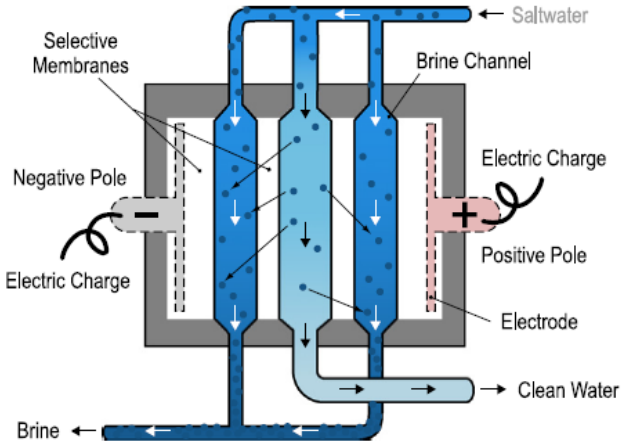

Figure 2.2: Electro-dialysis Unit [58]

Electro-dialysis desalination process consists of a separation of dissolved salts from water thanks to two electrodes with opposite charged. Dissolved ionic constituents in a saline solution, such as chloride (-), sodium (+), calcium (++) and carbonate (-), are dispersed in water, effectively neutralizing their individual charges. When flowing in the ED unit, salt ions tend to migrate to the electrode with opposite charge. Anion-selective and cation-selective membranes are utilized in this process to trap ions and prevent further movements towards the electrodes, thus leaving only concentrated and diluted solutions in the spaces between alternating membranes(see Figure 2.2) As for RO, also in ED pretreatment of feed salt water is needed to prevent fouling and pollution of the membranes. Beside classical ED there is also Electro-dialysis Reversal (EDR). In a EDR unit, polarity of electrodes is reversed at intervals of several times in an hour, thus switching channels of brine and product water. Reversal electro-dialysis is useful in that it breaks up and flushes out scales, slimes and other deposits in the cells before they can accumulate and cause problems.[17, 58].

ED units are generally used to desalinate brackish water, since their energy consumption (i.e. the current used to charge electrodes) is directly proportional to the quantity of salts removed.

In the following section, performance parameters used to analyze desalination systems are illustrated.

Forward Osmosis FO

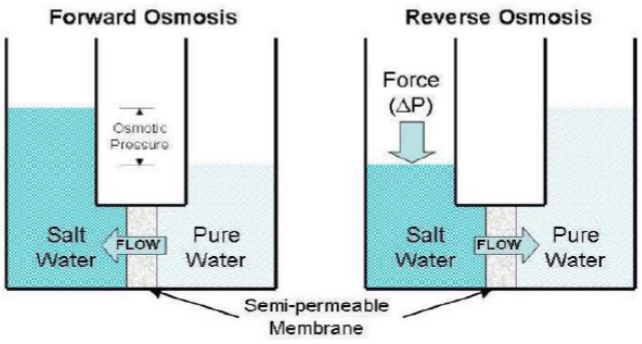

Figure 2.3: Flow directions in Reverse Osmosis and Forward Osmosis [15]

As RO, also Forward Osmosis (FO) utilizes a semi-permeable membrane to separate water from dissolved solutes. In FO however, the driving force is an osmotic pressure gradient between a highly concentrated solution, often referred to as *draw solution*, and a solution of lower concentration, referred to as *feed solution* (i.e. seawater stream for desalination purposes).The draw solution can consist of a single or multiple salts, usually for FO desalination purposes a solution containing NH_3 and CO_2 is utilized. Flow direction is thus opposite when compared to Reverse Osmosis (see Figure 2.3). Fresh water is obtained once draw solution is heated up to a temperature of about 65 °C, splitting into two streams:chemical additives, which will be recycled in the process, and fresh water. FO plants are still a niche technology due to the complex construction of membrane. However, FO systems present some advantages over RO processes: higher conversion capacity, lower pressure needed and thus lower energy consumption, lower need for chemical pretreatment of the feed seawater, lower amount of discharged brine.

Membrane Distillation (MD)

As suggested by the name, Membrane Distillation (MD) combines both distillation and membrane desalination techniques.Saline water is warmed, thus producing water vapor. Produced vapor then passes through a selective membrane, while liquid water cannot. After passing through the membrane, vapor is condensed on a cooler surface producing fresh water in liquid form. Product water, which cannot pass through the membrane, is then collected and represents the plant output. Main advantages of MD technology lie in its simplicity and the need for only small temperature differentials to operate.

2.1.2 Thermal Technologies

Among thermal technologies, evaporative desalination plants have for sure the largest market share, also because they usually operate in co-generation with large power plants (MSF and MED systems). However, there are other thermal technologies it is worth mention that will be described in the following sections. At the end, a paragraph on evaporative desalination systems will introduce the main aspects that need to be investigated when analyzing evaporative desalination systems. Chapter 3 to 6 will then develop these concepts in detail.

Vacuum Freeze Desalination (VFD)

Freezing desalination process is conceptually similar to evaporative system: dissolved salts are separated from water during the freezing process. Theoretically, freezing desalination has some advantages when compared to evaporative methods due to the minor theoretical energy involved in the process. However, this system involves handling ice and water mixtures, which are mechanically problematic to move. Also for this reason, VFD does not have large commercial application nowadays.

Solar Stills

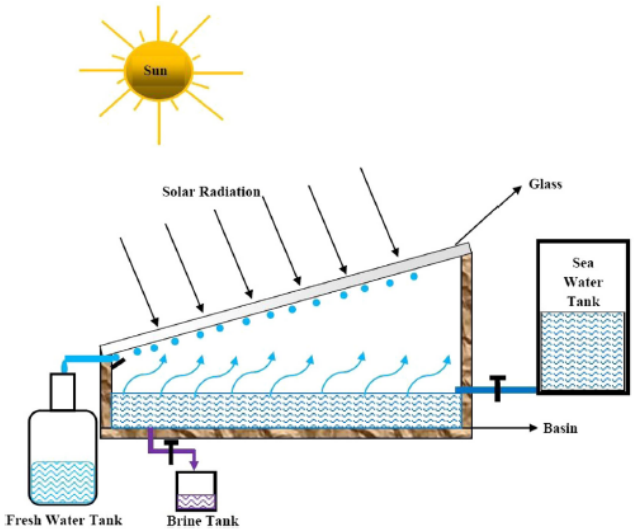

Figure 2.4: Solar Still [53]

A solar still is a simple device where salty (or dirty) water is heated and evaporated by solar energy while flowing in an airtight container. Distillate water vapor then

condenses on the inclined glass surface covering the system, and is collected. Several designs of solar stills have been developed, with different configurations and shapes of the container, integration of solar collectors and heat exchangers. [53, 28, 19, 39, 50, 26].

Humidification-Dehumidification (HDH)

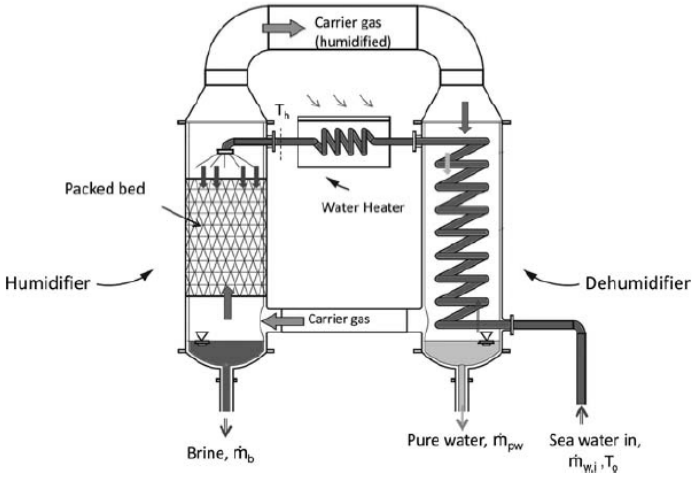

Figure 2.5: Humidification Dehumudification Unit [16]

In Humidification-Dehumidification process, a carrier gas, usually air, is saturated with water vapor and then, through cooling and dehumidification of humid air, fresh water is produced. HDH processes usually operate with forced fluid circulation, and normally humidification and dehumidification processes take place in separate chambers, both of them at temperatures below the boiling point of water (around 80 °C)and at ambient pressure. HDH technology was developed to overcome low efficiencies of solar stills, and is now considered a promising technique for small and medium capacities. [37, 51, 36]

Evaporative desalination technologies

Evaporative desalination technologies basically mimic the natural water cycle: by heating salt water, distillate water vapor is produced and then condensed to form fresh water. Critical features to keep under control in evaporative desalination plants are pressure and temperature, which influence both boiling process and scale formation. Moreover, for desalination plants that provides for brine discharge directly in the sea, maximum

salinity of brine at outlet of the plant is also a parameter to keep under control. Most plants use multiple evaporations to better utilize heat coming from the external heat source and thus increase their thermal efficiency. Clearly, having consecutive evaporations means that salt water has to be boiled at successively lower temperatures and hence lower pressures have to be kept in the system. As mentioned before, pressure and especially temperature are key points to control scale formation. In particular, there are substances in seawater, such as carbonates and sulphates, that dissolve more readily in cooler water. One of the most important is calcium sulphate ($CaSO_4$), which begins to leave solution when seawater approaches about 115 °C [17]. This material forms a hard scale difficult to remove, especially in MED plants, causing thermal and mechanical problems. Controlling the top temperature reached in the system by the salt water (Top Brine Temperature, TBT) or adding chemicals to the seawater for reducing scale precipitation are the most common ways to control and avoid scale formation. For this reason, MED plant can normally operate at a maximum Top Brine Temperature (TBT) of 70 °C. This is not the case of MSF plants, where the plant's structure allows an easier cleaning from fouling and deposits and thus TBT can reach also 120 °C [17, 48].

There are several types of evaporative desalination processes that differ one from each other basing on the way evaporation process is performed. In Multiple Effect Distillation (MED) water vapor is produced in a boiling process, that means evaporation takes place over a heat transfer area. In Multiple Stage Flash distillation processes (MSF), evaporation takes place in the liquid bulk thanks to a pressure difference, and water vapor is thus produced and condensed instantaneously in a flashing process. Both MED and MSF need an external heat source that provides sufficient heat to evaporate water in the first effect or stage. External heat sources could be separated power plants, a dedicated boiler unit, compressed vapor coming from the plant itself, solar energy. MED processes are often matched to a Vapor Compression unit, which provides the necessary heat to the system by compressing a portion of the water vapor produced in the last effect of the plant. Vapor Compression unit could be either Mechanical (MVC) or Thermal (TVC); in MVC mechanical compressors are used, while TVC provides for the use of steam jet ejectors.

According to HEATSEP method [59], it is always convenient to separate problems of definition of the structure of the heat transfer section and definition of the rest of the

system. A distinction is thus made among "basic" components and components involved in the internal heat transfer (heat exchangers). Basic components are those essential to implement the system working principle. Applying these concepts to energy systems firstly allows to better understand the system purpose and, in a second moment, to find the optimum heat exchangers network for the selected plant. Also for evaporative desalination systems, an HEATSEP approach would highlight main differences among several desalination techniques. Starting from clear definitions of each technology would then be possible to delineate the best internal heat transfer network. In Chapters 3 to 5, different evaporative desalination systems are described, starting from the definition of basic components and structure. Mathematical models are then built for complex plant configurations (multi-effect and multi-stage). Results are thus discussed and compared with data available in the literature.

2.2 Performance Parameters of Desalination Plants

Efficiency of evaporative desalination plants is usually expressed through two different parameters: Performance Ratio PR (or Gain Output Ratio GOR, which is similar) and Recovery Ratio RR. Recovery Ratio is defined as:

$$RR = \frac{M_d}{M_{sw,in}} \tag{2.1}$$

where M_d s the mass flow rate of product freshwater and $M_{sw,in}$ is the mass flow rate of feed seawater entering the desalination plant (sum of freshwater, brine and cooling water). PR and GOR definitions are slightly different from paper to paper. Referring to Blessiotis et al. [60] :

- PR: quantity of distillate water produced by the plant for 2326 kJ of heat input;
- GOR: quantity of desalinated water produced (expressed in kg) per kg of heating steam at inlet of the plant.

El-Dessouky and Ettouney [17] define PR as the ratio between mass flow rate of product freshwater and heating steam entering the evaporator at the tube side. In addition to PR, GOR and RR, specific electric consumption of the plant and specific area are often

considered when talking about efficiency of a desalination plant, although specific electric consumption is mostly utilized for describing efficiency of membrane desalination systems.

Defining efficiency of an evaporative desalination plant in this way has two main disadvantages:

1. Having at least two different parameters to consider (PR and RR or GOR and RR), comparison among different technologies or between different design conditions of the same technology is not immediate;

2. *Quality* of energy required by the system is not considered; this can induce to misleading evaluations, especially when comparing thermal driven and electrical driven desalination processes. For example, utilization of waste heat would not be taken into account with the present evaluation, thus leading to efficiencies probably lower than other plant configurations which, however, utilize high quality energy sources.

Moreover, Chapter 7 will point out that variables involved in the calculation of PR and GOR are not always representative of the desalination plant under consideration.

Shazad et al. [52] and Lienhard et al. [25] highlight disadvantage (2) cited before and refer PR to primary energy. In particular, they modify PR's definition of equation 2.2 into the Universal Performance Ratio (UPR) of equation 2.3:

$$PR = \frac{2326[kJ/kg]}{3.6[kWh_{el}/m^3] + [kWh_{therm}/m^3] + [kWh_{ren}/m^3]} \tag{2.2}$$

$$UPR = \frac{2326[kJ/kg]}{3.6[kWh_{el}/m^3] \cdot CF_1 + [kWh_{therm}/m^3] \cdot CF_2 + [kWh_{ren}/m^3] \cdot CF_3} \tag{2.3}$$

where CF_1,CF_2 and CF_3 are conversion factors of the different forms of energy into primary energy. Results of UPR are then related to the thermodynamic limit for desalination of $0.78kWh/m^3$, corresponding to $PR = 828$.

In a similar way, a new efficiency definition for evaporative desalination systems is developed in this work starting from chemical process of salts dilution in water. The desalination process itself is energy demanding, implying to pass from a higher entropy

state (water with dissolved salts) to a minor entropy state (freshwater and salts). In fact, chemical reaction of salts dilution is exothermic. Considering, for simplicity, only NaCL as salt in seawater, chemical process of salt dilution in water is:

$$[H_2O] + [NaCl] \rightleftharpoons [H_2O + NaCl] + E \tag{2.4}$$

Where E is the energy released by the process of salts dissolution in water (comprehending heat of dissolution, osmotic pressure and boiling point elevation). It is experimentally evaluated that at least 0.75 kWh are needed to desalinate 1 m^3 of water with salinity of 40000 ppm [48]. In addition, energy linked to inefficiencies of the desalination plant has then to be supplied to the process. As a consequence, it makes sense to define the efficiency of an evaporative desalination process as :

$$\eta = \frac{D_{real}}{D_{max}} \tag{2.5}$$

where D_{real} is the real amount of fresh water obtained from 1 kWh of primary energy input and D_{max} is the ideal amount of fresh water obtained from a desalination process ($\frac{1m^3}{0.75kWh} = 1.33m^3/kWh$). Equation 2.5 defines an efficiency parameter that can be compared to an iso-entropic efficiency. In fact, as iso-entropic efficiencies compare real processes with the ideal ones, also η compares the real performance of a desalination plant, in terms of $[m^3/kWh]$, to the reversible chemical process. Moreover, this way of estimating the efficiency of a desalination plant allows to take into account *quality* of energy in input just by considering primary energy as input of the plant. Primary energy can easily be determined by multiplying different forms of input energy of the plant by the corresponding correction factor. Table 2.4 reports conversion factors of the main energy sources utilized in desalination plants.

Also with this new definition of efficiency, value of RR is essential to estimate cooling or dilution needs of a plant. Therefore, new parameter η only improves the evaluation of a desalination plant's efficiency, but does not solve the problem of having two different parameters to take into consideration. Exergy analysis and the delineation of an exergetic efficiency in Chapter 7 aim to solve also this problematic.

As a conclusion to the presentation of the different desalination technologies, Table 2.5 reports main performance parameters and temperature ranges of operation for

Form of Energy	Conversion Factor
Electrical Energy from the grid	2.18
Natural Gas	1.32
Renewable Energy	1.00
Waste heat	1.00
On-site co-generation	1.00

Table 2.4: Primary energy conversion factors used in this work for different energy sources [54]

the different plants. reported data are average values of those found in the literature. Even though each desalination plant has to follow precise constraints (limits on rejected brine salinity, purpose of the plant, performance requirements, etc.), data available on performance parameters, electrical energy required at inlet and temperature ranges of operation clearly suggest that different technologies are suitable for different conditions. In particular, main differences between thermal and membrane technologies are evident. On the one hand, thermal technologies work at temperatures that are much higher than the ones needed by membrane technologies. However, membrane technologies require a high level of chemical pretreatment in order to avoid scale formation and fouling. Moreover, from Table 2.5 it can be noted how the "classic" definition of efficiency of an energy plant does not take into account quality of input energy: most of membrane desalination plants are electrical driven, whilst thermal desalination plants often utilize waste heat. By analyzing only PR and RR (or GOR and RR) it is impossible to differentiate the two forms of energy utilized in the plants, which would therefore be compared in a misleading way. In the following chapters different evaporative desalination technologies are modeled and efficiencies are evaluated with the method just described.

	Unit	MSF	MED-TVC	MED-MVC	RO	ED
Temperature of operation	°C	90-120	55-70	70	Ambient temperature	Ambient temperature
Thermal Energy consumption	kWh/m^3	70-160	40-120			
Electrical Energy consumption	kWh/m^3	3-5	1.5-2.5	8-15 1.5-2.5 for brackish water	3-5 for seawater;	1.5-4
Level of pretreatment required	[-]	low	low	very low	high	medium
Quality of product freshwater	ppm	< 10	< 10	< 10	200-500	150-500
GOR	[-]	8-12	12-14			
Recovery Ratio	%	35-45	35-45	23-41 50-95 for brackish water	20-50 for seawater;	50-90

Table 2.5: Performances of main desalination technologies.[52, 25, 17]

Chapter 3

Multi-Stage Flash

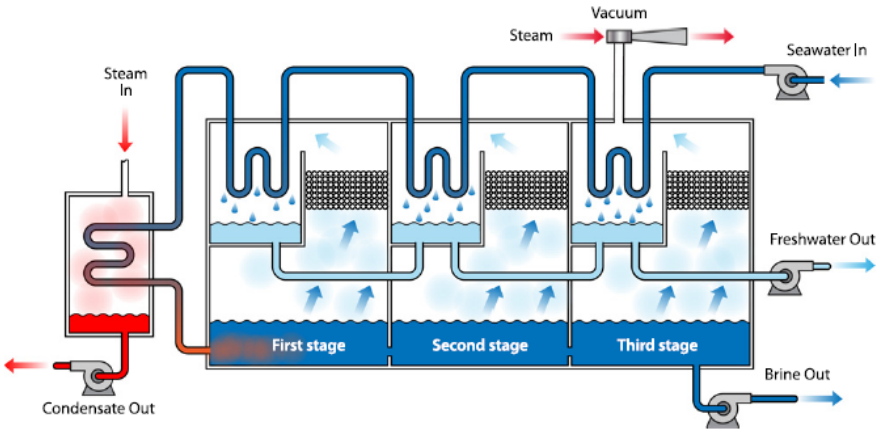

Figure 3.1: Multi Stage Flash desalination unit [58]

Multi Stage Flash desalination (MSF) was the dominant method in the 1960s. Even though nowadays MSF is mostly replaced by MED and RO, it still represents the main technology in some countries (North Africa and Middle East) [61]. MSF plants can be operated at high temperatures, high turbidity and high salinity of feed seawater; most of the times plants are integrated with power plants to produce both water and electricity. Different flow-configurations of MSF systems are possible; the most common are MSF once through (MSF-OT) and MSF with brine recirculation (MSF-BR). Even though MSF-BR are the state of the art for MSF plants, MSF-OT technology is a good starting point to analyze main operating features of this technology.

In this Chapter, MSF-OT process is described. A mathematical model is built and simulations are run under different conditions, comparing the results with data available

in the literature. Firstly, in a HEATSEP perspective [59], basic components of a MSF plant are analyzed, in order to figure out the simple working principle of this technology.

3.1 Basic Structure and Components

Multi Stage Flash technology differs from MED system in the way evaporation of seawater is driven. While for MED systems evaporation and condensation of distillate vapor are separate processes, in MSF desalination system they happen simultaneously in a flash process. Feed seawater itself absorbs the latent heat of condensation of the flashed vapor. Feed seawater has then to be heated in a brine heater in order to gain a temperature difference sufficient to evaporate inside the stage. Hence it is clear that for a MSF system the basic components, as shown in Figure 3.2, are:

- Brine heater;
- Flash stage.

A black-box representation of the system is given in Figure 3.3, valid for all plant configurations, which shows input and output streams of the plant and the internal path of each flow.

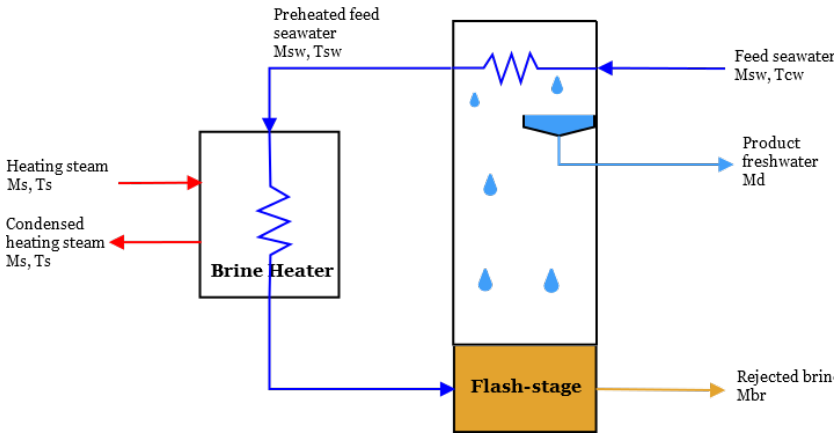

Figure 3.2: Basic components of a MSF desalination plant.

3.2 Process Description

Figure 3.1shows a simple schematic for a MSF-OT desalination plant. Heating steam from an external source ($M_{st,in}$) enters the brine heater in saturated vapor conditions.

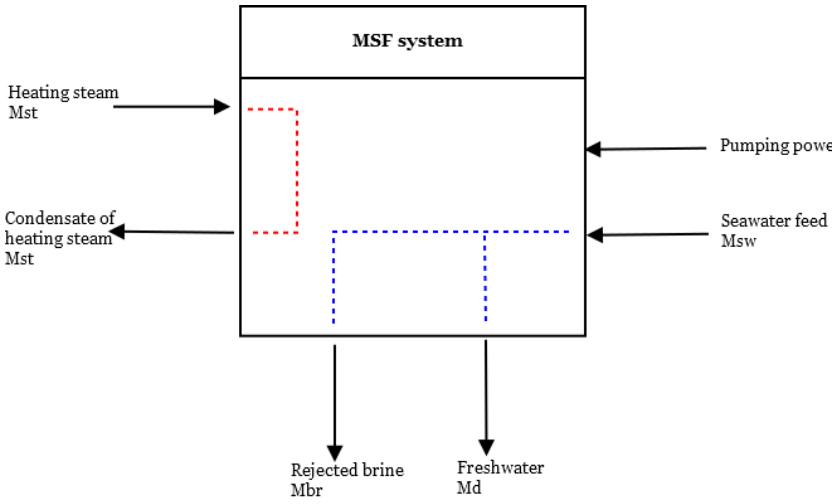

Figure 3.3: Black box representation of a MSF desalination plant.

Latent heat released by the condensing heating steam increases temperature of the feed seawater M_{feed} to the Top Brine Temperature $T_{br,0}$. Feed seawater then enters the first stage, kept at a temperature $T_{br,1}$ lower than $T_{br,0}$ by ΔT_{stage}. Temperature difference between each stage ΔT_{stage} is constant through all the stages. Pressure in each effect $p_{br,i}$ is the saturation pressure at the stage temperature $T_{br,i}$. Once entered in the first stage, a portion of the feed seawater, $M_{d,1}$, instantaneously evaporates and condenses in a flash process. The remaining part, $M_{br,2}$, flows into the second stage, a portion of it ($M_{d,2}$) flashes thanks to the pressure difference with the previous stage and the remaining part $M_{br,3}$ flows into the third stage. In each stage, heat necessary to evaporate the distillate mass flow rate $M_{d,i}$ is given by the mass flow rate of brine from the previous effect ($M_{br,(i-1)}$) decreasing its temperature by ΔT_{stage}. Latent heat of condensation of $M_{d,i}$ is transferred to feed seawater flowing at the tube side of the stage. Feed seawater is thus preheated when flowing from the last stage to the first one. In contrast with MED, no cooling water is needed in MSF processes. Moreover, as mentioned before, MSF plants can operate at higher Top Brine Temperatures and higher salinities of the feed seawater.

3.2.1 Mathematical Model

Mathematical model is built basing on mass and energy balances in each component. Figure 3.4shows the diagram used to develop the model. Assumptions made for mod-

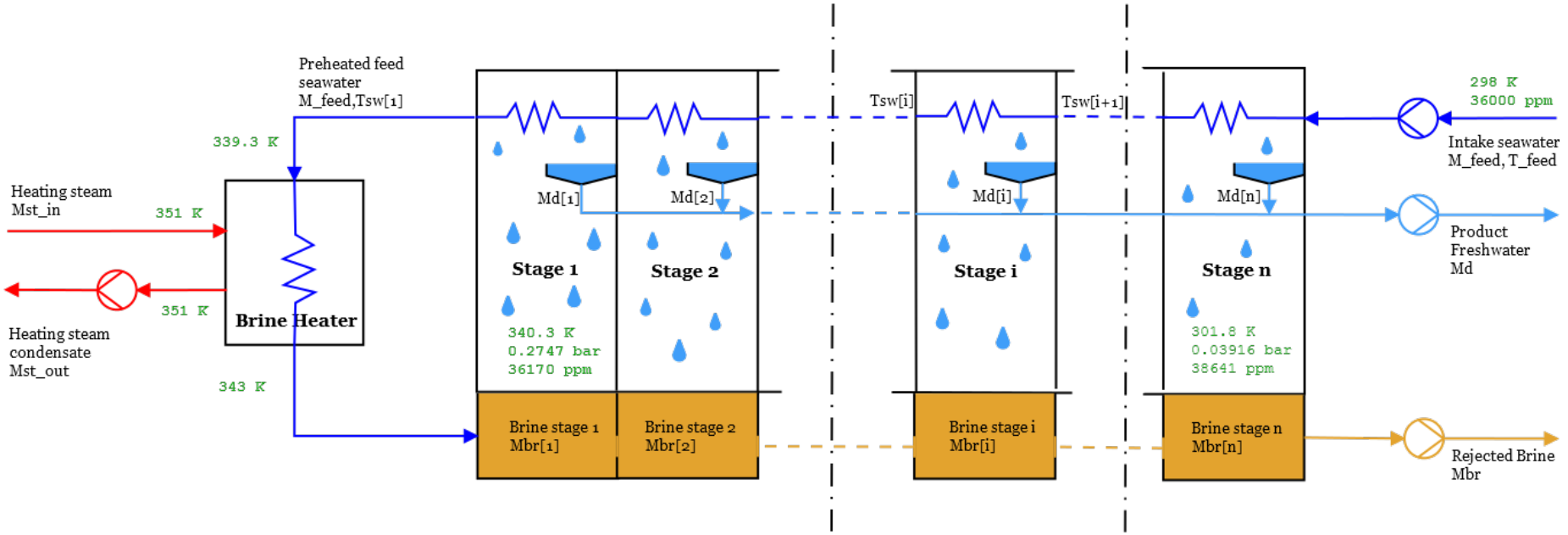

Figure 3.4: Schematic diagram of a Multi Stage Flash plant used for modeling. Reported values of temperature, pressure and salinity are referred to a plant with 15 stages.

eling are:

- Steady state operation;
- Salinity of the distillate product is considered null;
- Heating steam (M_s) enters the brine heater in saturation conditions, thus only releasing latent heat in the heat exchanger;

Mass balances in each component i are expressed as:

$$\sum_i M_{in,i} = \sum_i M_{out,i} \tag{3.1}$$

At the brine heater, preheated feed seawater coming from the tube side of the stages is heated up to the top brine temperature thanks to the latent heat released by the condensing heating steam. Energy balance of this process is:

$$M_s \cdot r_s = M_f \cdot c_p \cdot (TBT - T_{sw,1}) \tag{3.2}$$

Where M_s is the mass flow rate of heating steam, r_s is the latent heat of condensation of heating steam, c_p is the specific heat at constant pressure of feed seawater, TBT is the top brine temperature and $T_{sw,1}$ is the temperature of feed seawater at the end of the preheating process through the stages.

Temperature drop in each stage is equal to ΔT_{stage}. Therefore, temperature in each stage i is calculated as:

$$T_i = T_{i-1} - i \cdot \Delta T_{stage} \tag{3.3}$$

T_i is the same for brine and distillate at stage i. At each stage, at the tube side, feed seawater temperature is increased of ΔT_{stage}:

$$T_{sw,i} = T_{feed} + (n - (i-1)) \cdot \Delta T_{stage} \tag{3.4}$$

In equation 3.4, $T_{sw,i}$ is the feed seawater temperature at the end of the preheating process happening at stage i, n is the total number of stages and T_feed is the feed seawater temperature at plant inlet. Salt balances at each stage i are:

$$M_{br,i-1} \cdot C_{br,i-1} = M_{br,i} \cdot C_{br,i} \tag{3.5}$$

where $m_{br,i}$ is the mass flow rate of non evaporated brine at the stage i and $C_{br,i}$ is the salinity of brine at the stage i.

Flashing process in each stage can be modeled with equations 3.6 and 3.7, derived from the first law of thermodynamics applied to the single stage:

$$M_{br,i-1} \cdot c_p \cdot \Delta T_{stage} = M_{d,i} \cdot r_{d,i} \tag{3.6}$$

$$M_{d,i} \cdot r_{d,i} = M_{feed} \cdot c_p \cdot \Delta T_{stage} \tag{3.7}$$

Performance Ratio (PR) and Recovery Ratio (RR) are calculated as:

$$PR = \frac{M_d}{M_s} \tag{3.8}$$

$$RR = \frac{M_d}{M_{feed}} \tag{3.9}$$

where M_d is the amount of product freshwater, M_s is the heating steam flow rate and M_{feed} is the feed seawater flow rate.

The model is validated with experimental data available in the literature. As shown in Table 3.1, there is a good correspondence between the actual model results and values reported by El Dessouky and Ettouney [17].

3.3 Model Simulation

Variables that can be set as independent to solve the model are:

- C_f: salt concentration of feed seawater;
- T_{feed}: temperature of feed seawater;
- $p_{sw,in}$: pressure of feed seawater;
- $C_{b,max}$: maximum salinity of rejected brine;
- $T_{b,rej}$: temperature of the rejected brine;
- TBT: top brine temperature (brine temperature at the evaporator);
- $\eta_{is,p}$: iso-entropic efficiency of pumps;
- M_d: total amount of freshwater produced;
- n: number of stages;

	Unit	El-Dessouky and Ettouney Model [17]	Model
n		24	24
Feed Seawater Temperature	[K]	298	298
Salinity of feed seawater	[ppm]	42000	42000
Top Brine Temperature	[K]	379	379
Temperature drop per effect	[K]	2.75	2.75
PR		3.96	4.26
Distillate Product effect 1	[kg/s]	16.70	16.64
Distillate Product effect 2	[kg/s]	16.61	16.57
Distillate Product effect 3	[kg/s]	16.53	16.49
Distillate Product effect 4	[kg/s]	16.45	16.41
.		.	.
.		.	.
.		.	.
Distillate Product effect 15	[kg/s]	15.58	15.59
Distillate Product effect 16	[kg/s]	15.50	15.52
Distillate Product effect 17	[kg/s]	15.43	15.45
.		.	.
.		.	.
.		.	.
Distillate Product effect 23	[kg/s]	14.98	15.02
Distillate Product effect 24	[kg/s]	14.90	14.95

Table 3.1: Model validation: MSF model results compared to literature data [17]

- ΔT_{st}: temperature drop per stage;

- ΔT_{bh}: minimum temperature difference at the brine heater.

C_f, T_{feed}, ΔT_{bh} and $\eta_{is,p}$ are fixed from external conditions, depending on characteristics of feed seawater and machines (pumps) utilized in the plant. All the other variables listed before can be either fixed as independent or calculated by the model. Choice of independent variables depends on how the model is utilized. In contrast with MED plants, MSF plants do not have requirements on maximum top brine temperature to avoid hard scaling. Moreover, MSF plants can cope with high salinity of the feed seawater and slightly increase the salinity of the rejected brine. Therefore, it was decided not to fix $C_{b,max}$ as an independent variable. Pressure of feed seawater $p_{sw,in}$ is set at 6.5 bar, an indicative value high enough to win pressure losses in the system (as for the other plants previously described, pressure of feed seawater does not directly influence the system performance; obviously, higher values of $p_{sw,in}$ would require higher pumping power).

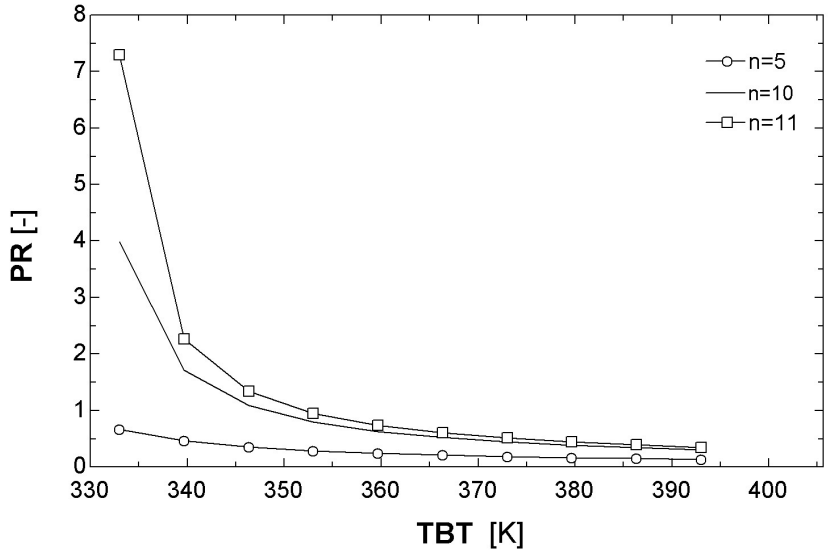

Figure 3.5: Performance Ratio of a MSF plant as a function of number of effects n and Top Brine Temperature TBT.

Number of effects (n) is set as independent variable in order to determine performance parameters in different design conditions. n strongly affects other parameters

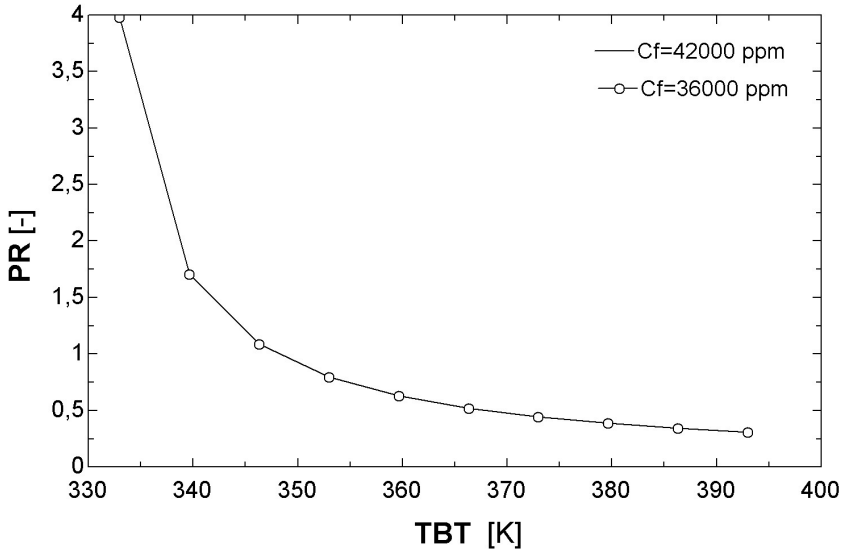

Figure 3.6: Performance Ratio of a MSF plant as a function of Top Brine Temperature and salinity of the feed seawater.

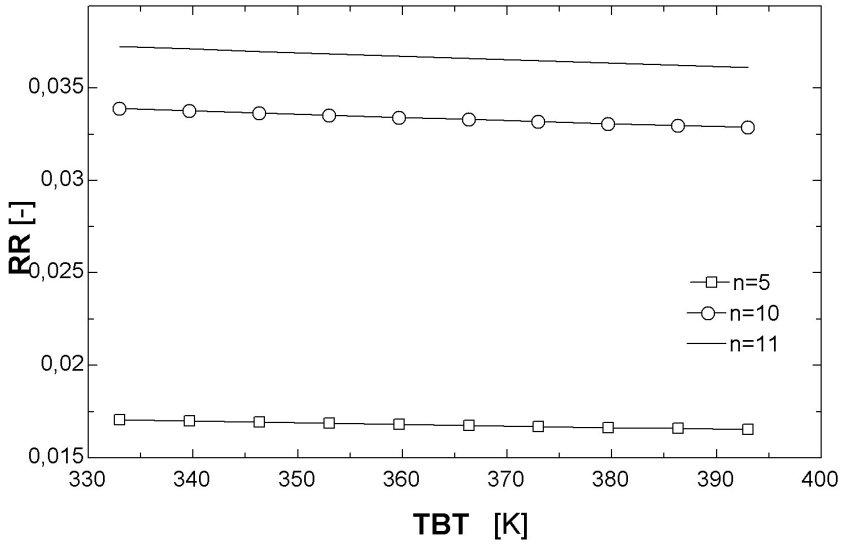

Figure 3.7: Recovery Ratio RR as function of number of effects n and Top Brine Temperature TBT of a MSF plant.

of the plant, thus representing a key point in the design of the entire process. Temperature of the rejected brine ($T_{b,rej}$) can be set as independent in order to cope with environmental constraints on plant output. Having set both n and $T_{b,rej}$, it is sufficient to set just one variable among top brine temperature TBT(or temperature of heating steam (T_s)) and temperature drop per effect (ΔT_{st}), because the other one will be calculated by the model. Adjusting value of minimum temperature difference at the brine heater (ΔT_{bh}), allows to control top brine temperature of the plant. Figures 3.5 to 3.7 illustrate main working parameters for the MSF plant described in Table 3.1. As mentioned before, seawater salinity does not affect performance of the plant. On the contrary, Performance ratio (PR) strongly depends on Top Brine temperature TBT and number of stages n. In particular, for a fixed number of stages n, higher TBT result in a drop of PR. This is due to the fact that increasing top brine temperature means increasing the temperature drop per stage, thus decreasing the thermal coupling at the heat exchangers (i.e. the efficiency of heat exchange itself). Number of stages affects PR at lower Top Brine Temperatures, while it is less influent for higher values of TBT. On the other hand, Recovery Ratio is slightly affected by different values of TBT, but strongly depends on number of stages.

Chapter 4

Multiple Effect Distillation

Multi-Effect Distillation (MED) represents one of the most widely used desalination techniques. It is based on the working principle of Single Effect Distillation, but it has better thermal performances due to the higher number of effects that allow to better utilize the heat provided from the external source.

In this Chapter, basic components of MED are described, working principle of MED is shown and mathematical model is built. Simulations are run in different conditions, and the model is validated with experimental results found in the literature.

4.1 Basic Structure and Components

Multiple Effect Distillation (MED) provides for the evaporation of salt water thanks to heat provided by an external heating source in order to form two streams: fresh water vapor and brine. Distillate water vapor has then to be condensed to obtain the desired output of the plant, fresh water. Basic components of a MED plant are therefore:

- Evaporator
- Condenser

Figure 4.1 reports the schematic diagram of a Single Effect Distillation system, that is the configuration of MED that provides only for the basic components. Intake seawater enters the condenser in the tube side. Here its temperature increases from T_{cw} to T_f thanks to the heat provided from the condensing fresh water vapor (M_d) coming from the evaporator. The increase in the feed seawater temperature is essential

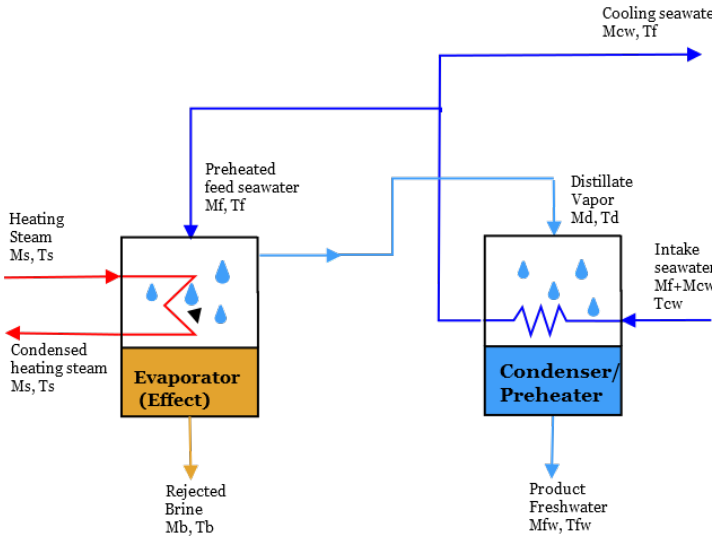

Figure 4.1: Schematic of Single Effect Evaporation, i.e. MED with only basic components.

to improve the thermal performance of the process. However, mass flow rate of feed seawater M_f alone is not enough to condense the freshwater vapor M_d produced in the effect. Therefore, intake seawater mass flow rate comprehends cooling water flow rate (M_{cw}), which is then rejected back to the sea after the condenser. The preheated feed seawater (M_f) is then sprayed into the evaporator. At the same time, steam from an external source (M_s) is introduced in the tube side of the evaporator. While flowing in the tubes bundle, the heating steam condenses, releasing its latent heat to the falling film of sprayed seawater. As a result, the feed seawater is heated up to the boiling temperature Tb, and a part of it (M_d) is able to evaporate. The generated vapor flows through a demister to remove the entrained brine droplets.

More in general, a MED desalination plant could be represented as a "black-box", which takes into account only flows entering and exiting from the whole system. Figure 4.2 thus represents all possible configurations of MED, highlighting also all the internal connections of the plant. Schematic representation of a MED system of Figure 4.2 is the starting point of complex analysis, such as exergy analysis performed in Chapter 7. Following sections will analyze more in detail MED plants, in which several evaporations (several "effects") improve the thermal performance of the whole system.

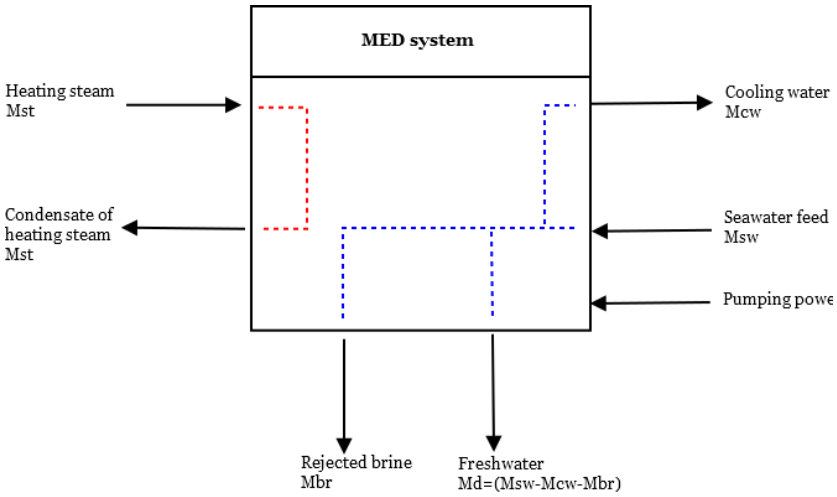

Figure 4.2: Black-box representation of a MED desalination system.

4.2 Process Description

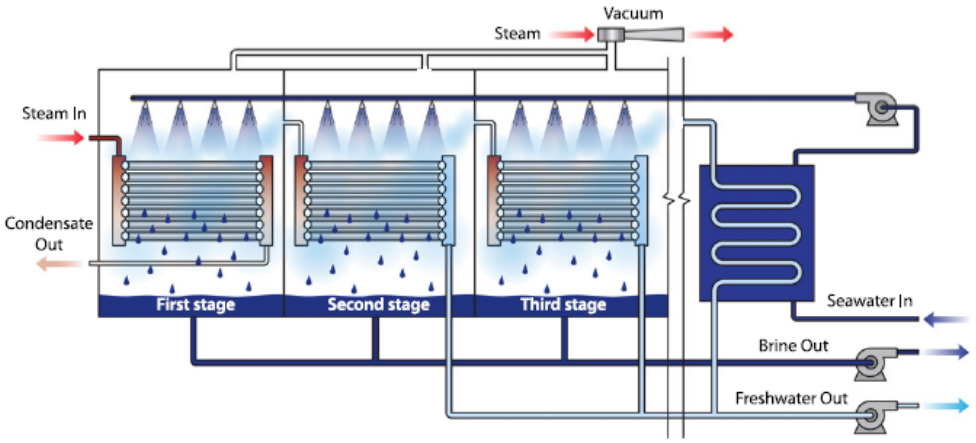

Figure 4.3: Multi Effect Distillation unit [58]

MED plant can have different flow configurations: forward feed, parallel feed and backward feed. The latter is not industrially utilized. In this Chapter, parallel feed configuration is analyzed. Figure 4.3 shows a schematic parallel feed diagram for a basic MED plant. Heating steam from an external source ($M_{st,in}$) enters the evaporator and condenses, releasing latent heat necessary to vaporize feed seawater in the effect ($M_{f,j}$). Brine ($M_{br,j}$) and distillate water vapor ($M_{d,j}$) are produced in the effect: brine is rejected and distillate vapor is transferred to the following effect, where it releases latent heat to the feed seawater entering that effect. This process is repeated in all the effects. Distillate vapor from the last effect ($M_{d,n}$) enters the condenser together with

the feed seawater ($M_{sw,in}$) and the cooling seawater (M_{cw}). Seawater, absorbing latent heat released from the distillate water vapor, increases its temperature from T_{cw} to $T_{sw,out}$. As for Single Effect Evaporation (SEE), increase of feed seawater temperature is essential to improve thermal performance of the system. The role of cooling water is to absorb the excess heat added to the system by the heating steam in the evaporator. [17]. After the condenser, the cooling water flow rate (M_{cw}) is dumped back to the sea or salt water source and the rest of the feed seawater (M_{feed}) is sent to the effects.

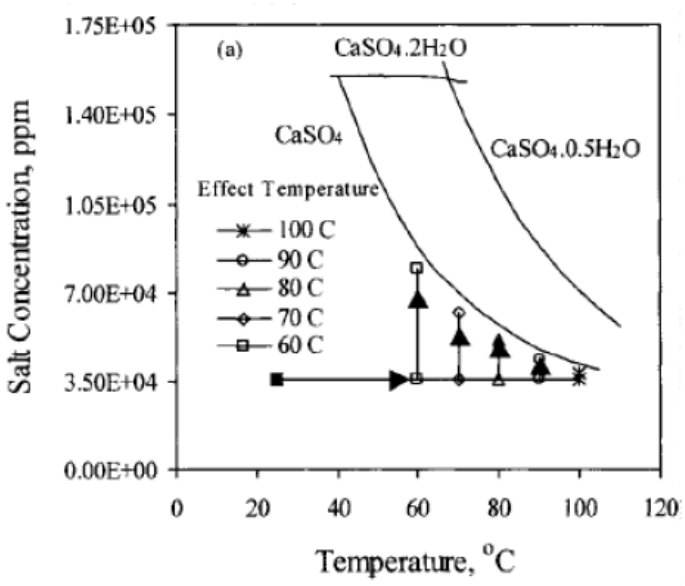

Figure 4.4: Calcium sulfate solubility and top brine temperature for parallel feed multiple effect evaporation. [17]

The nature of chemical additives to control scale formation dictates the magnitude of boiling temperature of the feed seawater in the evaporator. Temperature in each effect is decreasing when going from evaporator towards the condenser, according to the minimum temperature difference in each effect ΔT_{min} (see Figure 4.5). Thus, pressure decreases when going from evaporator (first effect) towards the condenser, being the effect's pressure the saturation pressure at the temperature in the effect.

Salinity of the brine stream leaving each effect is close to solubility limit of $CaSO_4$ at brine temperature of the fist effect (Figure 4.4).

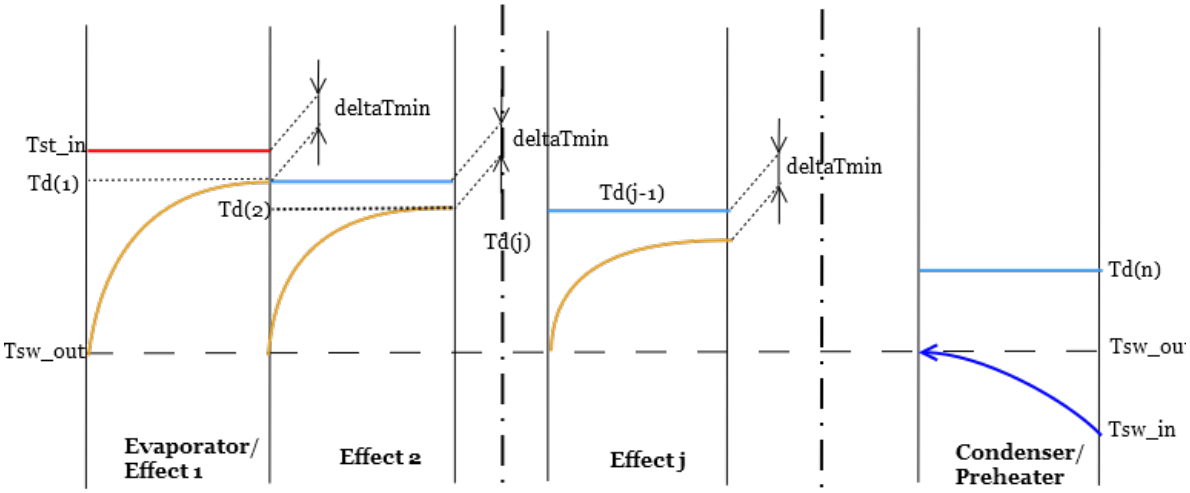

Figure 4.5: Thermal profiles of a Multi Effect Distillation plant used for modeling. Boiling Point Elevation is not represented in the scheme for simplicity.

4.3 Mathematical Model

Figure 4.6 shows the diagram used for developing the mathematical model of a basic MED plant. Assumptions made for modeling are:

- Steady state operation with negligible heat and pressure losses;
- Salt concentration in the distillate product is considered null;
- Heating steam ($M_{st,in}$) enters the evaporator as saturated vapor, thus it only releases latent heat in the heat exchanger;
- Distillate water vapor produced in evaporator and effects is in saturated vapor conditions;
- Seawater properties are calculated with correlations developed by Sharqawy et al. [54];
- Properties of pure water are calculated thanks equations of state incorporated in EES software;
- Salt concentration of the rejected brine at the evaporator is calculated from the correlation developed by El-Dessouky and Ettouney [17] (salt concentration is expressed in [ppm], temperature expressed in Celsius degrees):

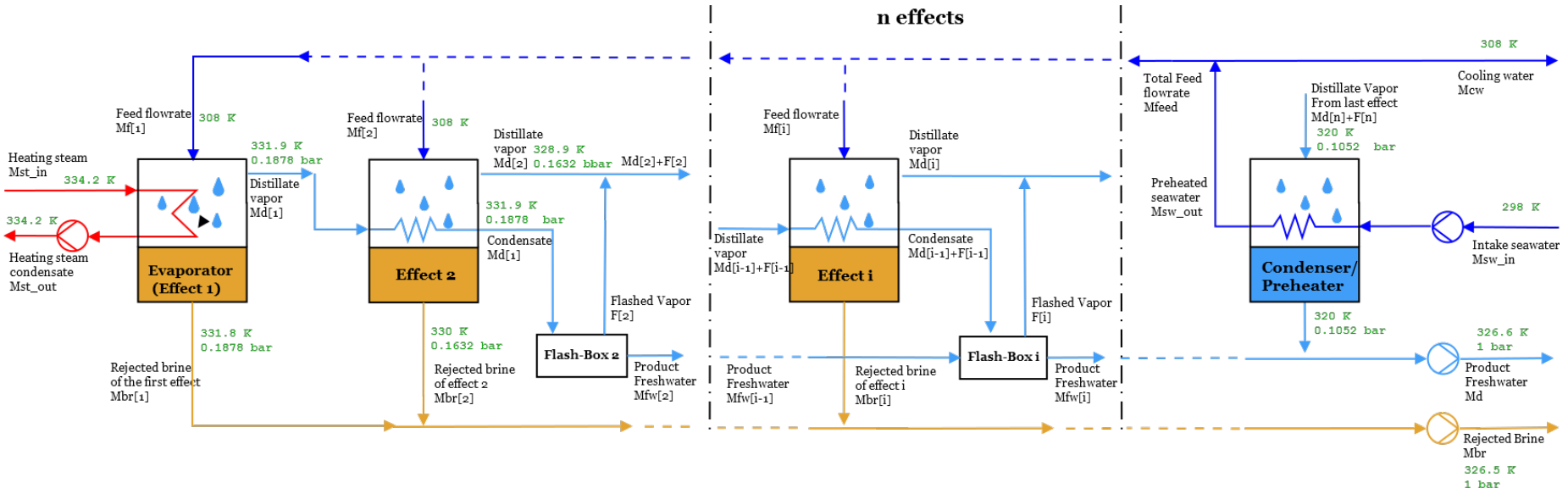

Figure 4.6: Schematic diagram of a Multi Effect Distillation plant used for modeling. Values of temperature and pressure reported refer to a MED plant with 5 effects.

$$C_b = 0.9 \cdot (457628.5 - 11304.11 \cdot T_b) + 107.5781 \cdot T_b^2 - 0.360747 \cdot T_b^3 \tag{4.1}$$

Mass balances in the i-th component are:

$$\sum_i M_{in;i} = \sum_i M_{out,i} \tag{4.2}$$

In the effects the salt balance is :

$$M_{feed} \cdot C_{feed} = M_{brine} \cdot C_{brine} + M_{distillate} \cdot C_{distillate} \tag{4.3}$$

where C is the salt concentration of the streams.

Energy balance for each effect is:

$$\begin{aligned} M_{distillate,(i-1)} \cdot r_{distillate,(i-1)} = M_{feed,(i)} \cdot cp_{feed,(i)} \cdot (T_{brine,(i)} - T_{seawater,out}) + \\ + M_{distillate,(i)} \cdot r_{distillate,(i)} \end{aligned} \tag{4.4}$$

Boiling point elevation was calculated as in equation 4.5 [17]

$$BPE_{(i)} = A_{(i)} \cdot S_{br,(i)} + B_{(i)} \cdot S_{br,(i)}^2 + C_{(i)} \cdot S_{br,(i)}^3 \tag{4.5}$$

with

$$\begin{aligned} A_{(i)} &= 8.325 \cdot 10^{-2} + 1.883 \cdot 10^{-4} \cdot T_{br,(i)} + 4.02 \cdot 10^{-6} \cdot T_{br,(i)}^2 \\ B_{(i)} &= -7.625 \cdot 10^{-4} + 9.02 \cdot 10^{-5} \cdot T_{br,(i)} - 5.2 \cdot 10^{-7} \cdot T_{br,(i)}^2 \\ C_{(i)} &= 1.522 \cdot 10^{-4} - 3 \cdot 10^{-6} \cdot T_{br,(i)} - 3 \cdot 10^{-8} \cdot T_{br,(i)}^2 \end{aligned} \tag{4.6}$$

where T is the temperature in Celsius degrees and $S_{br,(i)}$ is the salt weight percentage.

Model was validated with data available in the literature for real plants. Comparison between model and real data is reported in Table 4.1.

	Unit	Dessouky and Ettouney [17]	Model
n	[-]	4	4
Performance Ratio	[-]	3.7	3.6
Recovery Ratio	[-]	0.62	0.64
Heating steam temperature	[K]	333	333

Table 4.1: Model validation: MED model results compared to literature data [17]

4.4 Model Simulation

Variables that can be set as independent in order to solve the model are:

- C_f : salt concentration of the feed seawater;
- $C_{b,max}$: maximum salt concentration of the rejected brine;
- $\Delta\ T_{min}$: minimum temperature difference at each heat exchanger;
- $M_{fw,TOT}$: total amount of freshwater produced;
- $T_{st,in}$: temperature of heating steam from the external source;
- $M_{st,in}$: mass flow rate of heating steam;
- n : number of effects;
- $T_{sw,in}$: inlet temperature of feed seawater in the preheater/condenser;
- $p_{sw,in}$: pressure of feed seawater entering the preheater/condenser;
- ΔT_{cond}: temperature increase at the down condenser;
- $T_{sw,out}$: temperature of the preheated feed seawater.

C_f and $T_{sw,in}$, temperature and salinity of the salt water source (Table 2.1), result fixed from external conditions. The other variables mentioned before can be either fixed as independent or calculated. Choice of independent variables depends on how the model is utilized. For example, one possible choice could be to set $C_{b,max}$, $M_{fw,tot}$

and n as independent variables. This allows to analyze the plant performance with a fixed output ($M_{fw,tot}$ set at 1 kg/s for all calculations) and see which inputs are needed (temperature and mass flow rate of the heating steam, feed seawater and cooling water and temperature drop at each heat exchanger) in order to meet constraints on $C_{b,max}$. Pressure of feed seawater $p_{sw,in}$ is set at 6.5 bar (enough to win pressure losses in the system; this value does not directly influence the performance of the plant in terms of performance parameters calculated in the model, even though in real plants pressure losses play a key role in operation costs). The difference ($T_{sw,out}$-$T_{sw,in}$) is set at 5 K ([17]). The model is run for different values of heating steam temperature $T_{st,in}$ for a plant with a certain number of effects, calculating the minimum temperature drop at each heat exchanger (ΔT_{min}). Higher heating steam temperature means higher ΔT_{min} and thus lower costs, but also lower performance of the system. On the other hand, low temperatures of the heating steam require lower ΔT_{min} at the heat exchangers (considering that constraints on $C_{b,max}$ remain the same), resulting in higher costs and higher performances of the process. More detailed analysis on MED performance can be done referring to exergetic efficiency instead of Performance Ratio and Recovery ratio (Chapter 7).

With the same model it is also possible to analyze systems with different number of effects, thus evaluating how n affects the overall system efficiency. Figures 4.7 to 4.11 reports system performance parameters obtained in the model as functions of heating steam temperature at inlet of the evaporator, number of effects and feed seawater salinity.

As mentioned before, $C_{b,max}$ can be chosen as independent variable because it is normally constrained to environmental limits to avoid heavy impacts on ecosystems. Being the concentration of salts in the rejected brine a function of brine temperature (see Figure 4.4), value of $C_{b,max}$ also defines the brine temperature at the last effect $T_{br,n}$ and hence in all the other effects. As a result, limitations on $C_{b,max}$ point out temperature ranges of operation for the plant. As an alternative, Top Brine Temperature can be fixed as independent variable. In this case, however, it will be necessary to check whether value $C_{b,max}$ meets environmental constraints or not.

Figures 4.7 and 4.8 show that Performance Ratio is decreasing at increasing top Brine Temperature. This is due to the fact that at higher TBT lower salinity can be

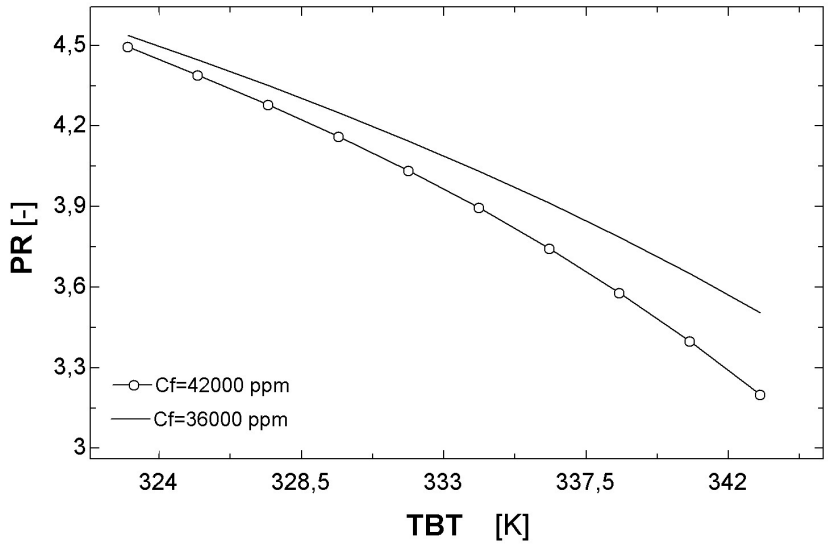

Figure 4.7: Performance Ratio PR of a MED plant as a function of feed seawater salinity C_f and Top Brine Temperature TBT.

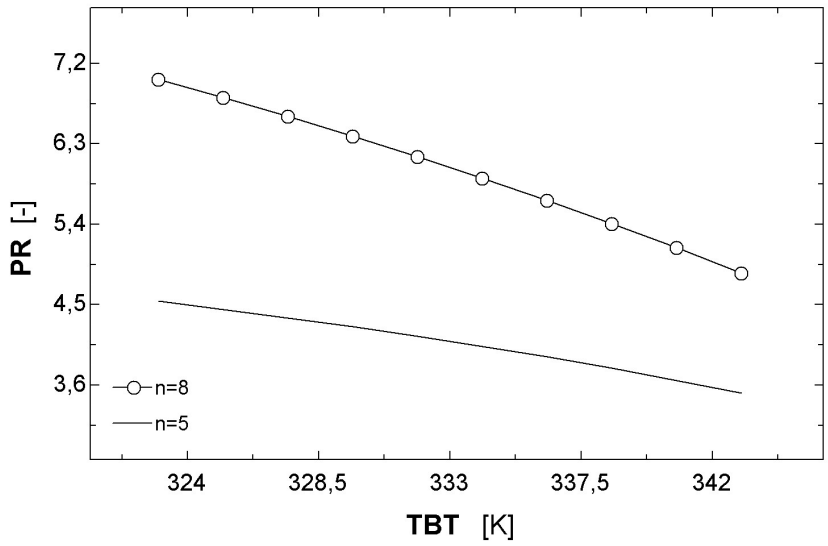

Figure 4.8: Performance Ratio PR of a MED plant as a function of number of effects n and Top Brine Temperature TBT. Feed salinity of seawater is set at 36000 ppm.

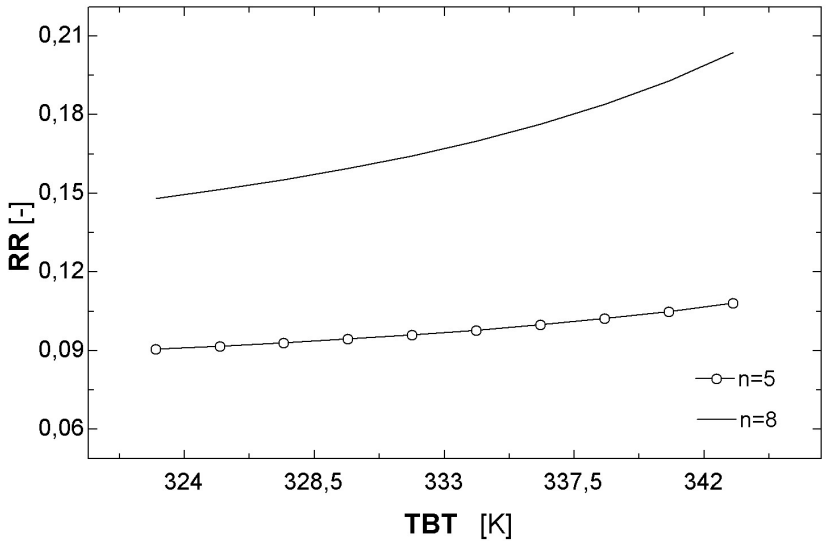

Figure 4.9: Recovery Ratio RR of a MED plant as a function of number of effects n and Top Brine Temperature TBT.

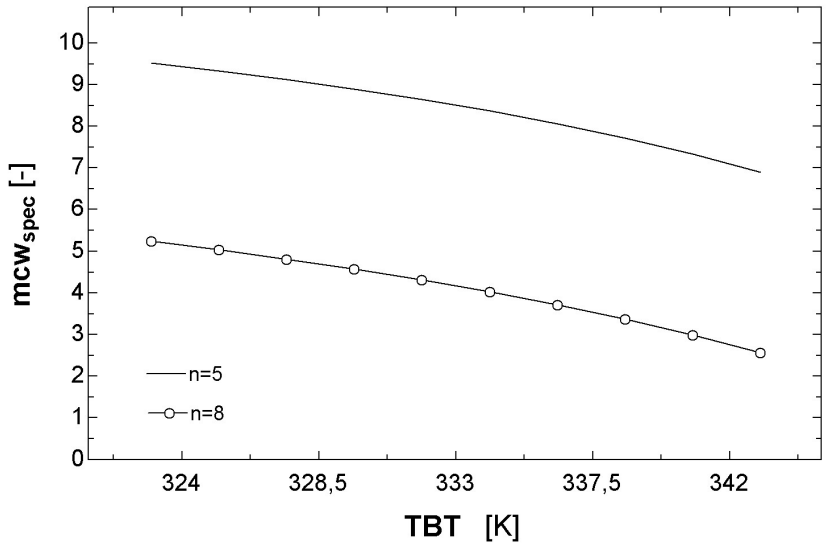

Figure 4.10: Specific cooling water flow rate mcw_{spec} of a MED plant as a function of number of effects n and Top Brine Temperature TBT.

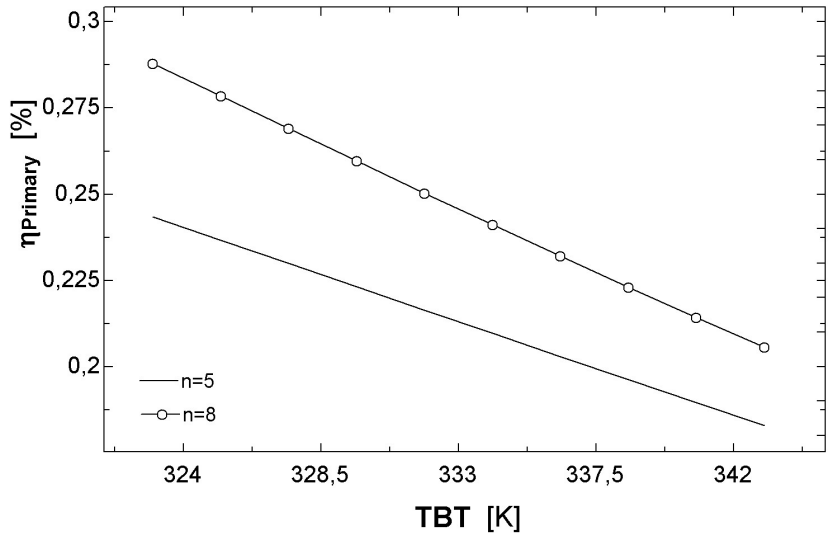

Figure 4.11: Efficiency parameter $\eta_{Primary}$ defined in Chapter 2 represented as a function of number of effects n and Top Brine Temperature.

reached at the evaporator to avoid precipitation of $CaSO_4$. As a consequence, higher amount of brine will be produced per effect and hence higher amount of feed seawater will be supplied to each effect (amount of distilled vapor is fixed). In order to evaporate higher amounts of feed seawater, higher amount of heating steam is required at the evaporator, thus decreasing PR.

In addition, PR also decreases for higher salinities of feed seawater (Figure 4.7) and for lower number of effects (Figure 4.8). On the one hand, higher salinities of feed seawater would increase the amount of necessary feed seawater and hence the mass flow rate of heating steam that must be supplied at the evaporator (see salt mass balance in eq. 4.3). Also, it should be noted that the influence of feed seawater salinity is higher at higher temperatures (and so at lower values of $C_{b,max}$). On the other hand, increasing number of effects will augment internal reutilization of heat, thus decreasing the need of heat supplied at the evaporator.

Figure 4.9 depicts Recovery Ratio RR as a function of Top Brine Temperature TBT and number of effects n. Increasing number of effects results in better heat reutilization in the plant, thus improving its performance. In contrast with PR, RR increases for increasing TBT. This is due to the decreasing mass flow rate (Figure 4.10) that has to

be supplied to the plant at higher temperatures.

Finally, trend of efficiency parameter η based on primary energy is reported in Figure 4.11. In this case, η has te same tendency of PR: increasing at higher number of effects,decreasing at higher temperatures.

Chapter 5

Multiple Effect Distillation with Thermal Vapor Compression

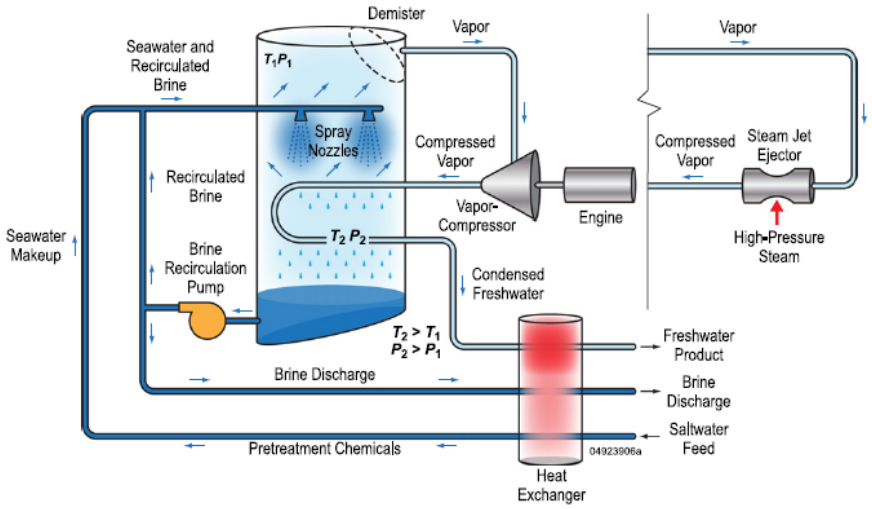

Figure 5.1: Multi Effect Distillation unit with Vapor Compression [58]

Desalination techniques based on vapor compression rely on heat generated by the compression of water vapor produced by the desalination plant itself to evaporate salt water in the evaporator. Two methods are available: thermal vapor compression (TVC) and mechanical vapor compression (MVC). Basic components of MVC and TVC, in a HEATSEP perspective, are exactly the same if the motive steam at inlet of the steam ejector in TVC is water vapor. Otherwise there will be some differences in the basic configuration. In this Chapter, MED-TVC system will be analyzed, while in Chapter 6 MED-MVC is described.

The advantage of MED-TVC, when compared to classical MED systems (Chapter 4), is the possibility to re-utilize part (or the whole) of the distillate vapor produced by the plant as heating steam at the evaporator. When disposing of a high pressure steam flow it is possible, through a steam ejector, to compress a portion (or the whole) of the mass flow rate of the distillate vapor exiting the evaporator. This leads to an internal *regeneration*, thus decreasing the need of heat from an external source. For MED-TVC systems, two situations must be considered, depending on the quality/nature of the motive steam at inlet of the steam ejector. In the following section, basic components of MED-TVC plants are described in the two possible situations.

5.1 Basic Structure and Components

As just mentioned, basic components of a MED-TVC desalination plant depend on the quality of motive steam entering the steam jet ejector. The two possible situations are:

1. Motive steam is freshwater vapor;

2. Motive steam is not freshwater vapor, but a different substance that will pollute the distillate vapor entrained by the ejector.

In the first case, basic components are:

- Evaporator/Condenser;

- Thermal Compressor (steam ejector).

Under these conditions, the whole mass flow rate of distillate vapor produced at the evaporator will be entrained by the steam ejector, where it will mix wit the motive steam. In contrast with simple MED plants, there is no need of condenser, since the mixture of distillate vapor and motive steam -once compressed- is directly condensed at the tube side of the evaporator, producing freshwater.

For the second case, i.e. "polluting motive steam", basic components are:

- Evaporator;

- Thermal Compressor (steam ejector);

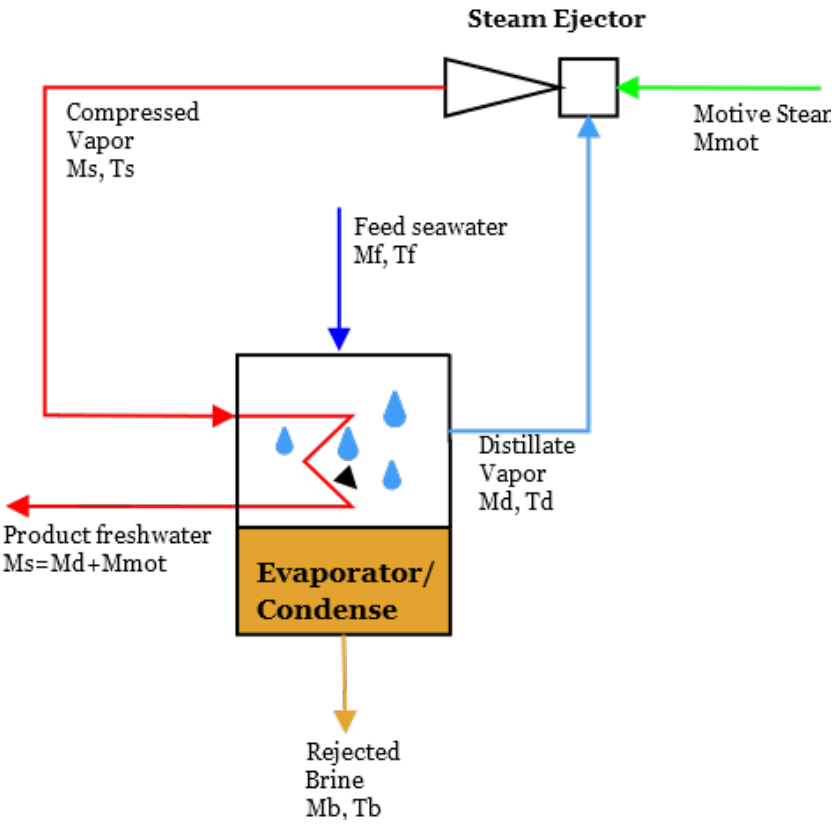

Figure 5.2: MED-TVC plant with potable motive steam entering the steam ejector provided only with basic components.

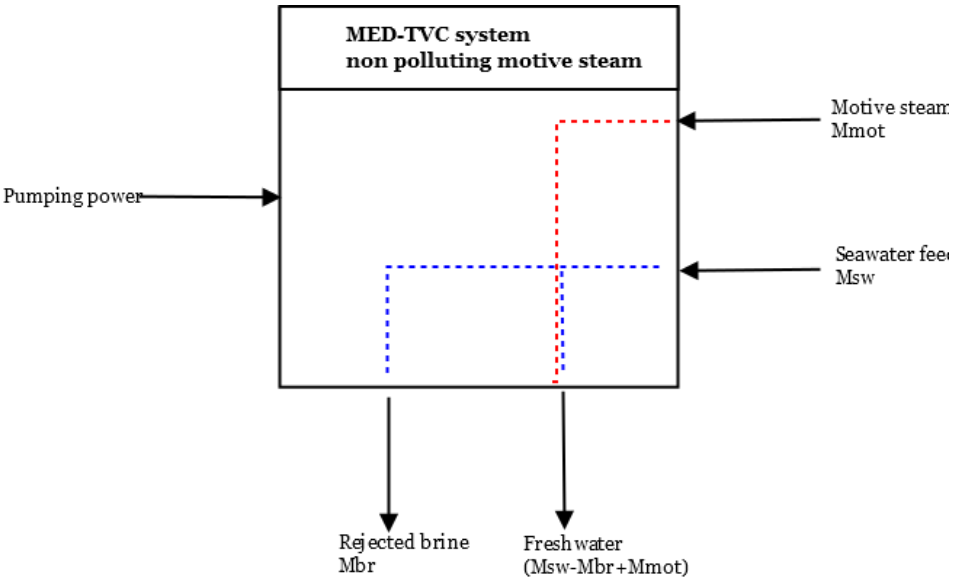

Figure 5.3: Black-box representation of MED-TVC systems in case of potable motive steam.

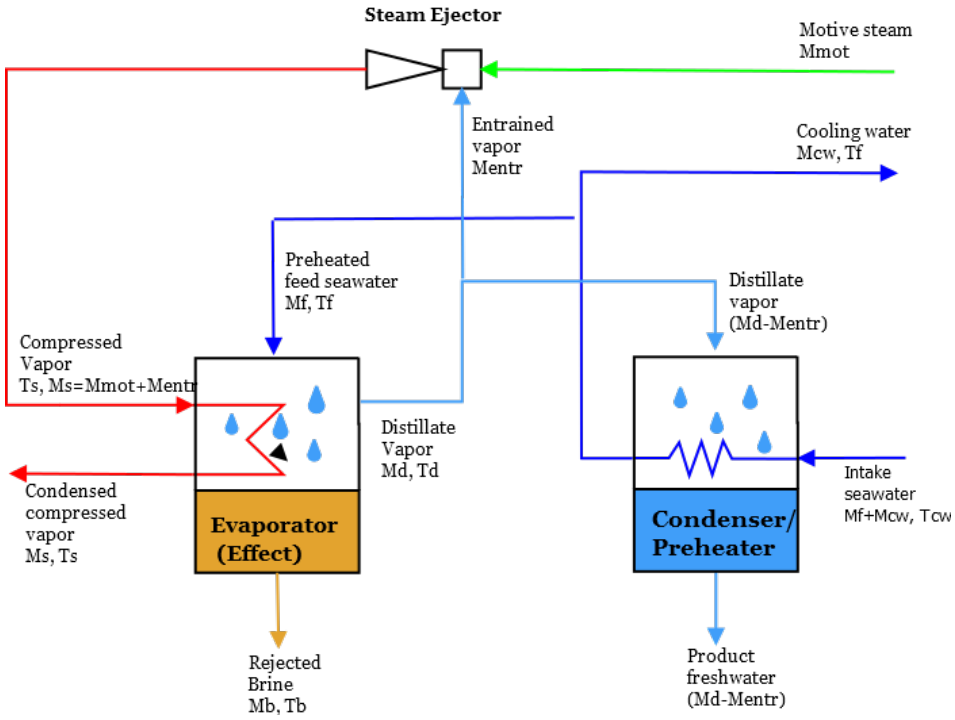

Figure 5.4: Schematic diagram of basic components of MED-TVC system with non-potable motive steam entering the steam ejector.

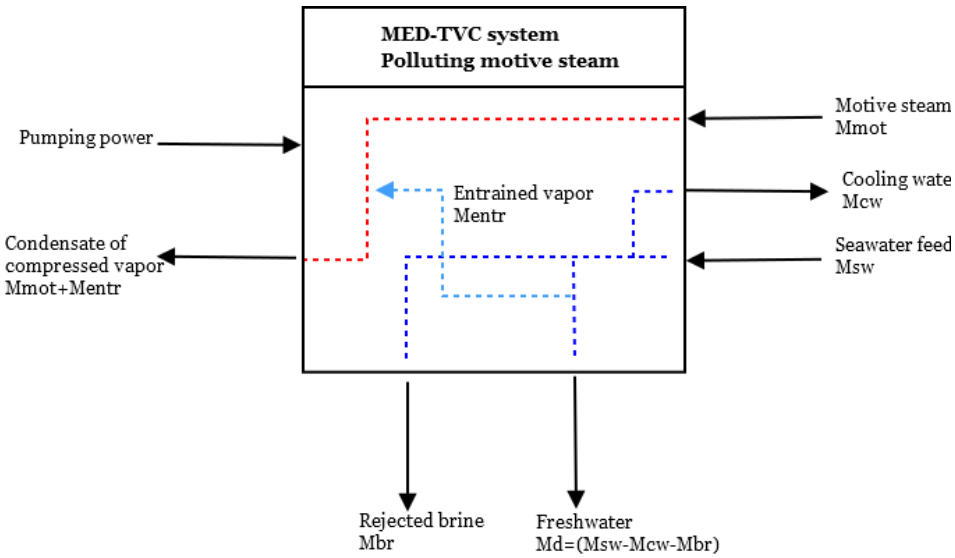

Figure 5.5: Black-box representation of MED-TVC systems in case of non potable motive steam.

- Condenser.

In fact, if the motive steam entering the steam ejector is not water, it will pollute the mass flow rate of distillate vapor entrained by the steam ejector. Therefore, the mixture of motive steam and entrained distillate vapor -once condensed at the evaporator- will not be freshwater. In this case, only a portion (M_{entr})of distillate vapor produced at the evaporator (M_d)will be sent to the steam ejector (this is a decision variable that depends on the characteristics of the steam ejector). The remaining part ($M_d - M_{entr}$) has to be condensed in order to produce freshwater, and thus a condenser is needed. As seen for classical MED, cooling water flow rate is needed at the condenser. Figures 5.2 and 5.4 show the schematic diagrams of MED-TVC (more precisely, single effect distillation unit with thermal vapor compression) systems with only basic components in both situations (1) and (2). Adding effects to these configurations will lead to better utilization of heat provided at the evaporator, improving thermal performances of the whole plant. Moreover, it is possible to increase the efficiency of the system by preheating the feed seawater in a heat recovery unit. In general, all configurations can be represented as black boxes as in Figures 5.3 and 5.5, which also report global internal paths of the different streams.

As for MED, there are different configurations of MED-TVC plants (forward feed, parallel feed and backward feed). Each arrangement differs from the other in the flow direction of heating steam and evaporating brine. In this section, parallel feed configuration is described and mathematical model is built for this arrangement.

5.2 Process Description

Figure 5.6 shows the plant flow-sheet for a MED-TVC desalination system with parallel flow configuration. Motive steam (considered as potentially pollluting in order to model the most general situation) from an external source (M_{mot}) enters the steam jet ejector at a pressure p_{mot} (usual values of p_{mot} are in the range of 15-45 bar). The thermal vapor compressor entrains and compresses a portion (M_{entr}) of the vapor generated in the last effect of the plant ($M_{d,n}$). Compressed steam $M_{st,in}$ (considered in saturated vapor conditions) flows into the tube side of the evaporator (that is also the first effect) and condenses. Latent heat released by $M_{st,in}$ is transferred to the feed seawater entering

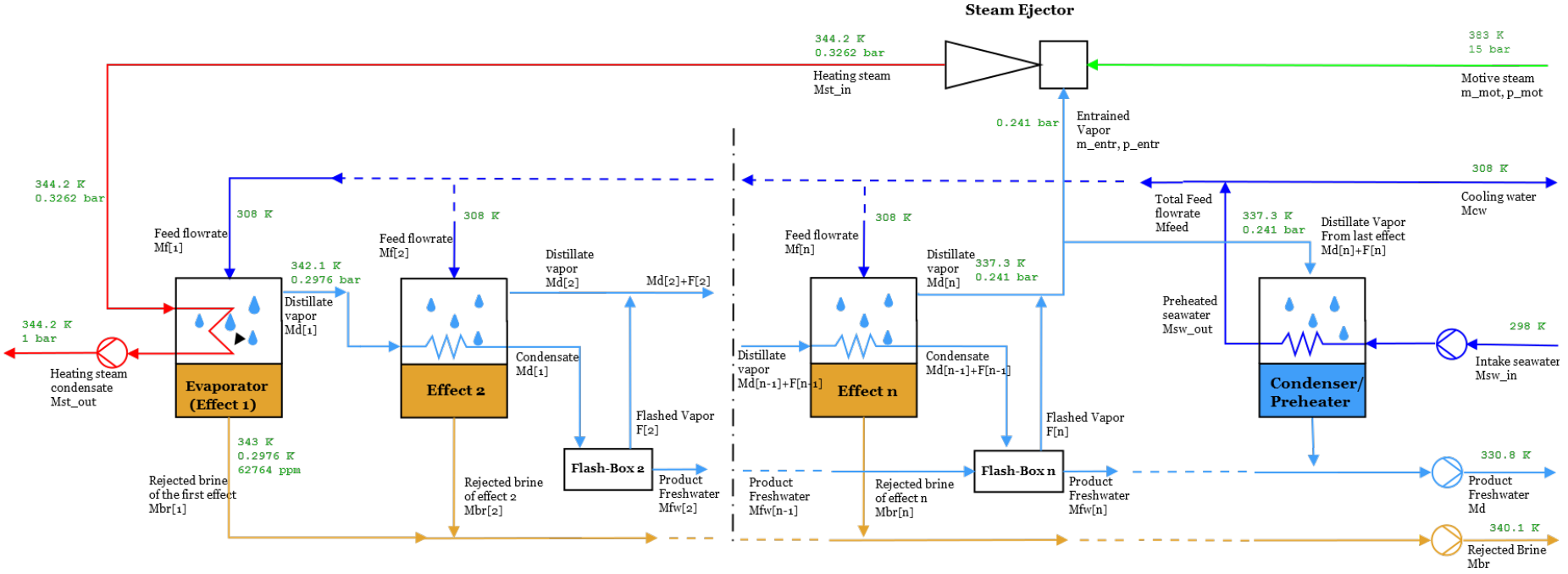

Figure 5.6: Schematic diagram of a Multi Effect Distillation plant with Thermal Vapor Compression used for modeling. Values of pressure and temperature reported on the diagram refer to a 5 effects plant.

the first effect ($M_{f,1}$) , vaporizing it. Brine ($M_{br,1}$) and distillate water vapor ($M_{d,1}$) are produced in the effect. Brine salinity in the first effect is approximately the solubility limit of $CaSO_4$ at that temperature (see Figure 4.4).Distillate water vapor then flows into the tube side of the following effect, acting as heating steam for that effect. This process is repeated till the last effect. As mentioned before, a portion of the distillate water vapor produced in the last effect is entrained by the steam jet ejector. The remaining part ($M_{d,n} - M_{entr}$) flows into the down condenser and condenses, releasing its latent heat necessary to preheat the entering feed seawater (M_{sw}). As for MED, also with TVC cooling water (M_{cw}) is needed in order to remove the excess heat added to the system in the evaporator. After the condenser, cooling water is dumped back to the salt water source, and the remaining feed seawater (M_{feed}) is sent to the effects.

Thermal profiles are the same of MED (see Figure 4.5 in Chapter 4). Also in this case, in each effect vapor is generated under saturation conditions, thus pressure is decreasing when proceeding from first to last effect.

5.3 Mathematical Model

Assumptions made for modeling are the same made for MED system (see paragraph 4). MED-TVC's mathematical model differs from the MED's one only for the equations regarding the Thermal Vapour Compressor. Therefore, only equations referred to thermal compression device will be reported in this section. Figure 5.7 reports variables involved in the steam ejector.

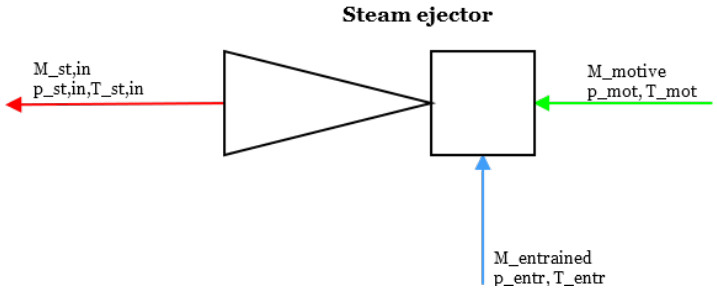

Figure 5.7: Schematic diagram of variables involved in steam ejector in a MED-TVC plant.

Mass balance at the steam jet ejector is:

	Unit	Rabigh Plant [3]	Model	Tripoli Plant [5]	Model
n	[K]	6	6	4	4
$p_{mot}[bar]$	[bar]	17	17	23	23
Top Brine Temperature	[K]	343	343	333.1	333.1
Minimum Brine Temperature	[K]	322.4	322.5	318.4	318.4
Temperature drop per effect	[K]	4.1	4.1	4.9	4.9
Feed Seawater Temperature	[K]	305	305	314.5	314.5
Seawater Temperature	[K]	296	296	304.5	304.5
Mass flow-rate of Motive steam	[kg/s]	7.06	7.06	8.8	8.8
Entrainment Ratio	[-]	NA	1.1	1.14	1.27
Expansion Ratio	[-]	NA	153.2	NA	258.1
Compression Ratio	[K]	NA	3.32	NA	2.79
Distillate Flow Rate	[kg/s]	57.9	58.04	57.8	57.7
GOR	[-]	8.2	8.2	6.51	6.56

Table 5.1: Model validation: MED-TVC model results compared to literature data [3, 5]

$$M_{st,in} = M_{mot} + M_{entrained} \tag{5.1}$$

Expansion Ratio (ER) and Compression Ratio (CR) are defined as:

$$ER = \frac{p_{mot}}{p_{entr}} \tag{5.2}$$

$$CR = \frac{p_{st,in}}{p_{entr}} \tag{5.3}$$

Both ER and CR are key values to calculate the entrainment ratio R_{entr} of the steam jet ejector:

$$R_{entr} = \frac{m_{mot}}{m_{entr}} \tag{5.4}$$

To calculate the entrainment ratio is the most important part in modeling the MED-TVC systems. An optimum value of this ratio will improve system performance by reducing the amount of motive steam [2]. In this work, entrainment ratio is calculated using the semi-empirical model presented by El-Dessouky and Ettouney [17]. According to semi-empirical model, entrainment ratio can be calculated as follow:

$$R_{entr} = 0.235 \cdot \frac{(p_{st,in})^{1.19}}{(p_{entr})^{1.04}} \cdot ER^{1.05} \tag{5.5}$$

Semi-empirical model is not the only possible way to evaluate entrainment ratio, but it is the simpler one. However, semi-empirical model is only applicable when motive stream is steam and entrained stream is water vapor [17, 2].

5.4 Model Simulation

Variables that can be set as independent to solve the model are:

- C_f: salt concentration of the feed salt water;
- $C_{b,max}$: maximum salinity of the rejected brine at the last effect;
- ΔT_{min}: minimum temperature difference at each heat exchanger;

- $M_{fw,tot}$: total amount of freshwater produced;
- n: number of effects;
- TBT: top brine temperature (brine temperature at the evaporator);
- $M_{st,in}$: mass flow rate of heating steam;
- T_{cw}: temperature of feed salt water entering the down condenser;
- $p_{sw,in}$: pressure of feed salt water;
- $T_{sw,out}$: temperature of feed salt water exiting the down condenser;
- p_{mot}: pressure of the motive steam;
- m_{mot}: mass flow rate of the motive steam;
- CR: compression ratio of the jet ejector;
- ER: expansion ratio of the jet ejector.

Considerations on the choice of independent variables and values assigned to them are the same made for MED systems. In addition, one parameter among the one defining the performance (or two defining the input) of the steam jet ejector has to be set as independent.

The model was validated basing on experimental data available in the literature. Table 5.1 reports model predictions against industrial data available in the literature.

As illustrated in Figures 5.8 to 5.12, interactions between the different variables in MED-TVC are essentially the same of MED (see Chapter 4 for precise considerations on different variables and model simulation). In fact, the main advantages of MED-TVC when compared to classical MED and MED-MVC are:

- the possibility to utilize high pressure steam at inlet of the desalination plant but in small quantities;
- better thermal performance due to internal *regeneration*;
- utilization of low quality energy compared to electrical energy required by mechanical compressor in MED-MVC systems.

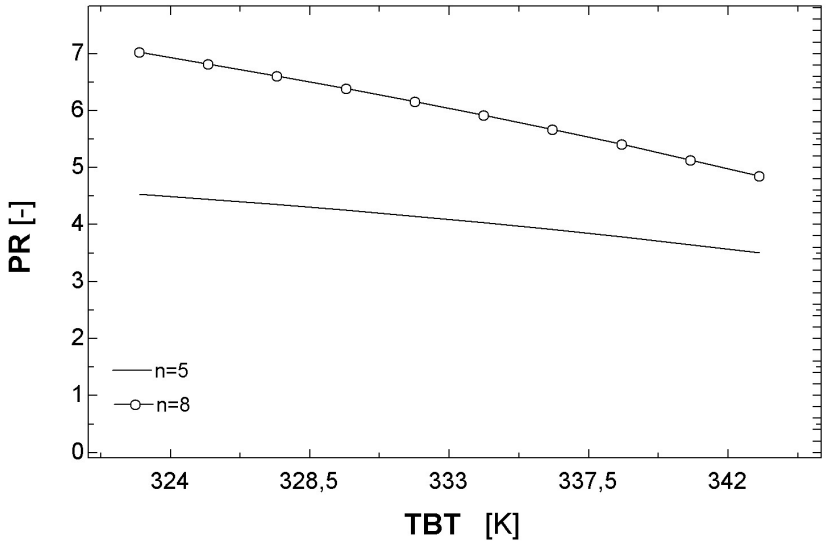

Figure 5.8: Performance ratio of a MED-TVC plant as function of top brine temperature TBT and number of effects n.

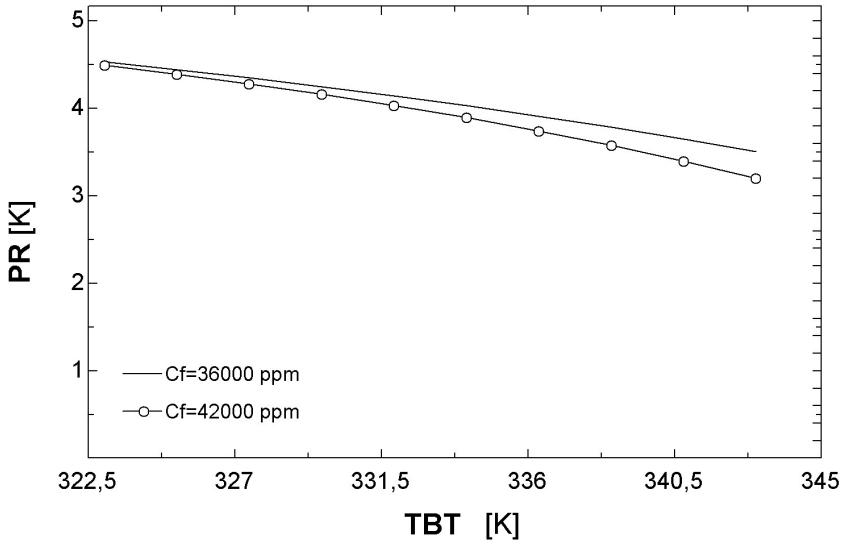

Figure 5.9: Performance Ratio of a MED-TVC plant as a function of feed seawater salinity C_f and top brine temperature TBT.

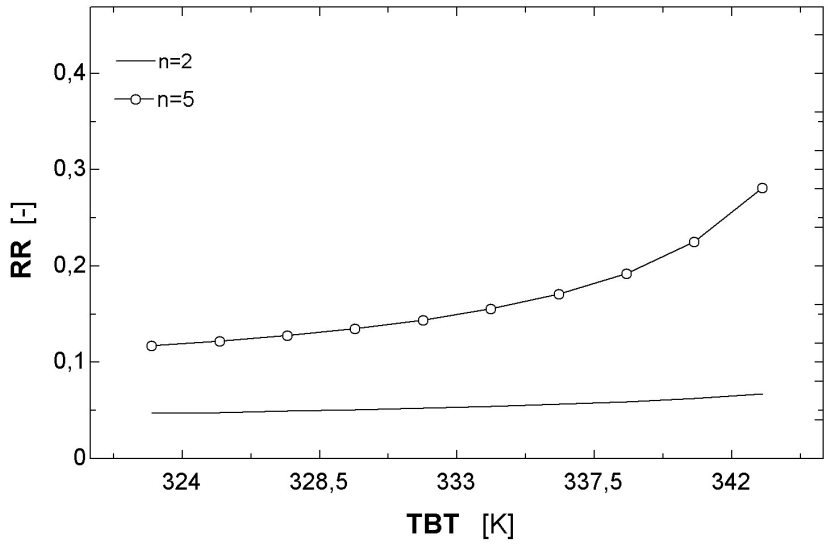

Figure 5.10: Recovery Ratio RR of a MED-TVC plant as a function of top brine temperature TBT and number of effects n.

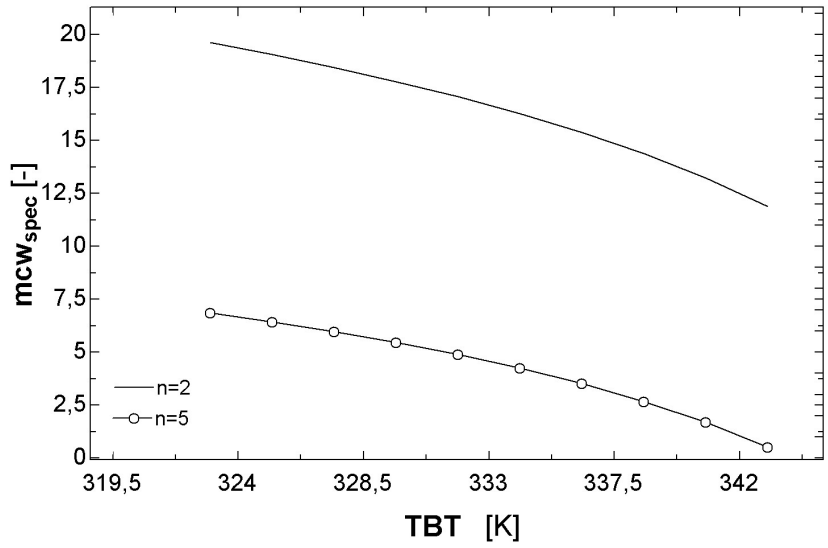

Figure 5.11: Specific mass flow rate of cooling water Mcw_{spec} of a MED-TVC plant as a function of top brine temperature TBT and number of effects n.

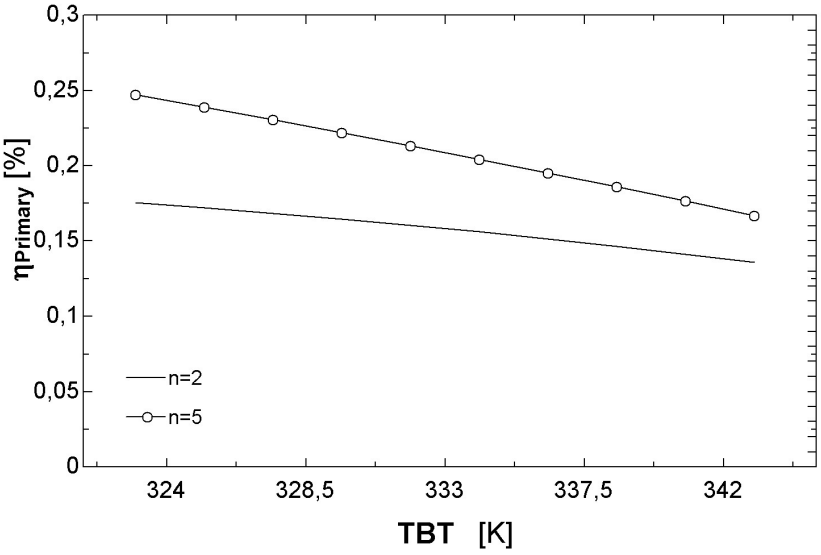

Figure 5.12: Efficiency parameter based on Primary energy as defined in Chapter 2 of a MED-TVC plant as a function of top brine temperature TBT and number of effects n.

Analyzing the plant performance with the new efficiency parameter η defined in Chapter 2 thus results more effective than with PR. Actually, trend of η (Figure 5.12) and PR (Figure 5.8) as functions of TBT and n are essentially the same. However, evaluating performance of MED-TVC system with η allows comparisons with the other technologies without the risk of misleading results. Even better results could be obtained by an exergy analysis as illustrated in Chapter 7.

Chapter 6

Multiple Effect Distillation with Mechanical Vapor Compression

As mentioned in Chapter 5, MED-MVC systems rely on heat generated by the compression of water vapor produced in the last effect of the plant. In this case, water vapor produced in the last effect is compressed by a mechanical compressor and thus the input energy to the system is the electrical energy at the inlet of the compressor. Conceptually, it is equivalent to the MED-TVC system with non polluting motive steam at the steam ejector, having electrical energy at input instead of motive steam stream. In this Chapter, basic structure of MED-MVC plants is illustrated along with the description of the process. Thereafter, mathematical model is built and validated with experimental data found in the literature, reporting simulation results for different design conditions.

6.1 Basic Structure and Components

Basic configuration of MED-MVC system is not affected by quality of energy at inlet as it was for MED-TVC. Since input is now electrical energy, the whole amount of distillate vapor produced at the evaporator is sent to the mechanical compressor. Basic components necessary to perform basic transformations in the systems thus are:

- Evaporator/Condenser (effect);
- Mechanical Compressor.

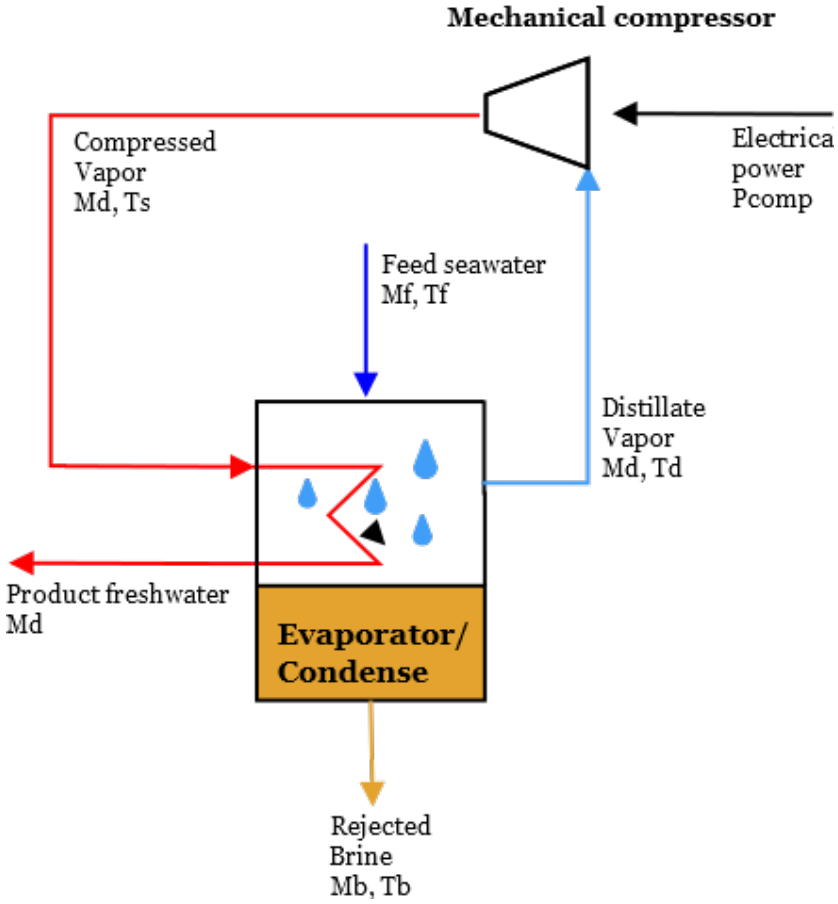

Figure 6.1: Schematic diagram of basic components of a MED-MVC system.

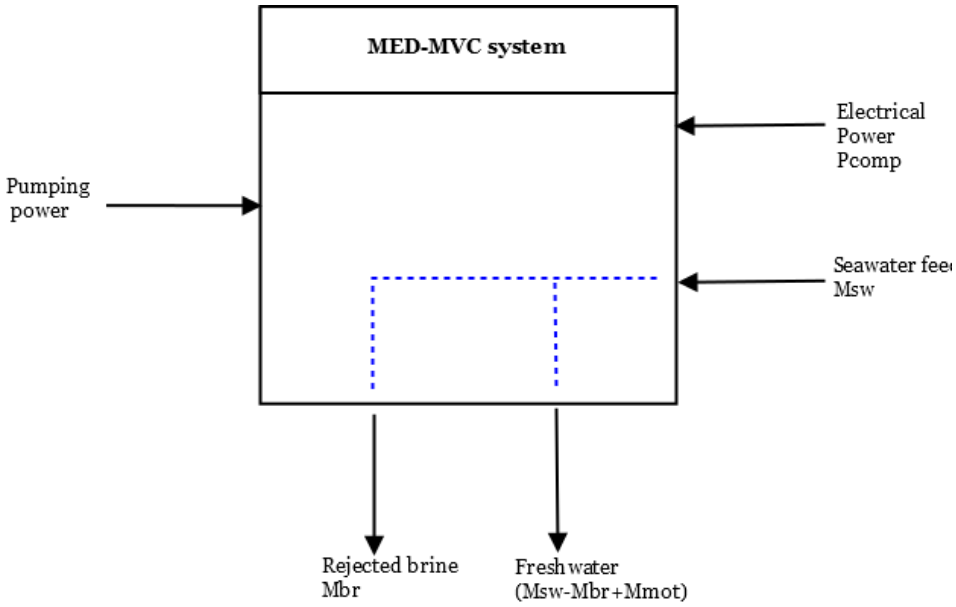

Figure 6.2: Black box representation of a general MED-MVC desalination system.

Figures 6.1 and 6.2 report basic component schematic and black box representation of a MED-MVC system, respectively. The whole process is described and modeled in the following sections.

6.2 Process Description

Plant flow-sheet for a MED-MVC desalination system with parallel flow configuration is shown in Figure 6.3, while Figure 6.1 represents a single distillation unit with mechanical vapor compression. The whole mass flow rate of distillate vapor produced in the last effect (M_d, n) is sent to the mechanical compressor. Here, $M_{d,n}$ is compressed and superheated to temperature $T_{st,suph}$. Compressed steam then flows into the tube side of the evaporator (that is also the first effect), cools down to $T_{st,in}$ and condenses. Latent heat released by $M_{st,in}$ is transferred to the feed seawater entering the first effect $(M_{f,1})$, vaporizing it. Brine $(M_{br,1})$ and distillate water vapor $(M_{d,1})$ are produced in the effect. Salinity of brine produced at the first effect corresponds to the solubility limit of $CaSO_4$ at that temperature (see Figure 4.4).Distillate water vapor then flows into the tube side of the following effect, acting as heating steam for that effect. This process is repeated till the last effect. Fresh water and brine streams exiting the last effect ($M_{fw,n}$ and $M_{br,n}$) flow into a pre-heater and cool down to temperature T_0. Heat released by $M_{fw,n}$ and $M_{br,n}$ is transferred to the feed seawater $M_{sw,in}$ entering the pre-heater. At outlet of the pre-heater, $M_{sw,in}$ has a temperature $T_{sw,out}$ higher than temperature at inlet $T_{sw,in}$.

6.3 Mathematical Model

Assumptions made for modeling are the same made for MED and MED-TVC systems (Paragraphs 4 and 5). Equations regarding mechanical compressor and feed seawater pre-heater models are reported in this section, while for material and energy balances in all the effects reference is made to paragraph 4.

Figure 6.4 reports variables involved in modeling the mechanical compressor. Mass balance is:

$$M_{d,n} + F_n = M_{st,in} \tag{6.1}$$

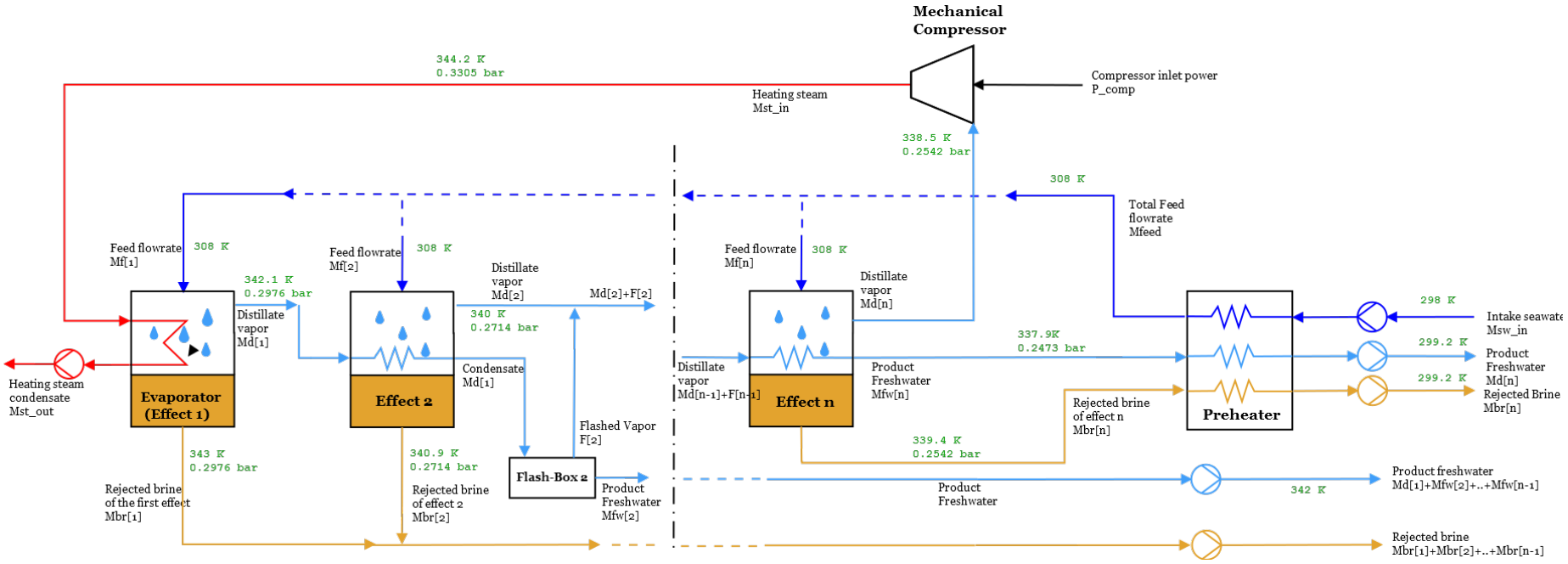

Figure 6.3: Schematic diagram of a Multi Effect Distillation plant with Mechanical Vapor Compression used for modeling. Values of pressure and temperature reported in the diagram refer to a 4 effects plant.

	Unit	Jamil et al. [24]	Model
Number of effects n	[-]	4	4
Seawater Temperature	[K]	294	294
Salinity of feed seawater	[ppm]	35000	35000
Salinity of rejected brine	[ppm]	70000	70000
Temperature of compressed vapor	[K]	345	345
Compression Ratio	[-]	1.35	1.35
Distillate mass flow rate	[kg/s]	35	35
Compression power	[kW]	553	553.8

Table 6.1: Model validation: MED-MVC model results compared to literature data [24].

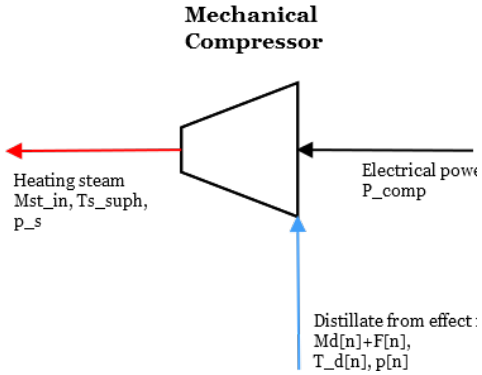

Figure 6.4: Schematic diagram of the mechanical compressor of a MED-MVC plant.

Where $M_{d,n}$ is the distillate vapor produced in effect n and F_n is the vapor produced by flashing process in the flash box of effect n. $M_{st,in}$ is the mass flow rate of compressed vapor that will enter the evaporator (first effect) at the tube side to condense. Compression ratio at the compressor is given by the ratio of Eq. 6.2, where p_s is the pressure of heating steam and p_n is the pressure of distillate vapor entering the compressor.

$$CompRatio = \frac{p_s}{p_n} \tag{6.2}$$

Steam exiting the compressor is superheated at the temperature $T_{s,suph}$ given by:

$$T_{s,suph} = T_{d,n} \cdot \frac{1 + CompRatio^{\frac{k-1}{k}}}{\eta_{is,comp}} \tag{6.3}$$

k is the specific heats ratio for water vapor, $T_{d,n}$ is the distillate vapor temperature and $\eta_{is,comp}$ is the iso-entropic efficiency of the mechanical compressor.

Mass balances for each stream i at the pre-heater can be expressed as:

$$\sum_i M_{in,i} = \sum_i M_{out,i} \tag{6.4}$$

Both the brine stream $M_{br,n}$ and the freshwater $M_{fw,n}$ coming from the last effect cool down to temperature T_0 and increase temperature of feed seawater (M_{feed}) from temperature T_{cw} to T_{feed}. Eq. 6.5 reports energy balance referred to this process.

$$M_{feed} \cdot c_p \cdot (T_{feed} - T_{cw}) = M_{br,n} \cdot c_p \cdot (T_{br,n} - T_0) + M_{fw,n} \cdot c_p \cdot (T_{fw,n} - T_0) \tag{6.5}$$

Model is validated with data available in the literature [24], showing a good correspondence between the built model and industrial data (Table 6.1).

6.4 Model Simulation

As discussed in previous sections, different variables can be set as independent. In particular, for MED-MVC processes the following variables can be either calculated od independent:

- C_f: salinity of feed seawater;
- $C_{b,max}$: maximum salinity of the rejected brine;
- ΔT_{min}: minimum temperature drop at each heat exchanger;

- T_{cw}: temperature of feed seawater;
- $p_{sw,in}$: pressure of feed seawater;
- k: specific heats ratio for water vapor;
- η_c: iso-entropic efficiency of the mechanical compressor;
- $CompRatio$: compression ratio at the mechanical compressor;
- ΔT_{cond}: seawater temperature increase at the down pre-heater;
- $M_{fw,tot}$: freshwater output of th plant;
- TBT: top brine temperature at the first effect (or temperature of the compressed steam entering the evaporator at the tube side);
- M_s: mass flow rate of compressed steam entering the evaporator;
- n: number of effects.

Considerations on the choice of independent variables are the same made for MED and MED-TVC systems (see Chapters 4 and 5). As for MED-TVC at least one performance parameter of the steam compressor has to be set. For MED-MVC iso-entropic efficiency $\eta_{is,c}$ and compression ratio of the mechanical compressor were set as independent.

Figures 6.5 to 6.9 report trends of efficiency parameters obtained by model simulations. In this case it is evident that PR refers to variables which are not representative of the process. In fact, while PR shows that performance of the plant is almost independent from the top brine temperature (Figure 6.6 and 6.5), efficiency parameter $\eta_{Primary}$, based on primary energy at inlet, shows how performance of MED-MVC system actually depends on top brine temperature (Figures 6.9 and 6.8). This is due to the fact that PR refers to heating steam mass flow rate M_s as input energy variable. However, in MED-MVC systems M_s corresponds to the amount of water vapor produced at the last effect, and thus only depends on the number of effects n (as stressed by Figure 6.6). The increase of TBT would actually result in higher amount of energy that has to be supplied from the outside,which however is represented by the electrical power at the

compressor and not by the mass flow rate of heating steam. For this reason $\eta_{Primary}$, which refers to primary energy at inlet, takes into account the increasing energy supply required at higher TBT and hence better describe performance of the plant at higher TBT. Same discussion is valid for plant performance at different feed seawater salinities: higher C_f require higher energy supply at inlet, which however is not accounted for in PR (Figures 6.5 and 6.9).

Finally, Figure 6.7 reports Recovery Ratio as a function of top brine temperature and number of effects. In contrast with MED and MED-TVC systems (Figures 4.9 and 5.10), MED-MVC plants do not need cooling water, since the whole amount of water vapor produced in the last effect is sent to the mechanical compressor. As a result, RR decreases at increasing top brine temperatures because of the drop in maximum salinity, which in turn cause an increase of rejected brine mass flow rate and hence of feed seawater (see material balances of water and salt in Equations 4.3 and 6.4).

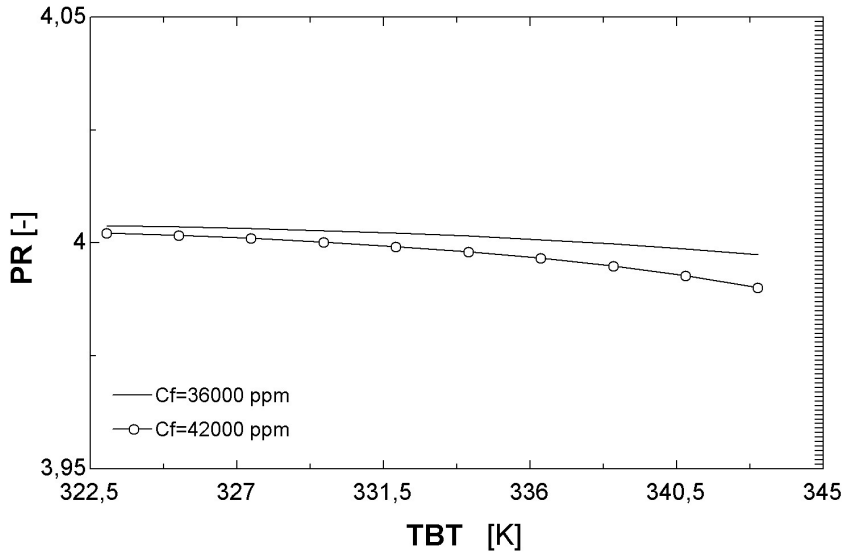

Figure 6.5: Performance Ratio PR of a MED-MVC plant as function of top brine temperature TBT and feed seawater salinity C_f.

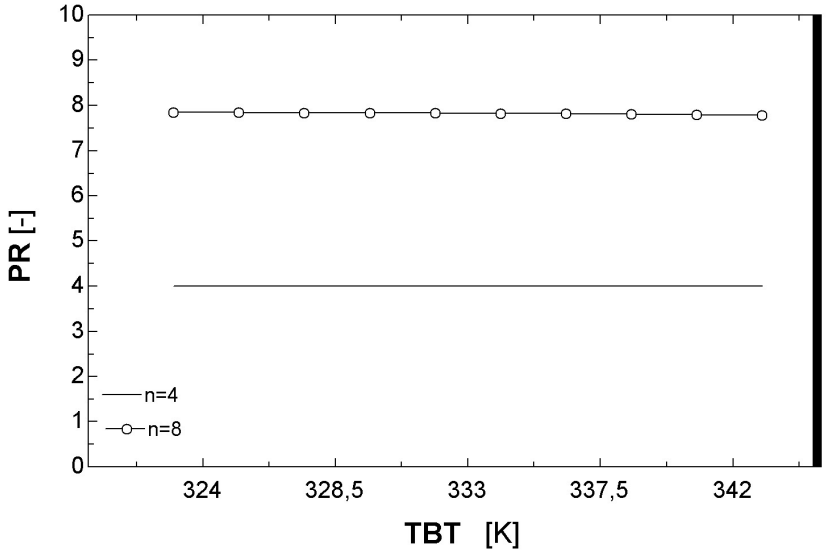

Figure 6.6: Performance Ratio PR of a MED-MVC plant as function of top brine temperature TBT and number of effects n.

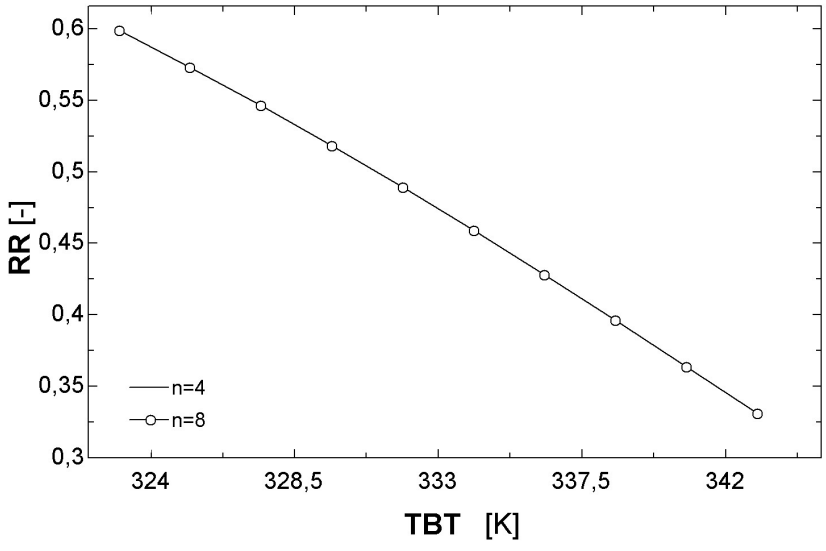

Figure 6.7: Recovery Ratio RR of a MED-MVC plant as function of top brine temperature TBT and number of effects n.

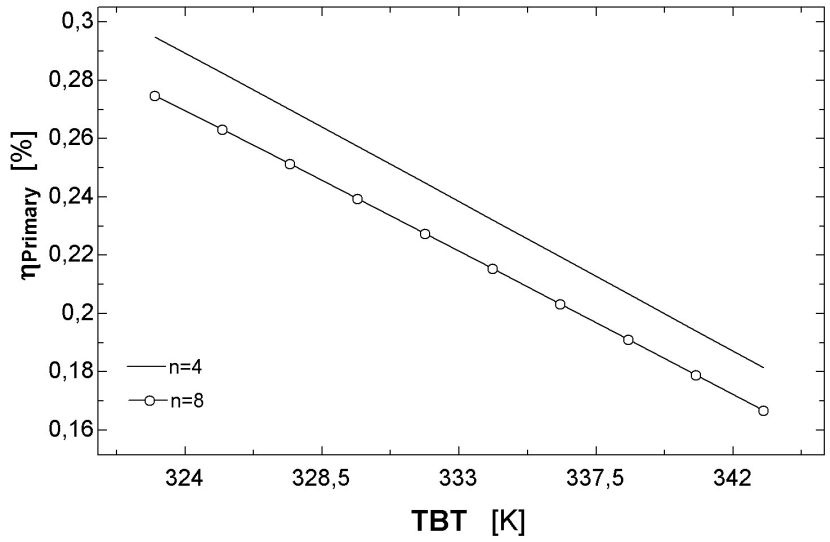

Figure 6.8: Efficiency based on primary energy $\eta_{Primary}$ of a MED plant as function of top brine temperature TBT and number of effects n.

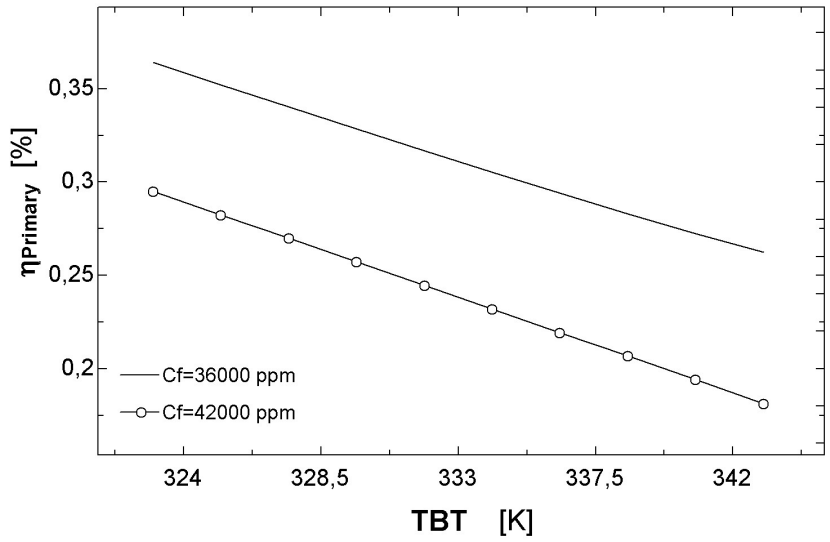

Figure 6.9: Efficiency based on primary energy $\eta_{Primary}$ of a MED plant as function of top brine temperature TBT and salinity of feed seawater C_f.

Chapter 7

Exergy Analysis of Evaporative Desalination Systems: a novel approach

Efficiency of evaporative desalination systems as defined in the previous Chapters refers to the first law of thermodynamics. However, energy conservation concept alone is not enough to properly describe the performance of a desalination system (or, more in general, of an energy system). For this reason, increasing attention has been given to exergy analysis for thermal systems, a widely recognized tool that allows to identify main sources of energy dissipations and quantify thermodynamic losses throughout the system. Informations on source, cause and real dimensions of energy losses are key points both in the design of new desalination configurations and in the improvement of efficiency of existing plants. Moreover, efficiency parameters of desalination plant commonly used (PR and RR, ref. Chapter 2)may not be sufficient to properly express the productive function of the plant, i.e. the removal of dissolved salts from seawater. Thus, exergy analysis applied to desalination plants not only allows to determine the sources of inefficiencies in the system, but seems also to be the only way to properly define the efficiency of a desalination process.

In this chapter a novel approach, based on SPECO method [32], is used to perform exergy analysis for some of the processes modeled in previous Chapters.

7.1 Exergy balance and exergetic efficiency of evaporative desalination plants

Exergy is defined as the maximum amount of work obtainable when bringing a system from its initial state to the dead state. Exergy of the system is considered to be null at the dead state. In the exergy analysis of a seawater desalination it is meaningful to considerate both physical and chemical exergy. Physical exergy is the maximum work obtainable when bringing temperature and pressure of the system to the environment temperature and pressure, with no change in concentration. Chemical exergy is the maximum work obtainable when changing concentration of a substance to the environment concentration, keeping temperature and pressure at environmental values. Properties at the environment state (those with "*" in the following equations) are evaluated at pressure and temperature of the feed seawater ($p_0 = p_{sw,in}, T_0 = T_{sw,in}$), while properties at the dead state are calculated at pressure, temperature and concentration of the environment state; in particular, concentration at environment state is considered to be equal to the feed seawater salinity C_f. In this work, environment state corresponds to the inlet conditions of feed seawater [54]. Specific seawater exergy can be calculated as:

$$e = (h - h^*) - T_0(s - s^*) + \sum_{i=1}^{n} w_i(\mu_i^* - \mu_i^0) \tag{7.1}$$

Where h is the seawater specific enthalpy, s the specific entropy, T_0 is the environment temperature, w_i is the concentration of element i in the mixture and μ_i is the chemical potential of substance i. Being seawater a multicomponent system, also chemical exergy (the last terms in equation 7.1)must be included in calculations. As done for all seawater properties, also chemical potentials are calculated thanks to the correlations developed by Sharqawy et al. [54].

Exergy balance in steady state conditions for a generic process i with streams flowing in and out the system boundaries can be expressed as:

$$\sum_i \dot{E}_{in,i} = \sum_i \dot{E}_{out,i} + \dot{I} \tag{7.2}$$

where $\dot{E}_{in}$ and $\dot{E}_{out}$ are exergy flows entering and exiting the boundaries of process i, respectively. $\dot{I}$ is the loss of exergy due to irreversibilities in the system. Although

Equation 7.2 gives an unambiguous definition of exergy destruction in the system, it does not give any information on the actual purpose of the plant. In order to highlight the real goal of the plant and define a consistent efficiency parameter it is convenient to identify *fuel* and *product* of the system. *Product* is the desired exergetic output of the system, *fuel* is the necessary exergy supply. There are several definitions of fuel and product that are consistent with the exergy balance. From a mathematical point of view different definitions of fuel and product simply correspond with moving exergy terms in the balance from one side to the other of equation 7.2. All definitions of fuel and product are consistent, however a choice should be done on the bass of the real purpose of the system. So that the efficiency calculated as the ratio between product and fuel is expected to increase when the plant performance is actually improved. For any definition of fuel and product is always possible to rewrite the exergy balance as:

$$\dot{E}_{fuel}=\dot{E}_{product} + \dot{I} \tag{7.3}$$

and to calculate an exergetic efficiency as:

$$\eta_{ex} = \frac{\dot{E}_{product}}{\dot{E}_{fuel}} \tag{7.4}$$

Several studies on exergy analysis of desalination plants propose different definitions of exergy-based efficiencies. In particular, Sharqawy et al. [54], Mistry et al. [31] and Brogioli et al. [9] define a second law efficiency as:

$$\eta_{II} = \frac{\dot{W}_{least,sep}}{\dot{W}_{sep}} \tag{7.5}$$

where $\dot{W}_{least_{sep}}$ is the minimum work of separation of dissolved salts from seawater and $\dot{W}_{sep}$ is the sum of flow thermal exergy of heating source (usally steam) and mechanical exergy at input to driving pumps and compressor (i.e. the actual work of separation). Exergy and other seawater properties in [54], [31] and [9] are calculated using correlations based on chemical analyses. Kahraman and Cengel [27] calculate second law efficiency in the same way of Sharqawy et al. but using an ideal mixture model, obtaining different values.

In the present work, a novel approach is utilized to define an exergy efficiency. The idea is that the real purpose of a desalination plant is to *decrease* the chemical exergy of seawater at expenses of heating steam entering the evaporator (i.e. at expenses of

the compressor in MVC systems or of the motive steam entering the steam ejector in TVC plants) and pumping power. In order to have the minimum exergy expense, this decrease in chemical exergy of seawater should not result in an increase of physical exergy of freshwater, cooling water and brine released to the environment. A similar problem can be conceptually met in a mechanical compressor, where the increase of the fluid pressure (i.e. the purpose of the compressor), always implies a temperature increase. As improving a compression process entails a lower increase of thermal exergy of the fluid, improving a desalination process would result in lowering the physical exergy increase of outlet streams (considering the decrease of chemical exergy of freshwater constant).Summarizing, for an evaporative desalination system:

- Product is the desired decrease of chemical exergy of seawater;
- Fuel is the sum of the whole exergy that is required to obtain the product, i.e.: input power (pumping and compressor for MVC), undesired chemical and physical exergy increases of brine, undesired physical exergy increase of cooling water and freshwater streams and desired physical exergy decreases of heating steam (or motive steam).

Actually, the SPECO method, as formulated in [32], does not explicitly refer to cases in which an exergy decrease is the desired product of a process, although it does not exclude it. As an example, considering a desalination system fed by heating steam and without cooling water is considered:

$$\dot{E}_{fuel} = P_{pumps} + \Delta \dot{E}^{PH}_{hst} - \Delta \dot{E}^{PH}_{br} - \Delta \dot{E}^{PH}_{fw} - \Delta \dot{E}^{CH}_{br} \tag{7.6}$$

$$\dot{E}_{product} = -\Delta \dot{E}^{CH}_{fw} \tag{7.7}$$

$$\eta_{ex} = \frac{\dot{E}_{product}}{\dot{E}_{fuel}} \tag{7.8}$$

where, in agreement with the SPECO approach, positive exergy changes Δ are the exergy increases at the product side and the exergy decreases at the fuel side. To include cases in which exergy decreases are desired products, a sign minus is added to exergy decreases that are to be considered at the product side and exergy increases that are to be considered at the fuel side. The meaning of the different terms is:

- P_{pumps}: pumping power;

- $\Delta \dot{E}_{hst}^{PH}$: decrease of heating steam physical exergy;
- $\Delta \dot{E}_{br}^{PH}$: increase of brine physical exergy;
- $\Delta \dot{E}_{fw}^{PH}$: increase of freshwater physical exergy;
- $\Delta \dot{E}_{br}^{CH}$: increase of brine physical exergy;
- $\Delta \dot{E}_{fw}^{CH}$: decrease of freshwater chemical exergy.

It can be easily verified that η_{ex} varies from 0 to 1. The maximum efficiency is reached when all fuel terms but $\dot{E}_{br}^{PH}$ are null, the minimum efficiency when no chemical exergy change is registered on the freshwater.

In the following sections, productive structures and deepened exergy analyses are shown for MED based technologies. The same discussion could be extended to MSF technology. However MSF plants are normally coupled with large power plants and therefore it would make more sense to perform a comprehensive exergy analysis of both power plant and desalination process instead of analyzing the desalination process alone.

7.2 Productive structure of MED based technologies

Figures 7.2 and 7.2 report schematics for inlet and outlet flows of MED and MED-MVC systems. Solid lines in the scheme represent physical streams in the process, while dashed lines show internal patterns in the system for the different flows. By considering definitions of fuel and product given in the previous section, it is possible to represent MED and MED-MVC systems as done in figure 7.3 and 7.4, which illustrate the productive structures of MED and MVC plants, respectively.

The main advantage of this representation is that it is possible to distinguish the different areas of interaction in the plant: physical, thermal, mechanical, chemical. Bold red lines in Figures 7.3 and 7.4 represent chemical exergy streams, while bold blue lines correspond to physical exergy flows. Bold dashed line constitutes the boundary of the whole system. Productive units of the systems are divided into chemical and physical ones. The first presents at inlet and outlet chemical exergy variations that constitute fuel and product exergies, respectively; the latter provides for fuel exergy stream at inlet and product one at outlet. In addition to productive units, there could be some

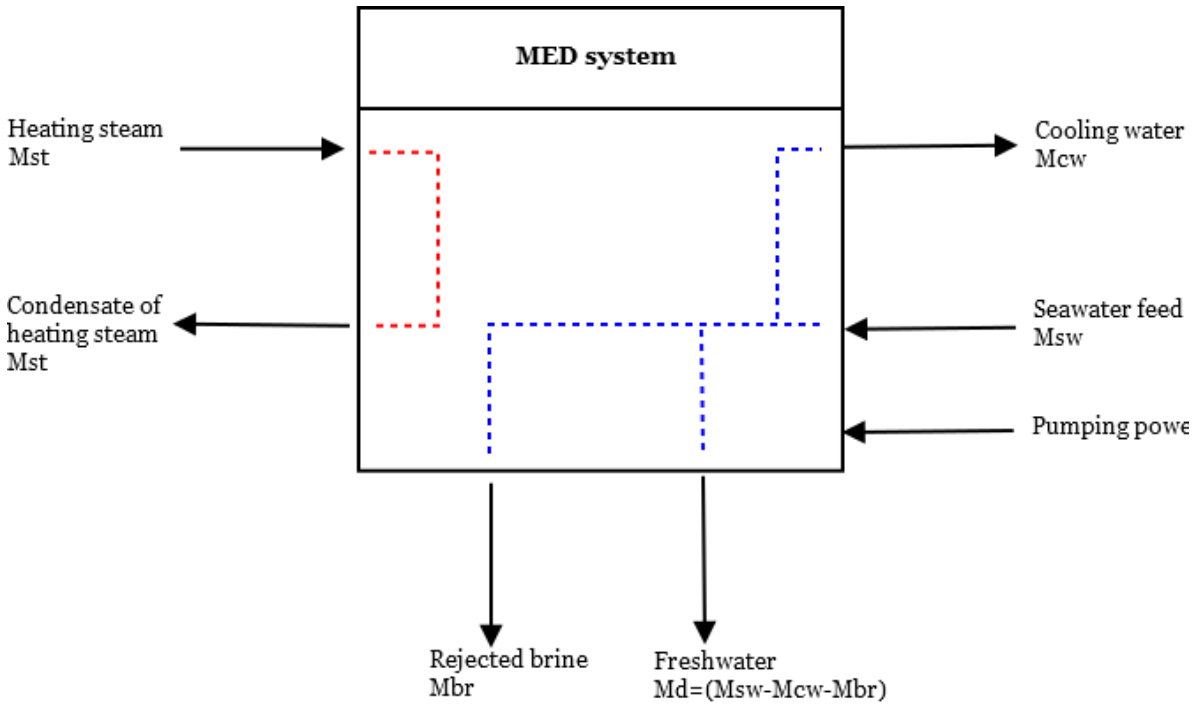

Figure 7.1: Schematics of inlet and outlet flows of MED desalination systems.

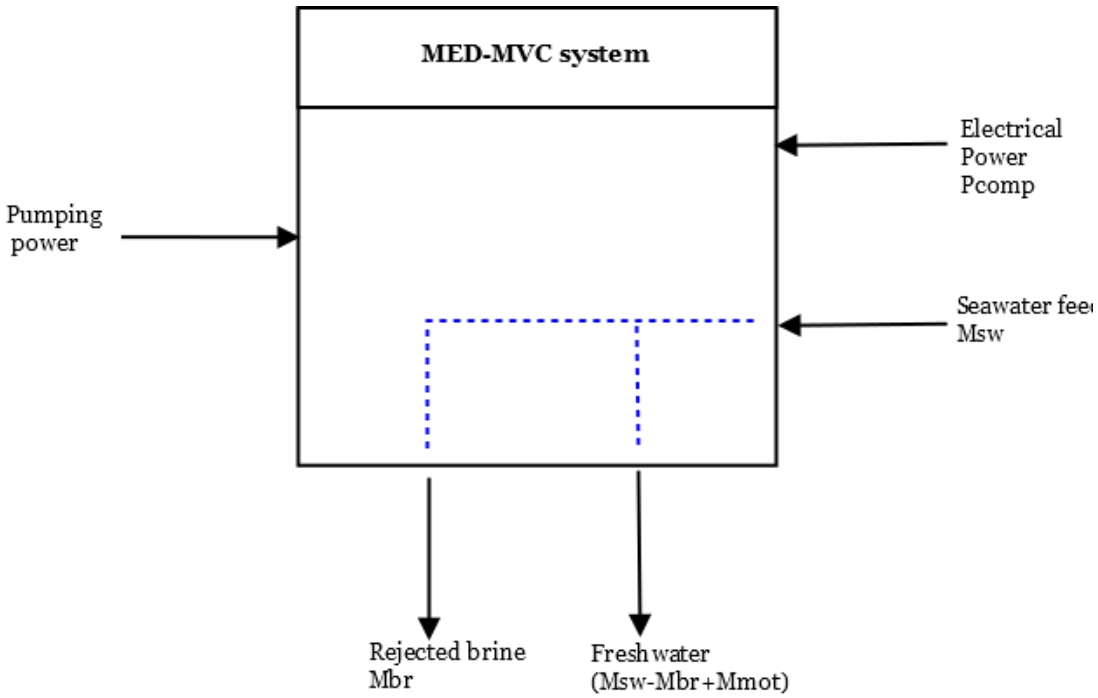

Figure 7.2: Schematics of inlet and outlet flows of MED-MVC desalination systems.

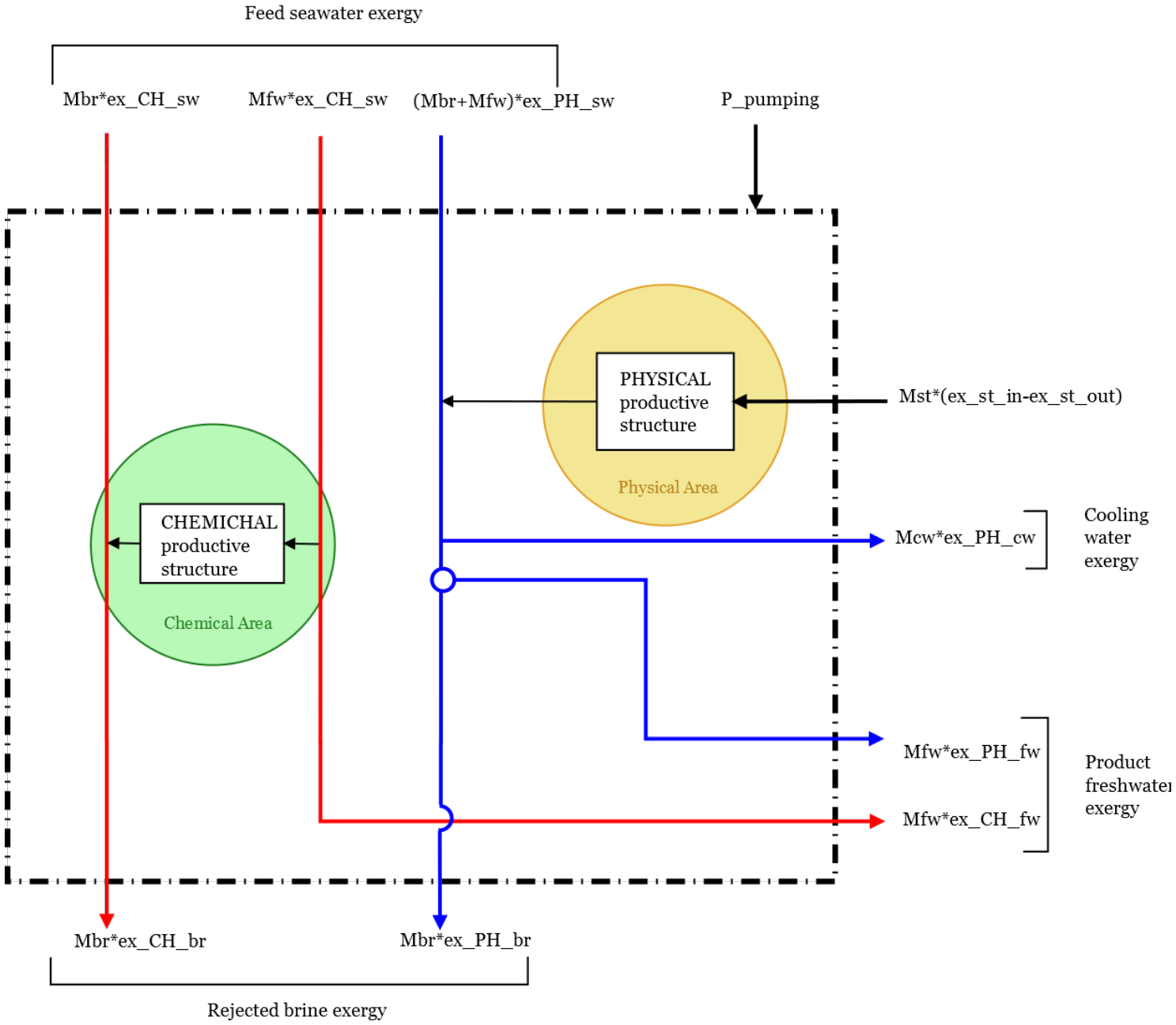

Figure 7.3: Productive structure of a MED desalination plant.

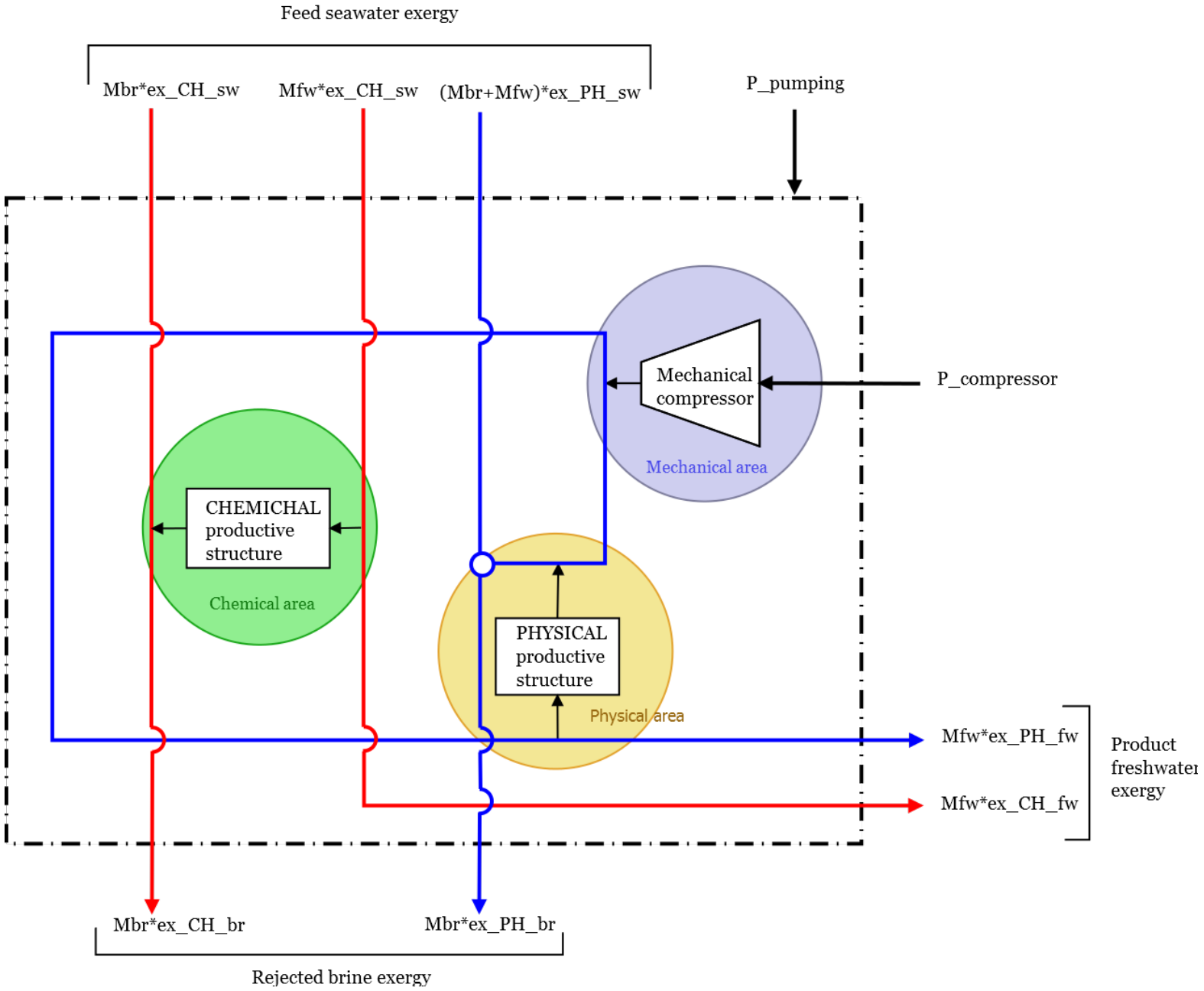

Figure 7.4: Productive structure of a MED-MVC desalination plant.

external components, such as the mechanical compressor in the case of MVC, which also is illustrated in a fuel-product perspective. As mentioned before, fuel and product streams can also be exergy variation between inlet and outlet streams.

7.3 Exergy analysis: model equations

Main equations of exergy analysis and definition of fuel and product are reported in this section. Systems analyzed are MED and MED-MVC, although the same discussion can be done for MED-TVC and MSF technologies too.

MED

MED desalination process is fed by condensing heating steam, which releases its latent heat to the feed seawater entering the evaporator. Therefore, the decrease in physical exergy of heating steam is considered at the fuel side of the exergy balance. In addition, in order to obtain the desired output (i.e. the decrease of chemical exergy of freshwater) other exergy variations are necessary. In particular, fuel components for MED systems are:

- $\Delta\ \dot{E}_{hst}$: exergy decrease of heating steam;
- $\Delta\ \dot{E}_{fw}^{PH}$: undesired increase of physical exergy associated to freshwater product;
- $\Delta\ \dot{E}_{br}^{PH}$: undesired increase of physical exergy associated to rejected brine;
- $\Delta\ \dot{E}_{cw}^{PH}$: undesired increase of physical exergy of cooling seawater mass flow rate;
- $\Delta\ \dot{E}_{br}^{CH}$: undesired increase of chemical exergy of rejected brine.

While product is the desired decrease of chemical exergy of product freshwater. Equations 7.9 to 7.13 report the extended expressions of the just mentioned variables. Letter e in lower case indicates specific exergy flows, chemical (exponent CH) or physical (exponent PH). Sign minus indicates undesired increases or decreases of exergy.

$$\Delta\ \dot{E}_{hst}=\dot{m}_{hst}\ (e_{st,in} - e_{st,out}) \tag{7.9}$$

$$\Delta\ \dot{E}_{fw}^{PH} = -\ \dot{m}_{fw}\ (e_{sw,feed}^{PH} - e_{fw}^{PH}) \tag{7.10}$$

$$\Delta \dot{E}_{br}^{PH} = - \dot{m}_{br} \, (e_{sw,feed}^{PH} - e_{br}^{PH}) \tag{7.11}$$

$$\Delta \dot{E}_{cw}^{PH} = - \dot{m}_{cw} \, (e_{sw,feed}^{PH} - e_{sw,out}^{PH}) \tag{7.12}$$

$$\Delta \dot{E}_{br}^{CH} = - \dot{m}_{br} \, (e_{sw,feed}^{CH} - e_{fw}^{CH}) \tag{7.13}$$

Exergy balance can thus be expressed in the form:

$$\dot{E}_{FUEL} = \dot{E}_{PRODUCT} + \dot{I} \tag{7.14}$$

where:

$$\dot{E}_{FUEL} = P_{pumping} + \Delta \dot{E}_{hst} + \Delta \dot{E}_{fw}^{PH} + \Delta \dot{E}_{br}^{PH} + \Delta \dot{E}_{cw}^{PH} + \Delta \dot{E}_{br}^{CH} \tag{7.15}$$

$$\dot{E}_{PRODUCT} = \Delta \dot{E}_{fw}^{CH} \tag{7.16}$$

Obviously, value of irreversibilities calculated with equation 7.14 is the same if calculated by the exergy balance of Equation 7.2. Exergetic efficiency of MED plant is calculated as $\dot{E}_{PRODUCT}$ divided by $\dot{E}_{FUEL}$.

MED-MVC

Definition of fuel and product in a MED-MVC plant only differs from the one of MED in that MED-MVC comprehends a mechanical compressor, while does not include a cooling water stream. As shown in Figure 7.4, a mechanical area is thus included in a MED-MVC plant. Clearly, power at the compressor P_{comp} is considered at the fuel side of the exergy balance; other terms remain the same of MED ones. Exergy balance of a MED-MVC is therefore:

$$\dot{E}_{FUEL} = \dot{E}_{PRODUCT} + \dot{I} \tag{7.17}$$

with:

$$\dot{E}_{FUEL} = P_{pumping} + P_{comp} + \Delta \dot{E}_{fw}^{PH} + \Delta \dot{E}_{br}^{PH} + \Delta \dot{E}_{br}^{CH} \tag{7.18}$$

$$\dot{E}_{PRODUCT} = \Delta \dot{E}_{fw}^{CH} \tag{7.19}$$

. Also in this case, exergetic efficiency will be the ratio of $\dot{E}_{PRODUCT}$ and $\dot{E}_{FUEL}$.

7.4 Exergy analysis results and discussion

Equations given in the previous section are implemented in mathematical models built with EES. For both MED and MED-MVC simulations are run under different conditions. In particular, performance of the plants is investigated in two situations:

1. fixed number of effects and varying top brine temperature;
2. fixed top brine temperature and varying number of effects.

7.4.1 Exergy efficiency for fixed number of effects and increasing top brine temperature

Top Brine Temperature [K]	Performance Ratio [-]	Recovery Ratio[%]	$\eta_{Primary}$ [%] (see chapter 2)	η_{ex} [%]
323.0	4.537	9.052	0.2434	4.755
325.2	4.446	9.168	0.2367	4.495
327.4	4.351	9.295	0.2299	4.240
329.7	4.250	9.437	0.2232	3.991
331.9	4.144	9.596	0.2164	3.749
334.1	4.032	9.776	0.2096	3.514
336.3	3.913	9.982	0.2029	3.287
338.6	3.786	10.22	0.1962	3.066
340.8	3.650	10.49	0.1896	2.854
343.0	3.505	10.82	0.1830	2.650

Table 7.1: Different efficiency parameters for MED plant with n=5 effects and Top Brine Temperature varying between 323 K and 343 K.

Tables 7.1 and 7.2 report different performance parameters defined in the previous Chapters. In particular, $\eta_{Primary}$ is the energetic efficiency defined in this thesis that refers to primary energy (see Paragraph on performance parameters in Chapter 2). For both MED and MED-MVC plants, higher Top Brine Temperature (TBT) means lower energetic efficiency $\eta_{Primary}$, due to increasing values of heating steam mass flow rate.

Top Brine Temperature [K]	Performance Ratio [-]	Recovery Ratio[%]	$\eta_{Primary}$ [%] (see chapter 2)	η_{ex} [%]
323.0	4.993	65.60	0.3705	4.634
325.2	4.992	63.41	0.3579	4.392
327.4	4.991	61.11	0.3453	4.153
329.7	4.990	58.71	0.3329	3.917
331.9	4.989	56.21	0.3208	3.685
334.1	4.988	53.62	0.3088	3.458
336.3	4.986	50.96	0.2972	3.236
338.6	4.984	48.23	0.2859	3.021
340.8	4.982	45.46	0.2750	2.812
343.0	4.979	42.64	0.2645	2.611

Table 7.2: Different efficiency parameters for MED-MVC plant with n=5 effects and Top Brine Temperature varying between 323 K and 343 K.

For MED plant this is due to the fact that at high temperatures maximum salinity reached by the rejected brine is lower. As a consequence, being the salt mass balance $M_{feed} \cdot C_{feed} = M_{br} \cdot C_{br}$, a higher amount of brine has to be rejected at the evaporator. Keeping constant the mass flow rate of freshwater product, increasing amount of rejected brine leads to increasing amount of feed seawater at the evaporator. Thus, since latent heat of heating steam is almost constant with temperature, a higher mass flow rate of heating steam is necessary to evaporate a higher amount of feed seawater. For the same reason, PR of MED plant decreases at higher Top Brine Temperatures. For what concerns MED-MVC plant, diminishing $\eta_{Primary}$ at high TBT is due to the higher power required by the compressor. In fact, in MVC plants mass flow rate of heating steam corresponds to the mass flow rate of the distillate water vapor at the last effect, which remains constant if freshwater product is fixed in the model. However, as it is for MED plants, also in this case higher TBT turns out to increase the feed seawater amount at the evaporator. Hence, distilled vapor entering the mechanical compressor need to be compressed to higher pressures, thus increasing the electrical power needed at the compressor. On thee other hand, PR of MED-MVC plant appears to be almost

constant for varying Top Brine Temperature, being calculated as ratio between freshwater product mass flow-rate (fixed) and heating steam flow rate (which is almost constant because it is the amount of fresh water vapor produced in the last effect). Recovery Ratio (RR) results to increase at increasing TBT for MED plants (because of the lower amount of cooling water needed). On the contrary, RR of MED-MVC decreases for higher temperatures because of the increase in feed seawater required by the process.

As already discussed in Chapter 2, having more than one performance parameter to analyze can be misleading. Calculating the exergetic efficiency η_{ex} for both processes as the ratio between product and fuel previously defined can clarify whether increasing Top Brine Temperature leads to better performances or not. Figure 7.5 and 7.6 clearly point out that exergy efficiency η_{ex} decreases at high top brine temperature for both MED and MED-MVC. Moreover, for both MED and MED-MVC it appears how, with a fixed number of effects, trend of η_{ex} is not so far from the situation with ideal thermal exchanges ($\Delta T_{min} = 0K$). However, the higher is ΔT_{min} (less efficient thermal exchanges at the effects), the higher are the losses for irreversibilities in the effects. This is particularly important when evaluating performance of a plant at increasing number of effects, as shown in the next section.

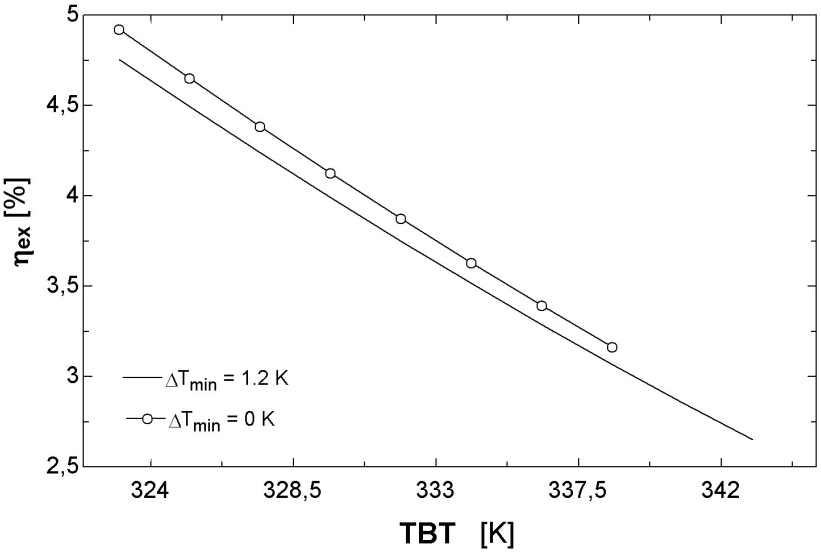

Figure 7.5: Exergetic efficiency for MED plant with 5 effects as a function of Top Brine Temperature and minimum temperature difference at the heat exchangers.

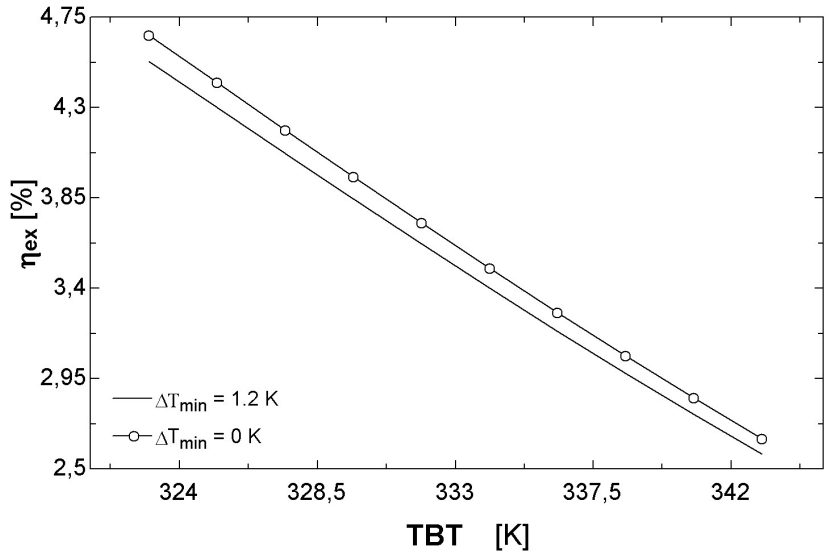

Figure 7.6: Exergetic efficiency for MED-MVC plant with 5 effects as a function of Top Brine Temperature and minimum temperature difference at the heat exchangers.

In order to better understand the exergy efficiency trend for different values of TBT, it is possible to analyze how the different components of fuel act at increasing temperature (in the case of $\Delta T_{min} = 1.2K$). With product kept fixed during the simulations, decreasing η_{ex} means higher fuel. In particular, as highlighted by Figure 7.7 to 7.10, at higher TBT there is a sharp increase of the brine physical exergy variation $\Delta \dot{E}_{br}^{PH}$ due to increasing amount of rejected brine and increasing values of temperature of the rejected brine. For the same reason, also pumping power raises at higher TBT. Other fuel components also grow at increasing TBT, except for the physical exergy variation of cooling water in MED (because of the reduced amount of cooling water at high TBT).

7.4.2 Exergy efficiency for fixed top brine temperature and increasing number of effects

Table 7.3 and 7.4 report performance parameters of MED and MED-MVC plants operating at $TBT = 333K$ for number of effects varying between 3 and 12. For MED process, RR augments in configuration with more effects, since this would result in lowering the amount of cooling water needed at the down condenser (having more effects,

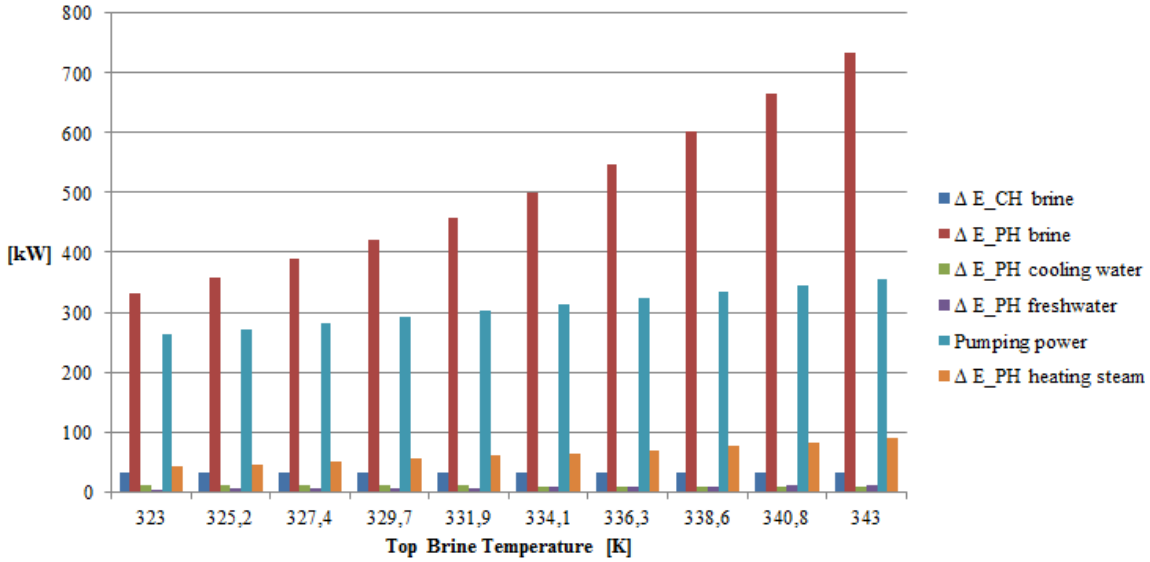

Figure 7.7: Fuel components for MED plant with 5 effects for Top Brine Temperature varying between 323 K and 343 K.

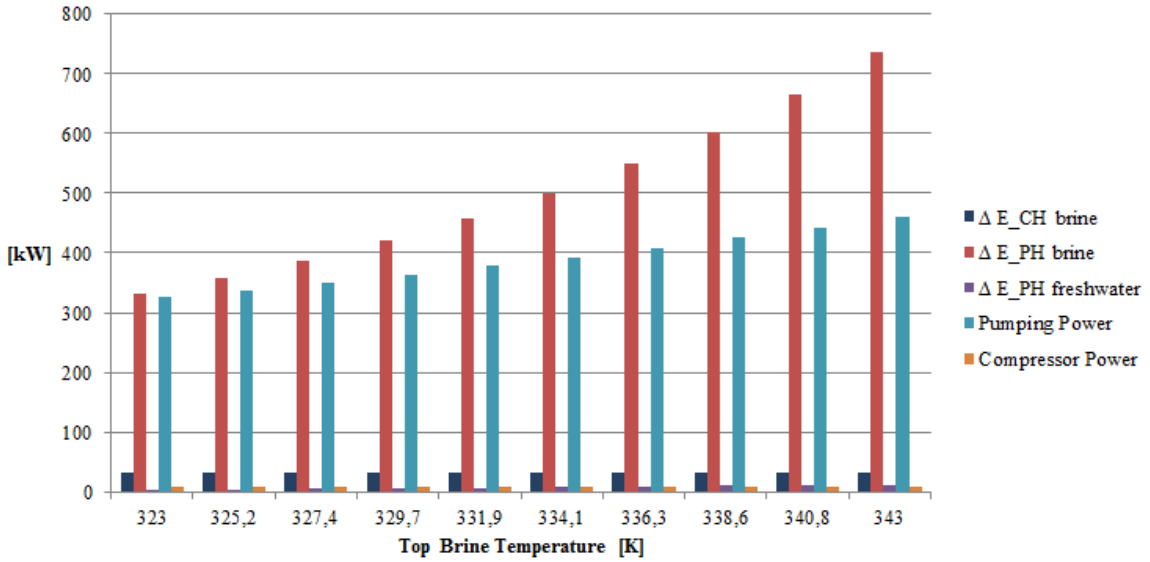

Figure 7.8: Fuel components for MED-MVC plant with 5 effects for Top Brine Temperature varying between 323 K and 343 K.

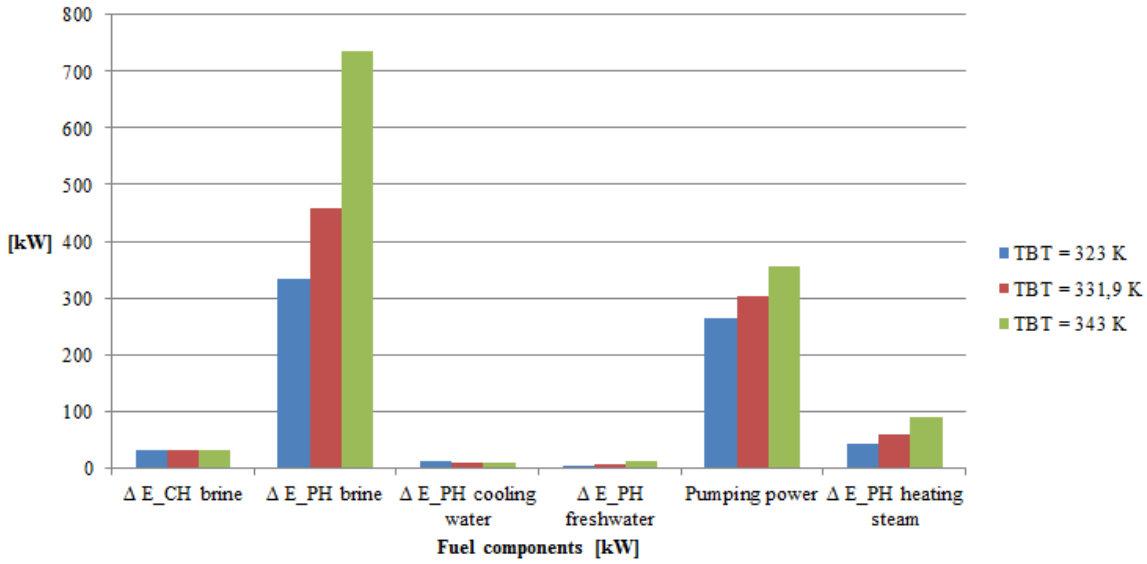

Figure 7.9: Fuel components trend of a MED plant with 5 effects for different values of Top Brine Temperature.

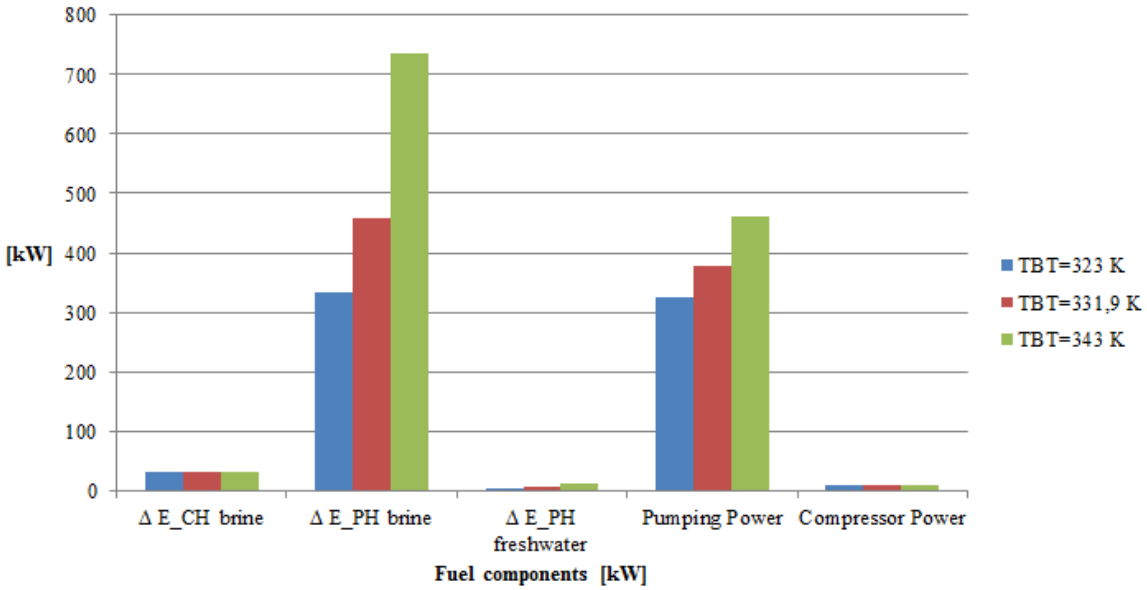

Figure 7.10: Fuel components trend of a MED-MVC plant with 5 effects for different values of Top Brine Temperature.

Number of effects [-]	Performance Ratio [-]	Recovery Ratio[%]	$\eta_{Primary}$ [%] (see chapter 2)	η_{ex} [%]
3	2.606	5.469	0.1689	3.486
4	3.369	7.523	0.1944	3.582
5	4.089	9.683	0.2130	3.631
6	4.771	11.94	0.2270	3.656
7	5.418	14.28	0.2376	3.667
8	6.036	16.70	0.2457	3.669
9	6.627	19.17	0.2520	3.666
10	7.194	21.69	0.2568	3.658
11	7.741	24.23	0.2606	3.648
12	8.269	26.78	0.2634	3.636

Table 7.3: Different efficiency parameters for MED plant operating at a top brine temperature of 333 K, with $\Delta T_{min} = 1.2K$ at increasing number of effects.

Number of effects [-]	Performance Ratio [-]	Recovery Ratio[%]	$\eta_{Primary}$ [%] (see chapter 2)	η_{ex} [%]
3	3.008	54.93	0.3158	3.590
4	4.003	54.93	0.3162	3.585
5	4.988	54.93	0.3148	3.571
6	5.964	54.93	0.3125	3.553
7	6.928	54.93	0.3097	3.532
8	7.878	54.93	0.3067	3.510
9	8.812	54.93	0.3035	3.487
10	9.730	54.93	0.3002	3.464
11	10.63	54.93	0.2969	3.440
12	11.51	54.93	0.2935	3.417

Table 7.4: Different efficiency parameters for MED-MVC plant operating at a top brine temperature of 333 K, with $\Delta T_{min} = 1.2K$ at increasing number of effects.

distillate water vapor amount produced at the last effect is lower). This is not the case of MED-MVC plant, which does not need the down condenser and therefore has a RR that is constant at increasing number of effects. For both plants PR increases at higher values of n, thanks to the decreasing amount of heating steam required at the evaporator. Conceptually, adding effects would augment the "internal re-utilization" of heat, thus improving the overall performance. The most important thing to notice, however, is that while PR increases for configurations with more effects, energetic efficiency $\eta_{Primary}$ drops, which means that higher amount of primary energy is necessary to obtain the same product.

In order to better understand how number of effects is affecting the performance of the processes, exergetic efficiency is calculated, obtaining trends shown in Figure 7.11 and 7.12. It is evident from the Figures that adding effects to the system increase losses for irreversibilities due to heat exchanges in the effect. In particular, for real effects ($\Delta T_{min} \neq 0K$), exergetic efficiency decreases at increasing number of effects, gradually distancing from ideal trend.

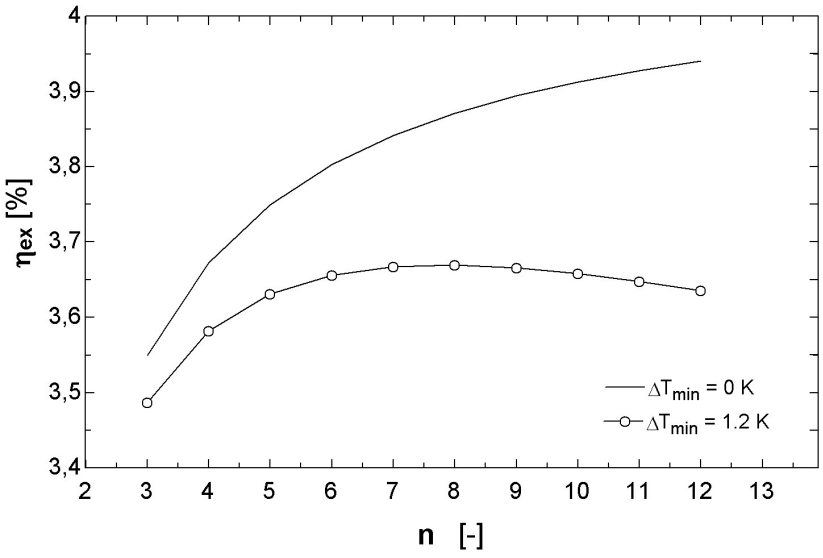

Figure 7.11: Exergetic efficiency as function of number of effects n and minimum temperature difference at the heat exchangers ΔT_{min} in a MED process with top brine temperature of 333 K.

Histograms in Figures 7.13 to 7.16 report trends of fuel components in MED and

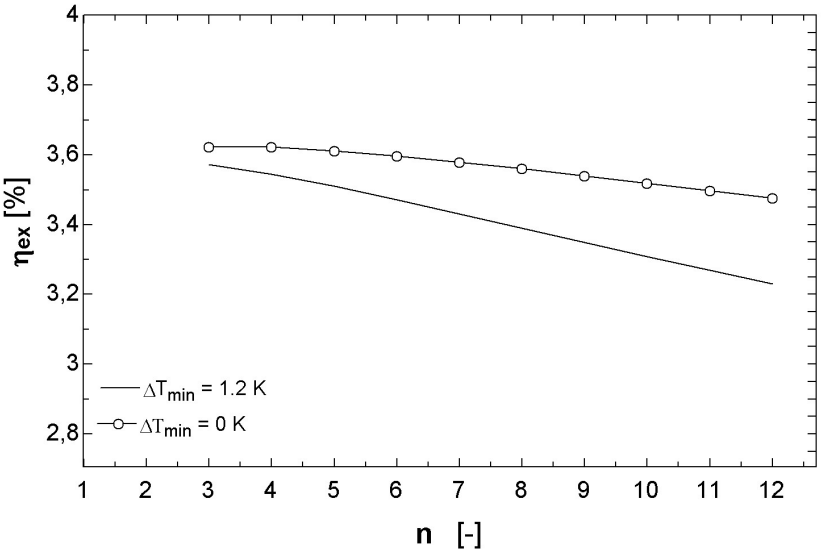

Figure 7.12: Exergetic efficiency as function of number of effects n and minimum tmperature difference at the heat exchangers ΔT_{min} in a MED-MVC process with top brine temperature of 333 K.

MED-MVC processes for varying number of effects n both for $\Delta T_{min} \neq 0K$ and $\Delta T_{min} = 0K$. It can be noted (Figure 7.11) that for MED process it is convenient to increase the number of effects up to an optimum value n_{opt}. Histograms of Figure 7.13 point out that this is due to the increasing values of $\Delta \dot{E}_{br}^{PH}$ and pumping power while other fuel components remain almost constant. At number of effects lower than n_{opt} the sharp decrease of $\Delta \dot{E}_{hst}^{PH}$ prevails on the slight growth of $\Delta \dot{E}_{br}^{PH}$ and Pumping power, leading to an increase of exergetic efficiency. For ideal effects ($\Delta T_{min} = 0K$, Figure 7.14), the drop of $\Delta \dot{E}_{hst}^{PH}$ at increasing number of effects leads to a growing trend of η_{ex}, while $\Delta \dot{E}_{br}^{PH}$ stays constant and pumping power slightly decrease thanks to lower heating steam mass flow rate.

Similar discussion can be done for MED-MVC system. However, MED-MVC does not have an optimum value of n. Instead, for the real case ($\Delta T_{min} \neq 0K$), exergetic efficiency has a monotonic decreasing trend at higher values of n (Figure 7.12). Also in this case it is clear that irreversibilities introduced by non-ideal effects cause the drop of exergetic efficiency. Trends of fuel components for both real and ideal conditions of MED-MVC are reported in Figure 7.15 and 7.16. For both real and ideal case,

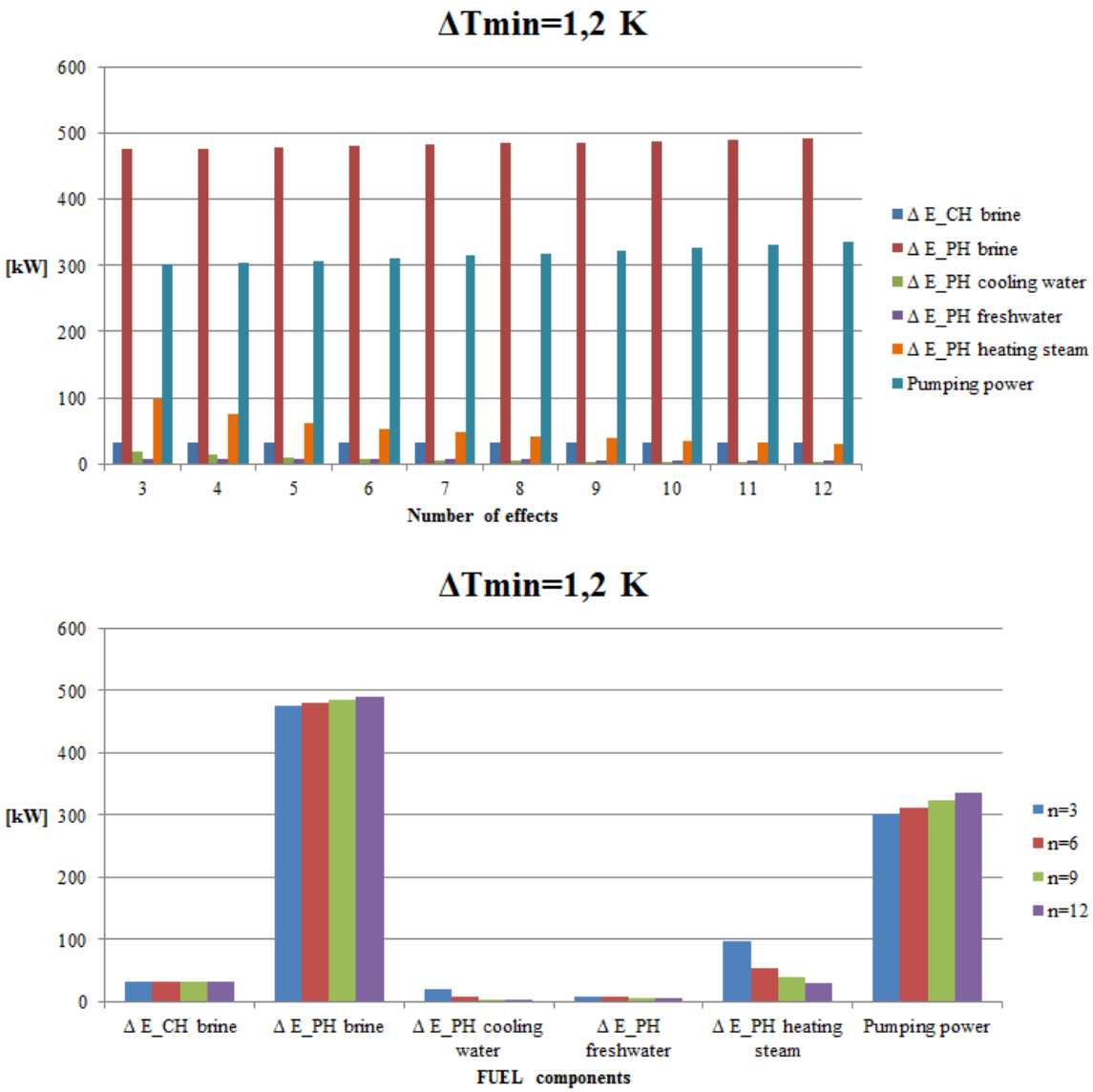

Figure 7.13: Fuel components trends as functions of number of effects n in a MED process with top brine temperature 333 K and $\Delta T_{min} = 1.2K$

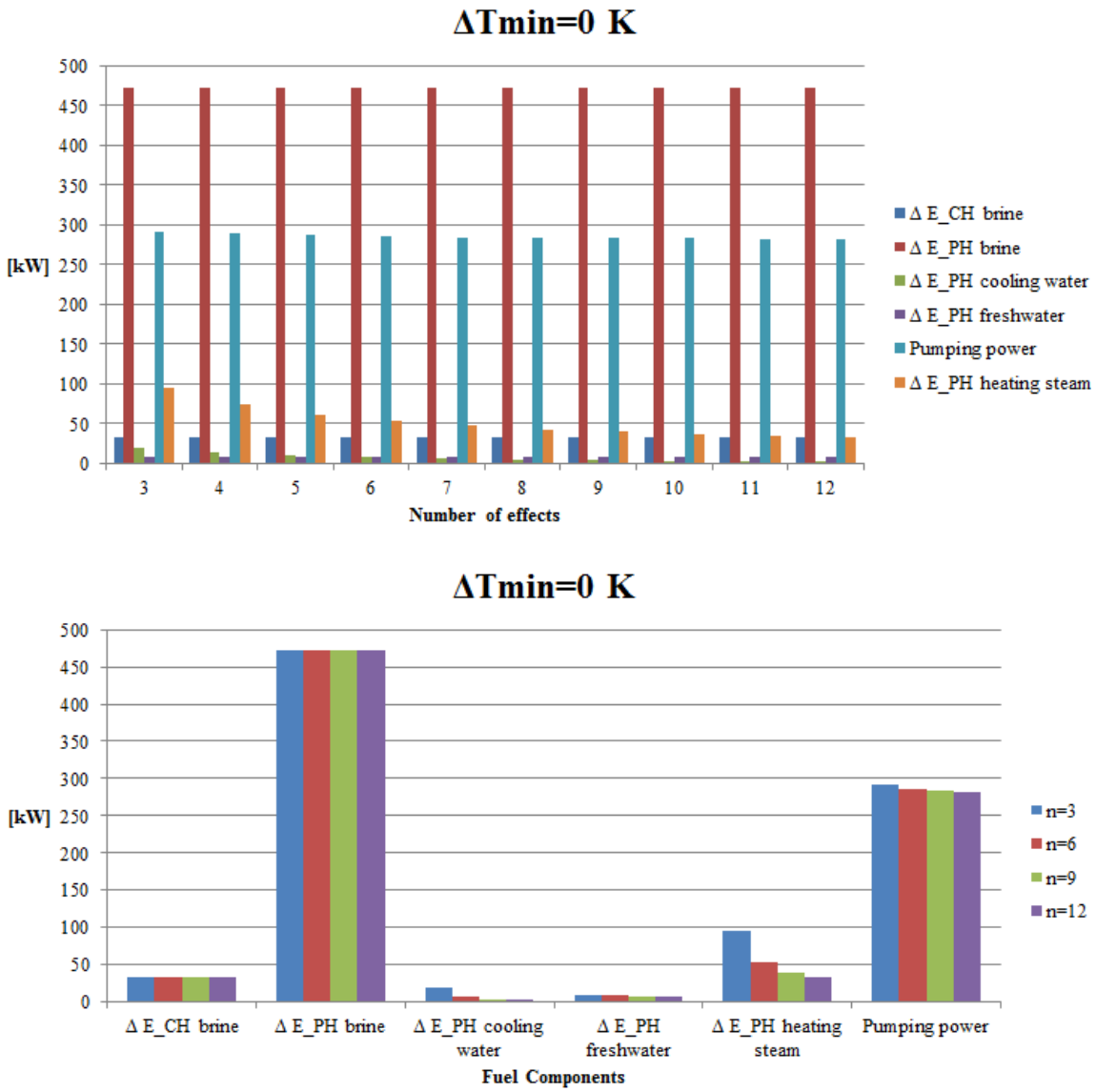

Figure 7.14: Fuel components trends as functions of number of effects n in a MED process with top brine temperature 333 K and $\Delta T_{min} = 0K$

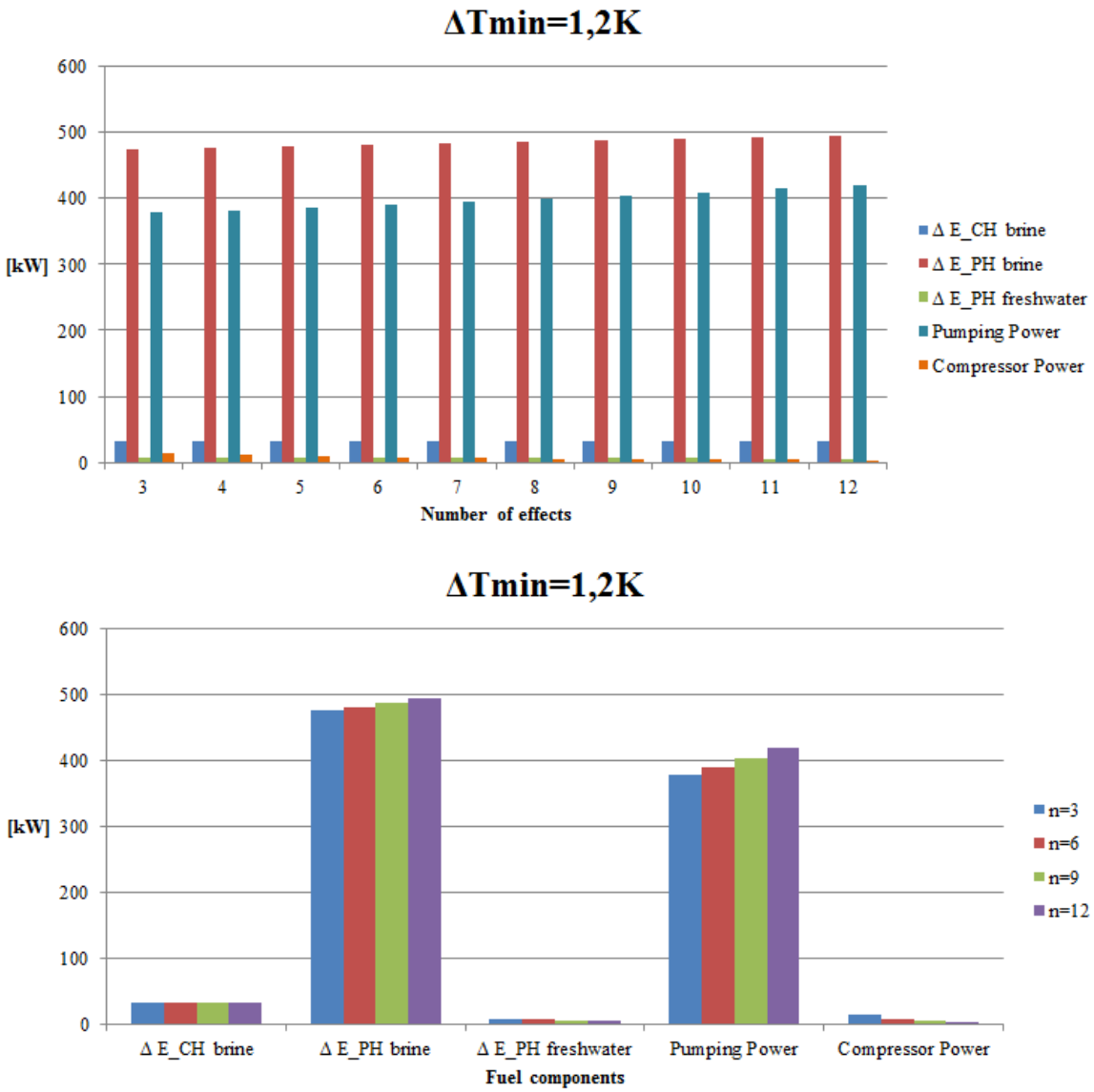

Figure 7.15: Fuel components trends as functions of number of effects n in a MED-MVC process with top brine temperature 333 K and $\Delta T_{min} = 1.2K$

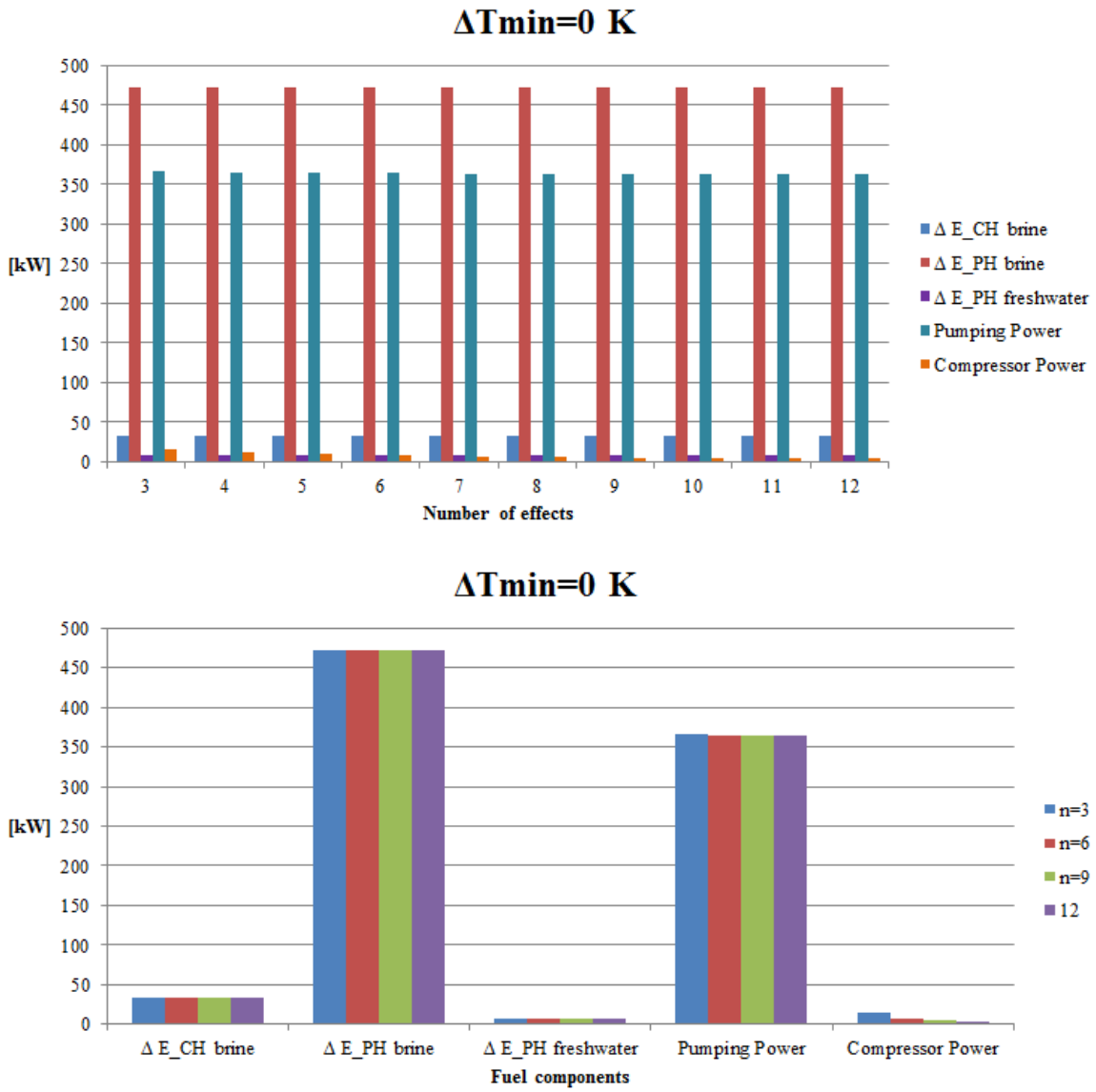

Figure 7.16: Fuel components trends as functions of number of effects n in a MED-MVC process with top brine temperature 333 K and $\Delta T_{min} = 0K$

power at the compressor decreases at increasing n, since higher number of effects means lower seawater mass flow rate per effect and hence lower heat amount required at the evaporator. On the other hand, in real conditions there is a global increase of fuel due to increasing $\Delta \dot{E}_{br}^{PH}$ and pumping power, which overcome the drop of compressor power (Figure 7.15). This is not the case of effects with $\Delta T_{min} = 0K$, where fuel globally decreases thanks to decreasing power at the compressor, while $\Delta \dot{E}_{br}^{PH}$ and pumping power remain constant.

Given the low values of exergy efficiency, it could be difficult to evaluate relevant changes in the performance of different configurations. For this reason, a new efficiency parameter can be introduced, which evaluates the exergy supply (in terms of energy, $[kWh_{ex}]$) necessary to obtain 1 m^3 of freshwater. Hence, from the definition of η_{ex} given in this chapter :

$$\eta_{ex} = \frac{[kg/s] \cdot [kW_{ex}]}{kW_{ex}} \tag{7.20}$$

From Equation 7.20 it is immediate to calculate the new performance parameter as:

$$1/SEV = \frac{3.6[kg/s]}{[kWh_{ex}]} \tag{7.21}$$

$$SEV = \frac{[kWh_{ex}]}{3.6[kg/s]} = \frac{[kWh_{ex}]}{[m^3_{fw}]} \tag{7.22}$$

In this way, all the considerations done before on the changes of fuel terms for different design configurations are still valid, since fuel definition does not change. However, parameter SEV (Specific Exergy Consumption per unit Volume of freshwater produced) could be easier to refer to for the higher values compared to η_{ex} and also for its meaning.

Table 7.5 reports values of different performance parameters under different design conditions of a MED-MVC plant. In particular, η_{Wsep} is the exergy efficiency calculated in the model using the definition given by Sharqawy et al. [54], Mistry et al. [31], [9] and Kahraman and Cengel [27] reported in equation 7.5. It can be noted that values of η_{Wsep} are considerably higher than those of η_{ex}. This is due to the fact that models built in this work refer to a control volume which matches with the system boundaries. As a consequence, disequilibrium of rejected brine and product freshwater with the environment are not taken into consideration. In fact, Mistry et al. used this definition of η_{Wsep} referring to a control volume "sufficiently far from the physical plant", so that all outlet streams are at environment temperature and freshwater (considered as the

only product) is already in thermal equilibrium with the environment. Values obtained in this way were significantly lower than those reported in Table 7.5, approximately around 7-8%, but still higher than the ones of η_{ex}, since rejected brine is not considered as a fuel, but only as an useless product.

			TBT=333 K	TBT=339 K	TBT=343 K
n=3	$\eta_{Primary}$	[%]	0.3134	0.2837	0.2653
	η_{ex}	[%]	3.5480	2.9670	2.6040
	η_{Wsep}	[%]	59.840	54.970	52.460
	SEV	$[kWh_{ex}/[m^3_{fw}]$	255.40	305.40	347.90
n=6	$\eta_{Primary}$	[%]	0.3014	0.2717	0.2530
	η_{ex}	[%]	3.4580	2.8930	2.5390
	η_{Wsep}	[%]	59.590	54.570	51.960
	SEV	$[kWh_{ex}/[m^3_{fw}]$	262.00	313.20	356.80
n=9	$\eta_{Primary}$	[%]	0.2850	0.2561	0.2378
	η_{ex}	[%]	3.3390	2.7980	2.4580
	η_{Wsep}	[%]	58.830	53.760	51.130
	SEV	$[kWh_{ex}/[m^3_{fw}]$	271.40	323.80	368.60

Table 7.5: Values of different efficiency parameters for a MED-MVC plant under different design conditions. Feed seawater is assumed at 298 K, 1 bar and 36000 ppm of salinity. Minimum temperature difference at the heat exchangers is set at $\Delta T_{min} = 1.2K$

.

In conclusion, from exergy analysis it appears how Performance Ratio and Recovery Ratio do not properly represent working principles of desalination systems. More in detail, they do not take into consideration the different forms of input energy (which in turn is done by the efficiency $\eta_{Primary}$ defined in Chapter 2) and are calculated from variables that are not always emblematic of the process (for example, heating steam mass flow rate in MED-MVC is not a representative variable as it is in MED). The

efficiency parameter $\eta_{Primary}$ defined in Chapter 2, which refers to primary energy for input of the system, better describes how the process are working. However, $\eta_{Primary}$ refers to an ideal chemical reaction (i.e. the reversible process of separation of salts from water) which would never be reached in reality and moreover does not explicitly take into account the effect of non-desired products (heating of brine, fresh water and cooling water). The latter can induce to misleading results. For example, from Table 7.3 and Figure 7.11 it is possible to notice that trend of $\eta_{Primary}$ does not highlight the presence of an optimum value of number of effect n in MED system operating at a fixed top brine temperature, which by contrast is done by η_{ex}. The low exergy efficiencies calculated in this chapter (or the high exergy expenses per cubic meter of desalinated water) confirm, once again, that evaporative desalination systems are highly energy intensive plants, which need to be improved before being considered sustainable. In this perspective, finding the exergy analysis approach that is totally consistent with the plant purpose could help to find out the right actions necessary to improve the global system.

Chapter 8

Conclusions

In the present work, main evaporative desalination technologies have been modeled and analyzed. Implementation of correlations by Sharqawy et al. [54] for seawater properties and inclusion of pumping energy in the mathematical models make results of model simulation more realistic.

In the first part of this work (Chapters 3 to 6) parametric analysis was driven through metrics based on the first law of thermodynamics. At increasing Top Brine Temperatures, both Performance Ratio PR and primary energy-based efficiency $\eta_{Primary}$ decrease, while they grow for higher number of effects. This result is also confirmed by other studies found in the literature, which refer to increasing level of heat reutilization at increasing number of effects/stages. However, efficiency parameters based on the first law of thermodynamics do not take into consideration the add of irreversibilities for non-ideal heat exchange at each effect/stage added to the system, which indeed is demonstrated by simulation results of exergy analysis performed in Chapter 7.

On the other hand, exergy analysis confirms the decreasing trend of plants performance at increasing Top Brine Temperature. More in detail, the new approach to exergy analysis allows to highlight which fuel exergy components increase at rising TBT, revealing that higher Top Brine Temperatures would result in higher levels of exergy released to the environment through brine and freshwater streams.

Even though low values of exergy efficiency demonstrate that evaporative systems are still far from being sustainable, finding the exergy analysis approach that is totally consistent with the plant purpose could help to find out the right actions necessary to improve the global system.

The accurate analysis proposed in the present thesis could also constitute a solid base for future studies. Extending the same approach for exergy analysis to other desalination technologies - both thermal and membrane ones - could lead to an organic comparative analysis based on a single and consistent efficiency parameter. Finally, for what concerns evaporative desalination technologies, a thermo-economic analysis would be the natural prosecution of the present study.

Bibliography

[1] World water temperature. *www.seatemperature.org*.

[2] Ibrahim S. Al-Mutaz and Irfan Wazeer. Development of a steady-state mathematical model for mee-tvc desalination plants. *Desalination*, (351):9–18, 2014.

[3] F. Alasfour, M. Darwish, and A. Bin Amer. Thermal analysis of me-tvc+mee desalination systems. *Desalination*, (174):39–61, 2005.

[4] N. H. Aly and A. K. El-Fiqi. Mechanical vapor compression desalination systems-a case study. *Desalination*, (158):143–150, 2003.

[5] M.M. Ashour. Steady state analysis of the tripoli west lt-ht-med plant. *Desalination*, (152):191–194, 2003.

[6] A.Subramani, M.Badruzzaman, J.Oppenheimer, and J.G.Jacangelo. Energy minimization strategies and renewable energy utilization for desalination: A rview. *Water research*, (45):1907–1920, 2011.

[7] C. S. Bandi, R. Uppaluri, and A. Kumar. Global optimization of msf seawater desalination processes. *Desalination*, (394):30–43, 2016.

[8] B.Rahimi, A.Christ, K.Regenauer-Lieb, and H.T.Chua. A novel process for low grade heat driven desalination. *Desalination*, (351):202–212, 2014.

[9] D. Brogioli, F. La Mantia, and Ngai Yin Yip. Thermodynamic analysis and energy efficiency of thermal desalination processes. *Desalination*, (428):29–39, 2018.

[10] D.M.Warsinger, K.H.Mistry, K.G.Nayar, H.W.Chung, and J.H.Lienhard. Entropy generation of desalination powered by variable temperature waste heat. *Entropy*, (17):7530–7566, 2015.

[11] A.M. Farooque, A.T.M. Jamaluddin, and Ali R. Al-Reweli. Comparative study of various energy recovery devices used in swro process. 2005.

[12] P. Fiorini and E. Sciubbba. Modular simulation and thermoeconomic analysis of a multi-ffect distillation desalination plant. *Energy*, (32):459–466, 2007.

[13] F.Zhang, S.Xu, D.Feng, S.Chen, R.Du, C.Su, and B.Shen. A low-temperature multi-effect desalination system powered bby the cooling water of a diesel engine. *Desalination*, (404):112–120, 2017.

[14] A. Gambier, A. Krasnik, and E. Badreddin. Dynamic modeling of a simple reverse osmosis desalination plant for advanced control purposes. *Proceedings of the 2007 American Control Conference*, pages 4854–4859, 2007.

[15] D. Gatto. Experimental investigation of ethanol separation by reverse osmosis. *Desalination*, 2012.

[16] G.P.Narayan. Thermal design of humidification dehumidification systems for affordable, small-scale desalination. *PhD thesis*, 2012.

[17] H. M. Ettouney H. T. El-Dessouky. In *Fundamentals of Desalination*. Elsevier, 2002.

[18] H.Fathia, K.Tahar, B.Yahia Ali, and B. Brahim Ammar. Exergoeconomic optimization of a double effect desalination unit used in an industrial steam power plant. *Desalination*, (438):63–82, 2018.

[19] S. Patel H.N. Panchal. An extensive review on different design and climatic parameters to increase distillate output of solar still. *Renewable Sustainable Energy Rev.*, (69):750–758, 2017.

[20] Shaobo Hou, Z.Zhang, Z Huang, and A. Xie. Performance optimization of solar multi-stage-flash desalination process using pinch technology. *Desalination*, (220):524–530, 2008.

[21] H.Sharon and K.S.Reddy. A review of solar energy driven desalination technologies. *Renewable and Sustainable Energy Reviews*, (41):1080–1118, 2015.

[22] IRENA. In *Renewable Energy in the Water, Energy and Food Nexus.*, 2015.

[23] I.S.Al-Mutaz and I.wazeer. Comparative performance evaluation of conventional multi-effect evaporation desalination process. *Applied Thermal Engineering*, (73):1194–1203, 2014.

[24] M. Ahmad Jamil and S.M. Zubair. Effect of feed flow arrangement and number of evaporators on the performance of multi-effect mechanical compression desalination. *Desalination*, (429):76–87, 2018.

[25] D.M. Warsinger J.H. Lienhard, G.P. Thiel and L.D. Banchik. Low carbbon desalination: status and research, development and demonstration needs. *Report of a workshop conducted at the MIT in association with GCWDA*, 2016.

[26] A.E. Kabeel, T. Arunkumar, and R. Sathyamurthy D.C. Denkenberger. Performance enhancement of solar still through efficient heat exchange mechanism-a review. *Applied Thermodynamics Engineering*, (114):815–836, 2017.

[27] N. Kahraman and Y.A. Cengel. Exergy analysis of a msf distillation plant. *Energy Conversion and Management*, (46):2625–2636, 2005.

[28] A.K. Kaviti, A. Yadav, and A. Shukla. Inclined solar stills desgns: A review. *Renewable Sustainable Energy Rev.*, (54):429–451, 2016.

[29] K.H.Mistry and J.H.Lienhard. Generalized least energy of separation for desalination and othr chemical separation processes. *Entropy*, (15):2046–2080, 2013.

[30] K.H.Mistry and J.H.Lienhard. Exergetic and thermoeconomic analysis of a trigeneration system producing electricity, hot water and fresh water driven by low-temperature. *Energy Conversion and Management*, (157):266–276, 2018.

[31] K.H.Mistry, R.K.McGovern, G.P.Thiel, E.K.Summers, S.M.Zubair, and J.H.Lienhard. Entropy generation analysis of desalination technologies. *Entropy*, (13):1829–1864, 2011.

[32] A. Lazzaretto and G. Tsatsaronis. Speco:a systematic and general methodology for calculating efficiencies and costs in thermal systems. *Energy*, (31):1257–1289, 2006.

[33] Chandrashekara M. and A. Yadav. Water desalination system using solar heat: A review. *Renewable and Sustainable Energy Reviews*, (67):1308–1330, 2017.

[34] M.A.Jamil and S.M.Zubair. Design and analysis of a forward feed multi-effct mechanical vapor compression desalination system: An exergo-economic approach. *Energy*, (140):1107–1120, 2017.

[35] A. Nannarone, C. Faoro, and E. Sciubbba. Multi-effect distillation desalination process: Modeling and simulation. *Proceedings of ECOS 2017*, 2017.

[36] G. Prakash Narayan and J. Lienhard. Humidification dehumidification desalination. *Desalination*, pages 427–472, 2014.

[37] G. Prakash et al. Narayan. Thermodynamic analysis of humidification-dehumidification desalination cycles. *Desalination and Water Treatment*, 2010.

[38] o. Samaké, N. Galanis, and M. Sorin. On the design and corresponding performance of steam jet ejectors. *Desalination*, (381):15–25, 2016.

[39] Z.M. Omara, A.E. JKabeel, and A.S. Abdullah. A review of solar still performance with reflectors. *Renewable Sustainable Energy Rev.*, (68):638–649, 2017.

[40] O.Samaké, N. Galanis, and M.Sorin. Thermo-economic analysis of a multiple-effect desalination system with ejector vapour compression. *Energy*, (144):1037–1051, 2018.

[41] S.M. Mahmoud P.G. Youssef, R.K. AL-Dadah. Comparative analysis of desalination technologies. *Energy Procedia*, (61):2604–2607, 2014.

[42] WWAP (United Nations World Water Assessment Programme). In *World Water Development Report 2015: Water for a sustainable world.* UNESCO, 2015.

[43] Q.Chen, M.Kum Ja, Y. Li, and K.J.Chua. On the second law analysis of a multi-stage spray-assisted low-temperature desalination system. *Energy Conversion and Management*, (148):1306–1316, 2017.

[44] Q.Chen, M.Kum Ja, Y. Li, and K.J.Chua. Energy, economic and environmental (3e) analysis and multi-objective optimization of a spray-assisted low-temperature desalination system. *Energy*, (151):387–401, 2018.

[45] Q.Chen, Y. Li, and K.J.Chua. On the thermodynamic analysis of a novel low-grade heat driven desalination system. *Energy Conversion and Management*, (128):145–159, 2016.

[46] Q.Chunhua, Lv Hongqing, F.Houjun, Lv Qingchun, and X. Yulei. Performance and economic analysis of the distilled seawater desalination process using low-temperature waste hot water. *Applied Thermal Engineering*, (122):712–722, 2017.

[47] D.A. Roberts, E.L. Johnston, and N.A. Knott. Impacts of desalination plant discharges on the marine environment: A critical review of published studies. *Water Research*, (44):5117–5128, 2010.

[48] M. Rognoni. In *La dissalazione dell'acqua di mare-Descrizione, analisi e valutazione delle principali tecnologie*. Dario Flaccovio Editore, 2010.

[49] Klein SA. Engineering equation solver (ees). *www.fchart.com/ees/*.

[50] R. Sathyamurty, S.A. El-Agouz, P.K. Nagarajan, J. Subramani, T. Arunkumar, D. Mageshbabu, B. Madhu, R. Bharathwaaj, and N. Prakash. A review of integrating solar collectors to solar still. *Renewable Sustainable Energy Rev.*, 2016.

[51] B. Seifert, A. Kroiss, M. Spinnler, and T. Sattelmayer. About the history of humidification-dehumidification desalination systems. *The International Desalination Association World Congress on Desalination and Water Reuse*, 2013.

[52] M.W. Shahzad, M. Burhan, Li Ang, and K. Choon Ng. Energy-water-environment nexus underpinning future desalination sustainability. *Desalination*, (413):52–64, 2017.

[53] H. Sharon and K.S. Reddy. A review of solar energy driven desalination tchnologies. *Renewable and Sustainable Energy Reviews*, (41):1080–1118, 2015.

[54] M.H. Sharqawy, J.H. Lienhard, and S.M.Zubair. On exergy calculations of seawater with applications in desalination systems. *International Journal of Thermal Science*, (50):187–196, 2011.

[55] S. Shen, S. Zhou, Y. Yang, and L. Yang. Study of steam parameters on the performance of a tvc-med desalination plant. *Desalination and water treatment*, (33):300–308, 2011.

[56] T.Mezher, H.Fath, Z.Abbas, and A.Khaled. Techno-economic assessment and environmental impacts of desalination tehcnologies. *Desalination*, (266):263–273, 2011.

[57] T.M.Ismail, A.K.Azab, M.A.Elkady, and M.M.Abo Elnasr. Theoretical investigation of the performance of integrated seawater desalination plant utilizing renewable energy. *Energy Conversion and Management*, (126):811–825, 2016.

[58] Letter to the Editor. Energy consumption and water production cost of conventional and renewable-energy-powered desalination processes. *Renewable and Sustainable Energy Reviews*, (24):343–356, 2013.

[59] A. Toffolo, A. Lazzaretto, and M. Morandin. The heatsep method for the synthesis of thermal systems: An application to the s-graz cycle. *Energy*, (35):976–981, 2010.

[60] E. Delyannis V. Belessiotis, S. Kalogirou. In *Thermal and Solar Desalination - Methods and systems*. Elsevier, 2016.

[61] Y.Roy, G.P. Thiel, M.A. Antar, and J.H. Lienhard. The effect of increased top brine temperature on the performance and design of ot-msf using a case study. *Desalination*, (412):32–38, 2017.